

**INDUSTRIAL WASTEWATER TREATMENT USING  
MEMBRANE NANOFILTRATION**

CERAMIC MEMBRANE NANOFILTRATION FOR INDUSTRIAL WASTEWATER  
TREATMENT – A COMPARISON WITH CONVENTIONAL POLYMER MEMBRANES &  
DATA-DRIVEN MODELING OF ORGANIC COMPOUNDS REMOVAL

By

SATYAM AGNIHOTRI, B.TECH

A Thesis Submitted to the School of Graduate Studies  
in Partial Fulfillment of the Requirements for the Degree  
Master of Applied Science

McMaster University © Copyright by Satyam Agnihotri, August 2020

MASTER OF APPLIED SCIENCE (2020)

McMaster University

(Chemical Engineering)

Hamilton, Ontario

**TITLE:** Ceramic membrane nanofiltration for industrial wastewater treatment – a comparison with conventional polymer membranes & data-driven modeling of organic compounds removal

**AUTHOR:** Satyam Agnihotri

**SUPERVISOR:** Dr. D Latulippe

**CO-SUPERVISOR:** Dr. P Mhaskar

**NUMBER OF PAGES:** 108

## LAY ABSTRACT

Conventional technologies for Industrial wastewater (IWW) treatment include biological treatment, coagulation, flocculation, adsorption and filtration. Many industries produce IWW with high concentration of biologically toxic organics ruling out the option of biological treatment. Moreover, with stricter regulatory laws in place for effluent discharge, adoption of new treatment technologies is needed. Nanofiltration (NF) is one such treatment technology that has seen a lot of growth in the past decade since its advent in 1980s. Polymer nanofiltration has been successfully used in applications such as dye removal in textile industry, as a pre-treatment method in desalination plants, for organic solvent nanofiltration in pharmaceutical industry and many more. More recent development of ceramic nanofiltration membranes has seen a lot of interest from researchers around the world due to their superior physical and chemical robustness, fouling resistant properties and higher permeability as compared to polymer NF membranes, though only a small amount of ceramic NF membranes are applied in industrial projects. To this end, we have conducted laboratory scale testing of 4 state of the art ceramic NF membranes on multiple real industrial wastewater samples collected from a specialized IWW treatment plant, along with 3 polymer NF membranes for comparison purposes. Additionally, a data-driven modeling approach leveraging the wastewater composition dataset is shown. The models can be used to predict % rejection of an unseen compound based on its chemical properties and provide insights into complex interactions between compounds and the membrane.

## ABSTRACT

Industrial wastewater treatment using conventional treatment technologies is becoming challenging day-by-day due to presence of ‘newer’ refractory compounds, lower treatment efficiencies and stricter environmental laws. Combination of conventional treatment techniques with modern treatment technologies like membrane filtration or advanced oxidation processes (AOPs) has shown promise in achieving high efficiencies. In this work we have worked towards development of a membrane nanofiltration unit to treat coagulation-flocculation pretreated IWW from a specialized treatment facility. More specifically, state-of-the-art TiO<sub>2</sub> ceramic NF membranes with low molecular weight cut off (MWCO) (200, 450, 750, 8500 Da) purchased from Inopor GmbH were tested on 6 different IWW samples due to their superior chemical stability, higher flux and high fouling resistance along with 3 commercial polymer NF membranes (NF90, NFX, NFS) for comparison purposes. Additionally, wastewater characterization dataset including composition analysis using Gas-chromatography Mass-spectroscopy (GC-MS) is leveraged to build data driven models for membrane performance prediction. ‘200 Da’ ceramic NF membrane was able to reject significant COD with an average rejection of 77% and 60% for two IWW samples with permeate flux between 5-15 LMH at 100-120 psi trans-membrane pressure (TMP). ‘200-Da’ membrane was also found to achieve more flux than ‘450 Da’ membrane while rejecting more COD at the same time. ‘200 Da’ membrane also showed lower flux decline than polymer membranes. Additionally, the ceramic NF membranes were found to be easily chemically cleanable restoring wastewater flux after fouling. Since polymer NF membranes were found to reject at higher COD rejection efficiencies (60-90%) and permeate flux, further improvement in ceramic membranes is needed to treat at higher efficiencies. 200 Da, NF90 and NFX membranes were found to be promising to reduce COD below target (600 mg/L) and should be studied further for this application.

## ACKNOWLEDGMENTS

First of all, I would like to thank my supervisor Dr. David Latulippe for giving me this opportunity to carry out this project. I am thankful for his continuous support in providing critical feedback and suggestions during the whole project. I also want to thank him for giving me the opportunity to present my work to our industry partners multiple times during the project. I am truly thankful for his numerous hours of work writing grants and proposals to ensure continuous funding for this project. Secondly, I would like to thank my co-supervisor Dr. Prashant Mhaskar for his continuous support and frequent meetings to discuss my work. I would also like to thank him for suggesting new ideas for my work and all the knowledge that he shared with me during the meetings. Also, would like to thank him for providing me a desktop and licenses for data-modeling softwares.

I would like to take this opportunity to thanks all my lab mates, Abhishek Premachandra, Patrick Morkus, Ryan LaRue, Melissa Larocque, Karina Kawka, Evan Wright, Salman Alizadeh for helping me around the lab during initial days. Also, would like to thank them for providing feedback on my work during group meetings. All the testing that went into this work and others would not have been possible without your help in the lab. I would also like to thank undergraduate students Jacob McGivern and Susie O'Brien for their time in understanding and carrying out some experiments for this project during their co-op term.

Next, I would like to thank Dr. Kirk Green and Dr. Fan Fie at MRCMS (McMaster Regional Centre for Mass Spectroscopy) facility in training me on GC-MS instrument and allowing testing of samples seamlessly. Special thanks to Dr. Kirk Green for insightful discussions about GC-MS and also setting up and maintaining remote desktop connection for data analysis during the COVID-19 pandemic. I would also like to thank Monica Han from Civil Engineering department

for providing multiple instruments from undergraduate lab for testing. Also thanking Dr. Shiping Zhu's lab for giving access to rotary-evaporator.

I would also like to highly acknowledge the help and support from team at Aevitas specially Richard Mock and Jo-ann Livingston for collecting wastewater samples for testing and giving multiple plant tours. I would also like to thank Milos Stanisavljevic, Tom Maxwell, Jo-ann Livingston and Richard Mock for their comments and questions during presentations.

I would also like to thank Paul Gatt for his help in setting up fittings for ceramic module and continuous help with the membrane system. I would also like to thank Tim Stephens, Michael Clarke, and Doug Keller for their help on numerous occasions.

In terms of funding, I would like to thank our department and Aevitas for providing graduate and research scholarship to sustain my living expenses, nothing would be possible without this.

Lastly, I would like to thank my friends and family, specially my parents, my father Mr. Ramesh Kumar Agnihotri, and my mother Mrs. Saroj Agnihotri, and my brother Shivam Agnihotri for their endless love and support. Also, special thanks to my friends Debanjan Ghosh, Aniket Anand and Carlos Rodriguez for their spiritual support during this course.

## TABLE OF CONTENTS

Lay Abstract.....	iii
Abstract.....	iv
Acknowledgements.....	v
Table of Contents.....	vii
List of Tables.....	x
List of Figures.....	xii
List of Abbreviations.....	xv
<b>CHAPTER 1. Introduction.....</b>	<b>1</b>
1.1 Background – Industrial Wastewater (IWW) treatment facility at Aevitas.....	1
1.2 Wastewater treatment using Nanofiltration membranes.....	4
1.2.1 Introduction - Understanding separation mechanisms.....	4
1.2.2 Conventional nanofiltration using polymer membranes.....	7
1.2.2.1 Synthesis & applications.....	7
1.2.2.2 Previous studies on IWW treatment.....	10
1.2.3 Nanofiltration using inorganic membranes.....	12
1.2.3.1 Synthesis & applications.....	12
1.2.3.2 Previous studies on IWW treatment.....	13
1.3 Objectives.....	14
<b>CHAPTER 2. Materials and Methods.....</b>	<b>15</b>
2.1 Industrial wastewater samples.....	15
2.1.1 Sample collection and storage.....	15
2.1.2 Wastewater characterization.....	15
2.2 Ceramic NF membranes.....	19
2.2.1 Pre-treatment and storage.....	19
2.2.2 Pristine membrane performance testing.....	21
2.3 Polymer NF membranes.....	22
2.3.1 Pre-treatment and storage.....	23

2.3.2	Pristine membrane performance testing .....	23
2.4	Experimental setup.....	23
2.4.1	Ceramic membrane testing module.....	26
2.4.2	Polymer membrane testing module.....	26
2.5	Filtration test procedures.....	27
2.5.1	Clean water permeability.....	27
2.5.2	Industrial wastewater filtration.....	28
2.5.3	Salt rejection testing.....	28
2.5.4	Clean-in-place chemical cleaning.....	29
2.6	Chronology of filtration tests.....	31
2.6.1	Ceramic Nanofiltration.....	31
2.6.2	Polymer Nanofiltration.....	31
2.7	Analytical Procedures.....	31
2.7.1	Total & soluble chemical oxygen demand test.....	31
2.7.2	pH & Conductivity test.....	32
2.7.3	Turbidity test.....	33
2.7.4	Gas-chromatography Mass-spectroscopy test.....	33
<b>CHAPTER 3.</b>	<b>Performance comparison among ceramic NF membranes.....</b>	<b>36</b>
3.1	Introduction.....	36
3.2	Results – Filtration & chemical cleaning.....	38
3.2.1	COD rejection performance.....	38
3.2.2	Permeate wastewater flux comparison.....	42
3.2.3	Effect of wastewater filtration & chemical cleaning on CWP.....	46
3.3	Chemical cleaning & filtration repeatability study – 750 Da membrane.....	49
3.3.1	Procedure for multiple filtration & cleaning cycles.....	50
3.3.2	Permeate flux and COD rejection performance.....	51
3.3.3	Chemical cleaning efficiency over multiple filtration cycles.....	53
3.4	Conclusion.....	54
<b>CHAPTER 4.</b>	<b>Comparison with Polymer Nanofiltration membranes and Predictive modeling of membrane rejections.....</b>	<b>56</b>
4.1	Polymer NF filtration performance.....	56

4.1.1	COD rejection & permeate flux.....	56
4.1.2	Effect of wastewater filtration on membrane performance.....	60
4.2	Performance comparison – Polymer vs Ceramic membranes.....	63
4.2.1	Permeate COD and wastewater flux.....	63
4.2.2	Removal of organic compounds – GCMS analysis.....	66
4.3	Predictive modeling using GCMS compound removal dataset.....	73
4.3.1	Introduction.....	73
4.3.2	Preliminary PLS model.....	77
4.3.3	Grouped PCA-PLS predictive modeling approach.....	80
4.3.4	Grouped PCA-PLS models training.....	81
4.3.5	Model training and testing results.....	83
4.3.5.1	Performance metrics – $R^2$ , $Q^2$ , RMSEE, RMSEP.....	84
4.3.5.2	Observed vs Predicted plots.....	89
4.3.5.3	Cross testing results.....	91
4.4	Key learnings – Polymer vs Ceramic membranes.....	93
<b>CHAPTER 5. Conclusions and future work.....</b>		<b>94</b>
5.1	Conclusions.....	94
5.2	Future work.....	96
<b>APPENDIX.....</b>		<b>100</b>
<b>REFERENCES.....</b>		<b>103</b>

LIST OF TABLES	Page
<b>Table 1.</b> Commercial nanofiltration membranes and specifications by manufacturers.....	6
<b>Table 2.</b> Previous IWW treatment studies using polymer nanofiltration membranes.....	11
<b>Table 3.</b> Previous IWW treatment studies using ceramic nanofiltration membranes.....	14
<b>Table 4.</b> Bulk property characterization of all wastewater samples shown in Figure 5. Two aliquots of each sample were used to calculate the average and error values shown in the table..	17
<b>Table 5.</b> GC-MS characterization of all wastewater samples shown in Figure 5. Compounds present in a wastewater samples are denoted by tick marks and highlighted in green. Compounds are sorted based on frequency of occurrence (out of 6 samples) of a compound shown in the last column. Note that RT stands for ‘retention time’ for a peak/compound.....	18
<b>Table 6.</b> Membrane nomenclature and properties as reported by the manufacturers and present in literature. MWCO stands for molecular weight cut off which refers to the lowest molecular weight solute in which 90 % of the solute is retained by the membrane. MWCO is usually measured using a mixture of Polyethylene glycols (PEGs). Zeta-potential values reported here were measured at pH 8 using 0.01 M NaCl solution [62, 63].....	20
<b>Table 7.</b> Summary of experimental conditions during various filtration tests. Note that a pump frequency of 16 Hz corresponds to a feed flow of 2 L/min through the system and a cross-flow velocity of 1 m/s through the ceramic tubular membrane.....	30
<b>Table 8.</b> Summary of feed and permeate characterization from cross-flow microfiltration pre-treatment step using Synder V0.2 membrane. Highlighted values in the parenthesis show % drop in bulk property. Permeates collected from this step are then used to test the ceramic & polymer NF membranes.....	37
<b>Table 9.</b> COD rejection summary from experiments with 4 ceramic membranes and 3 WW samples (A, B, C). Average and standard deviations are calculated using COD values at three time points (t=10, 60, 120 min).....	40
<b>Table 10.</b> Summary of % drop and % recovery in CWP during testing of ceramic membranes. **Note that the cleaning protocol followed for 8500-Da was different from others which led to very low % recovery in CWP.....	48
<b>Table 11.</b> Summary of chemical cleaning conditions for mild and aggressive cleaning steps.....	51
<b>Table 12. a.</b> Organic compounds rejection for 6 membranes tested on WW-A. Peaks are sorted in decreasing order of area under peak found in the feed sample, so major contributors to organic concentration are found towards the top of the table. Unidentified peaks are marked using ‘?’. Compounds/peaks which observed more than or equal to 90% rejection are highlighted in green. A count of total peaks reduced ( $\geq 90\%$ ) is present in the last row for each membrane out of 70 peaks. <b>b.</b> Segregation of peaks based on 6 different criteria to analyze the differences in rejection for ceramic and polymeric membranes, where ‘Diff’ stands for  Polymeric – Ceramic . For unidentified peaks, corresponding retention time (RT) is mentioned.....	69
<b>Table 13. a.</b> Organic compounds rejection for 6 membranes tested on WW-C. Peaks are sorted in decreasing order of area under peak found in the feed sample, so major contributors to organic concentration are found towards the top of the table. Unidentified peaks are marked using ‘?’.	

Compounds/peaks which observed more than or equal to 90% rejection are highlighted in green. A count of total peaks reduced ( $\geq 90\%$ ) is present in the last row for each membrane out of 76 peaks. **b.** Segregation of peaks based on 6 different criteria to analyze the differences in rejection for ceramic and polymeric membranes, where ‘Diff’ stands for |Polymeric – Ceramic|. For unidentified peaks, corresponding retention time (RT) is mentioned.....71

**Table 14.** Complete dataset showing 41 observations, 4 input variables (MW: Molecular weight, pKa: Dissociation constant,  $K_{ow}$ : Octanol-water partition coefficient, Sol: Solubility) and 7 output variables (one for each membrane tested 200-Da, 450-Da, 750-Da, 8500-Da, NF90, NFX and NFS). 7 highlighted observations were selected randomly and separated into a testing dataset; remaining observations were used for training models.....76

**Table 15.** Grouping of chemical compounds present in the training set using PCA score plot....81

**Table 16.** PLS model nomenclature. One PLS model is trained for each group and each membrane type. No PLS model was trained for Group-3 compounds for ceramic membranes due to less number of observations.....83

**Table 17.** Testing set compounds and their estimated groups based on PCA score plot analysis in Figure 27.....86

**Table 18.** Group-wise model summary for ceramic and polymeric membranes.....87

**Table 19.** Membrane-wise performance metrics for all 5 membranes. Corresponding Grouped PCA-PLS models were used to calculate predictions for each membrane.....87

**Table 20.** Summary of cross testing results. Cells highlighted in red are instances when a test subset was better predicted (low RMSEP) using a model that was not trained on observations from the same group as the test subset. Cells highlighted in gray show RMSEP values when a test subset was predicted using a model trained on observations from the same group as the test subset.....92

**Table 21.** Membrane area calculations based on flux achieved by 200-Da, NF90 and NFX membranes.....95

LIST OF FIGURES	Page
<b>Figure 1.</b> Schematic of different pathways for industrial wastewater treatment.....	2
<b>Figure 2.</b> Treatment train of batch treatment processes at Aevitas and WW sampling points. RW is raw incoming wastewater, RWT are raw water tanks, PTT are primary treatment tanks for acid cracking and coagulation-flocculation and FTT denote finishing treatment tanks used for aeration and peroxide treatment.....	3
<b>Figure 3.</b> Separation range and examples of feed for 4 major classes of membrane filtration processes [6] .....	5
<b>Figure 4.</b> Thin film composite membrane structure taken from [19].....	8
<b>Figure 5.</b> Pictures of 6 IWW samples collected from Aevitas. A unique identifier of each WW is mentioned on the top left corner of each panel. Bulk properties of all samples are tabulated in Table 4. ....	16
<b>Figure 6.</b> Pictures of single channel tubular ceramic membranes stored in DI water. Note that a total of 6 ceramic membranes are shown in the picture but only 4 of them were used for wastewater filtration studies in this report. Panel on the right shows the hollow feed channel inside the tubular membrane which contains the membrane active surface. Each membrane was 25 cm in length with an active membrane area of 55 cm <sup>2</sup> .....	20
<b>Figure 7.</b> Pristine ceramic membranes CWP plot. Permeability values in LMH/bar are shown in legend.....	21
<b>Figure 8.</b> Salt rejection (NaCl) for pristine ceramic membranes. Error bars are calculated using triplicate conductivity measurements.....	22
<b>Figure 9.</b> Pictures of the flatsheet polymer membrane testing module (right panel) with a membrane cutout placed inside (left panel) .....	23
<b>Figure 10.</b> Schematic of the experimental setup is shown with membrane module in place. Both ceramic and polymer testing modules can be easily detached from the system using push-to-connect adapters for easy replacement.....	25
<b>Figure 11.</b> Pictures of the ceramic membrane testing module. Top panel shows the module with ends detached and o-rings placed on the side. Bottom panel shows the module attached to the setup and in operation. Note that the membrane had two permeate outlets (top panel) one of which was blocked (bottom panel) to redirect all permeate from only one outlet.....	25
<b>Figure 12.</b> Feed and permeate COD bar plots for ceramic membrane testing. Horizontal dashed line represent the COD target for Aevitas to safely discharge the treated effluent (600 mg/L). Corresponding % COD rejection values can be found in Table 9. ....	41
<b>Figure 13.</b> Permeate flux profiles during wastewater filtration tests for ceramic membranes. Legends also show the operating pressure during each experiment. Error bars denote the standard deviation in flux measured using triplicate measurements. ....	44

**Figure 14.** Relative permeate flux profiles during wastewater filtration tests for ceramic membranes. Legends also show the operating pressure during each experiment. Error bars denote the standard deviation in relative flux measured using triplicate measurements. .... 45

**Figure 15.** Summary plot showing effect of wastewater filtration & chemical cleaning on CWP for ceramic membranes. Error bars are calculated by conducting the complete CWP experiment twice. CWP experiment was only performed once for bars which do not have an error bar. .... 47

**Figure 16.** Summary of chemical cleaning experiments with various chemicals for 8500-Da membrane. .... 48

**Figure 17.** Summary of wastewater flux and membrane permeability (CWP) results from 3 filtration-cleaning cycles on 750-Da membrane with WW-C. Note that all experiments are stacked in chronological order from left to right. Intermediate chemical cleaning steps are annotated on the chart showing cleaning conditions (% w/w Tergazyme, Temperature). Permeate flux is denoted by black markers with corresponding values present on the primary y-axis. Membrane permeability is denoted by red bars with corresponding values present on secondary y-axis. Error bars in CWP denote absolute error from duplicate CWP tests and error bars in permeate flux denote the standard deviation from 5 flux measurements. .... 52

**Figure 18.** Feed and permeate COD during repeated filtration-cleaning cycles of 750-Da membrane with WW-C. Error bars denote standard deviation in COD measured at three time points during filtration (t = 10, 60, 120 min) ..... 53

**Figure 19.** Feed and permeate COD's for 3 polymer membranes tested on 5 IWW samples. .... 57

**Figure 20.** Absolute permeate flux profiles for 3 polymer membranes tested on 5 IWW samples. .... 59

**Figure 21.** Membrane permeability (CWP) before and after filtration for polymer membranes tested on 5 IWW samples. Solid bars represents the CWP for the clean membrane cutouts before filtration and pattern bars represent the CWP of the membranes after wastewater filtration. IWW samples are denoted by different colored bars. .... 60

**Figure 22.** Monovalent (NaCl) and divalent (MgSO<sub>4</sub>) salt rejection performance for polymeric membranes before and after wastewater filtration. Error bars are generated using triplicate feed and permeate conductivity measurements at steady state. 4 IWW samples are denoted by different colored bars. % rejection of pristine membranes as reported by the manufacturers is shown by the red dashed line. .... 62

**Figure 23.** A comparison of COD rejection between 4 ceramic NF (200-Da, 450-Da, 750-Da and 8500-Da) and 3 polymer NF (NF90, NFX, NFS) membranes on two IWW samples namely, WW-A and WW-C. Red dashed line denote the target COD of 600 mg/L for discharge at Aevitas. Feed and permeate COD values are time averaged using three time points during the filtration experiment (t = 10, 60, 120 min). Error bars denote standard deviation of COD values at those three time points. .... 63

**Figure 24.** Comparison of permeate flux between ceramic NF and polymeric NF membranes. Top two panels compare the absolute flux values for WW-A and WW-C. Bottom two panels compare the relative flux values for WW-A and WW-C. 4 ceramic membranes (200-Da, 450-Da,

750-Da and 8500-Da) are shown using black markers while polymeric membranes (NF90, NFX, NFS) are shown using red markers. .... 65

**Figure 25.** Overlaid feed and permeate GC-MS total ion chromatogram (TIC) for WW-A treated using 200-Da ceramic membrane. Example of a partially reduced peak (RT = 5.6 min) and a completely reduced peak (RT = 17.3 min) is annotated on the plot ..... 66

**Figure 26.** Plots for 2 component preliminary PLS model; **a.** Model summary showing  $R^2$  and  $Q^2$  values for Y-space ; **b.**  $w^*,c$  loadings plot between 1<sup>st</sup> and 2<sup>nd</sup> component; **c.** Score plot between 1<sup>st</sup> and 2<sup>nd</sup> components for the PLS model, where region A consisted of short chain monocarboxylic and dicarboxylic acids, region B had long chain monocarboxylic acids, region C consisted mainly of alcohols and regions D had short chain acids or alcohols. .... 79

**Figure 27.** Grouped PCA-PLS modeling flowchart. The prediction layer is highlighted in yellow. Complete prediction layer is trained twice in this report, once for ceramic membranes (200-Da & 450-Da) and second time for polymeric membranes (NF90, NFX, NFS). .... 80

**Figure 28.** Plots for 2 component PCA model on X ; **a.** Model summary showing  $R^2$  and  $Q^2$  values ; **b.** Loadings plot between 1<sup>st</sup> and 2<sup>nd</sup> component, each point on the loadings plot refers to an input variable which is shown as a data label ; **c.** Score plot between 1<sup>st</sup> and 2<sup>nd</sup> components for the PCA model, compounds were found to be weakly clustered into four groups highlighted with different backgrounds on the plot (gold: Group-1, blue: Group-2, green: Group-3, red: Group-4) ..... 82

**Figure 29.** PCA score plot with both training and testing sets. Score values (T[1] & T[2]) for 7 testing set observations are shown in orange circles alongside training data to visualize how testing set observations are classified based on their position on the score plot ..... 86

**Figure 30.** Observed vs Predicted plots for 200-Da (left) and 450-Da (right) ceramic membranes. Each point on the plot correspond to an observation either from the training set (blue) or the testing set (red).  $R^2$  and RMSEE reported on each plot are calculated using points from the training set while RMSEP is calculated using points from the testing set. Error bars denote the standard deviation in % rejection for compounds that occurred in multiple wastewater samples. 89

**Figure 31.** Observed vs Predicted plots for NF90 (top left), NFX (top right) and NFS (bottom) polymer membranes. Each point on the plot correspond to an observation either from the training set (blue) or the testing set (red).  $R^2$  and RMSEE reported on each plot are calculated using points from the training set while RMSEP is calculated using points from the testing set. Error bars denote the standard deviation in % rejection for compounds that occurred in multiple wastewater samples ..... 90

LIST OF ABBREVIATIONS

AC.....	Activated Carbon
COD.....	Chemical Oxygen Demand
CWP.....	Clean Water Permeability
FTT.....	Finishing Treatment Tank
GC-MS.....	Gas Chromatography Mass Spectroscopy
IWW.....	Industrial Wastewater
LMH.....	$L.m^{-2}.h^{-1}$
MF.....	Micro-Filtration
MW.....	Molecular Weight
NF.....	Nano-filtration
PLS.....	Partial Least Squares
PhAC.....	Pharmaceutically Active Compounds
PPCP.....	Pharmaceuticals and Personal Care Products
PTT.....	Primary Treatment Tank
PCA.....	Principal Component Analysis
RWT.....	Raw Water Tank
RT.....	Retention Time
RO.....	Reverse Osmosis
RMSEE.....	Root Mean Square Error in Estimation
RMSEP.....	Root Mean Square Error in Prediction
sCOD.....	Soluble Chemical Oxygen Demand
TFC.....	Thin Film Composite
TDS.....	Total Dissolved Solids
TS.....	Total Solids
UF.....	Ultra-Filtration
WW.....	Wastewater

## **CHAPTER-1: Introduction**

### **1.1 Background – Industrial wastewater (IWW) treatment facility at Aevitas**

Wastewater treatment facilities are broadly classified under three categories, (i) Municipal wastewater treatment facilities, (ii) On-site IWW treatment/recycle facilities, and (iii) Specialized IWW treatment facilities. Municipal treatment facilities cater to very large volumes of wastewater collected from multiple point sources. These point sources generally include domestic households, small businesses, industrial facilities etc. The feed wastewater streams treated at a municipal treatment facility are usually characterized by low concentration of contaminants and low bio-toxicity. Much of the IWW generated does not comply with these standards and therefore cannot be sent directly to a municipal plant for treatment. In such cases, an intermediate treatment step is needed to bring the wastewater to a level that can be easily processed further at a municipal plant as shown in Figure 1. On-site treatment facilities are designed and operated at many plants which provide a two-fold advantage, the treatment technology can be chosen and designed based on the composition of the wastewater generated, and the treated wastewater can be either recycled or sent to a municipal plant for further treatment.

Aevitas is a specialized IWW treatment facility located in Brantford ON, Canada, which takes in wastewater from multiple industries/clients who cannot send their wastewater directly to a municipal plant. Once the IWW is treated as per the sewer discharge regulations of the City of Brantford, the wastewater can be discharged directly into city's sewer system which then takes it to the municipal plant for the final stage of treatment. Aevitas receives anywhere between 10-40 tanker trucks of wastewater every day. Every new batch of wastewater goes through a series of batch treatment processes as shown in Figure 2. The wastewater is treated until it meets the discharge targets which are shown in Table A1 in Appendix, following which the wastewater is sewerred.

Major unit operations include (i) acid cracking to remove oil and grease, (ii) coagulation & flocculation, (iii) activated carbon adsorption, and (iv) aeration and hydrogen peroxide disinfection. The incoming raw wastewater from tanker trucks is passed through mesh filters to catch any big solids and sent to Raw Wastewater Tanks (RWTs) where acid cracking takes place. Treated wastewater is then transferred to one of the Primary Treatment Tanks (PTTs) for coagulation & flocculation process to take place. Treated wastewater is passed through Activated Carbon (AC) column and sent to one of the multiple Finishing Treatment Tanks (FTTs) where hydrogen peroxide and aeration is used to disinfect and separate finer flocs, respectively. Treated wastewater is tested against the target limits and discharged if the targets are met, otherwise it is shipped to one their subsidiary facilities in USA for further treatment.

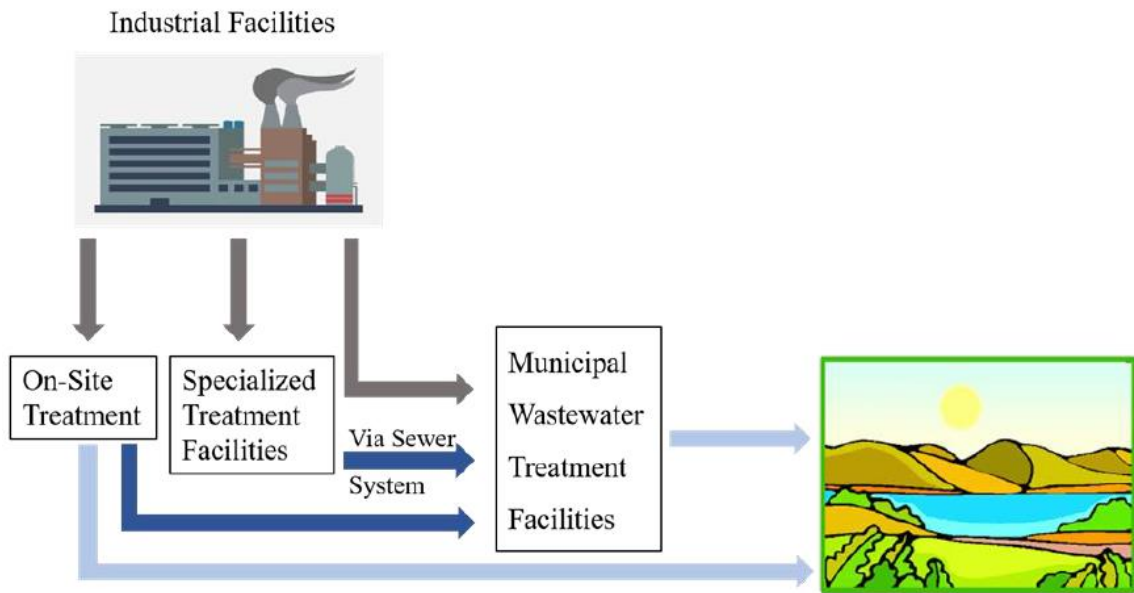


**Figure 1.** Schematic of different pathways for industrial wastewater treatment

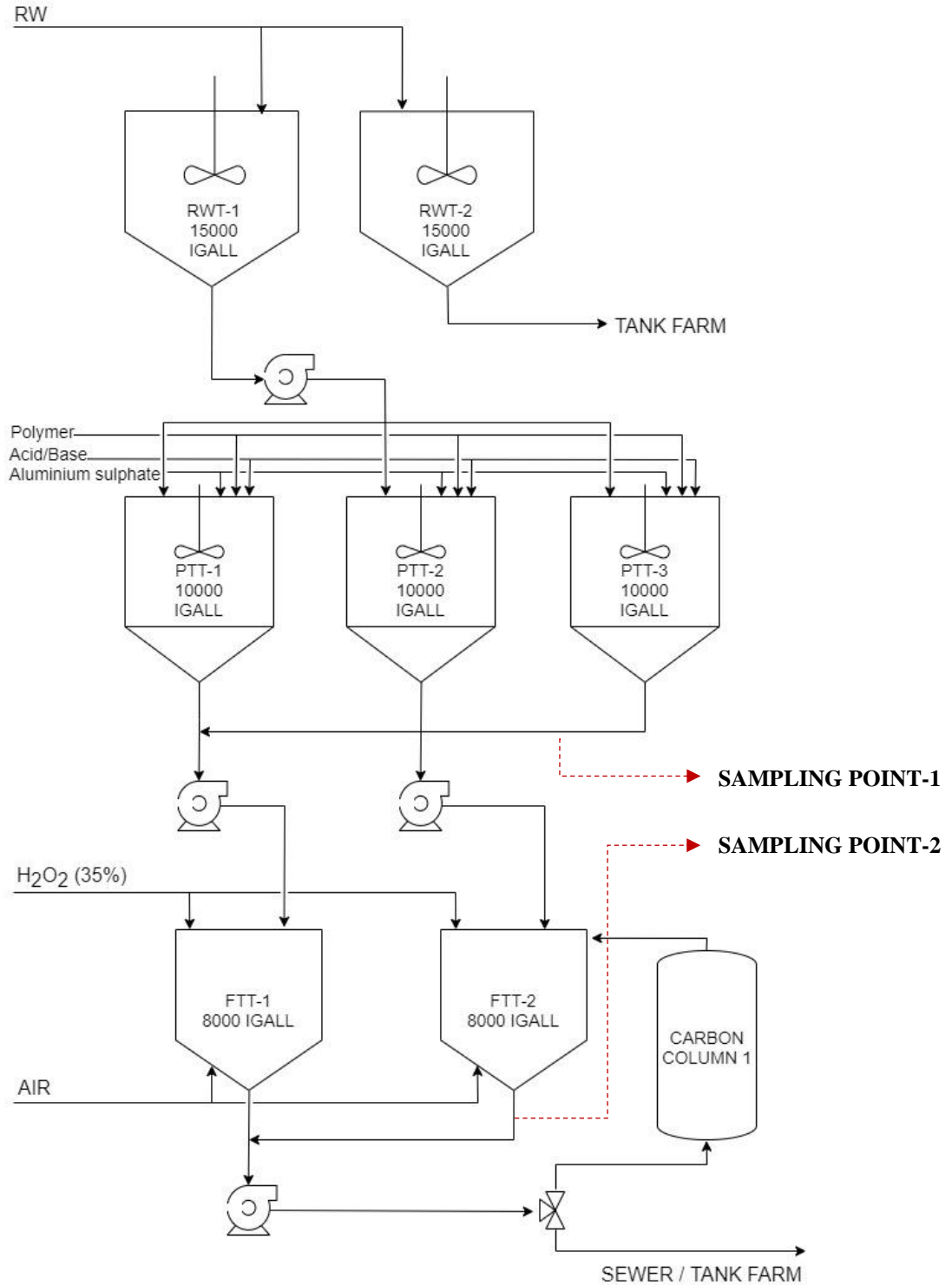


**Figure 2.** Treatment train of batch treatment processes at Aevitas and WW sampling points. RW is raw incoming wastewater, RWT are raw water tanks, PTT are primary treatment tanks for acid cracking and coagulation-flocculation and FTT denote finishing treatment tanks used for aeration and peroxide treatment

## **1.2 Wastewater treatment using Nanofiltration membranes**

### *1.2.1 Introduction – Understanding separation mechanisms*

A membrane is a physical barrier between phases which allows selective passage of some molecules through the membrane and hinders the passage of others. Usually a driving force is applied to the active side of a membrane pushing the fluid through the pores to the other side. The history of membrane filtration dates back to 1920s when the first microfiltration (MF) membranes were commercialized for use [1]. These membranes were made out of a polymer material called cellulose-acetate. Since then, the researchers have shown immense interest in developing membranes from different materials and technologies in order to improve membrane performance. The whole spectrum of membranes developed since 1920 can be divided into four major categories based on the average pore size of the membranes and the driving force required for their operation, (i) Microfiltration (MF), (ii) Ultrafiltration (UF), (iii) Nanofiltration (NF), and (iv) Reverse Osmosis (RO) [2, 3, 4, 5]. Average pore size and approx. molecular mass of compounds that can be typically separated using such membranes is shown in Figure 3 [6]. While separation in a RO membrane is believed to be through diffusion, convective separation and sieving effect is dominant in MF and UF membranes [7]. Properties of an NF membrane lie somewhere between UF and RO membranes and were first developed under the name of ‘hybrid membranes’ as a pre-treatment to RO membranes for desalination purpose [7].

NF membranes are characterized by low rejection of monovalent ions, high rejection of divalent ions and higher flux compared to RO membranes. They are also characterized based on the average pore radius offered by the selective top layer, usually in 0-5 nm range. These properties allow NF to be used in niche applications in many areas such as water and wastewater treatment, pharmaceutical and biotechnology and food engineering. Some commercial NF membranes

together with their properties and top-layer composition as specified by the manufacturer are given in Table 1.

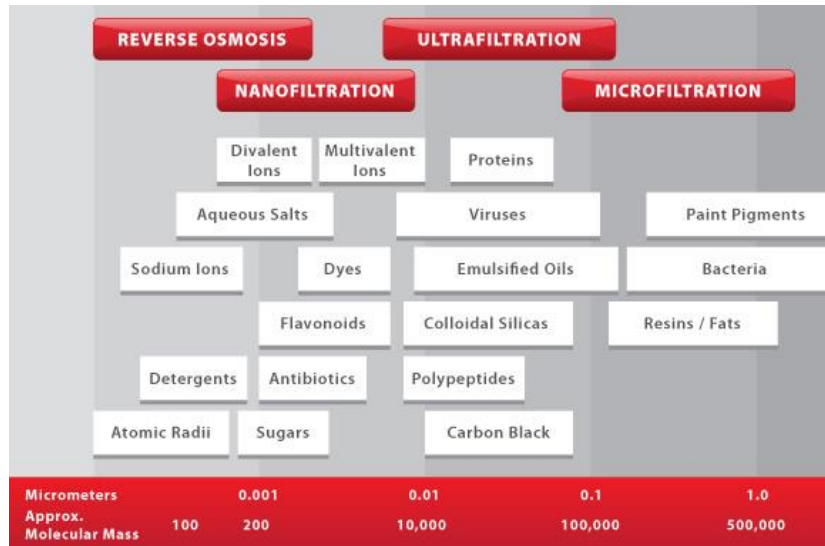


**Figure 3.** Separation range and examples of feed for 4 major classes of membrane filtration processes [6]

Membrane	Manufacturer	MWCO (Da)	Max Temperature	pH range	Stabilized salt rejection	Composition on top layer
NF270	Dow Filmtec	200-400	45	2-11	>97%	Polyamide TFC
NF200	Dow Filmtec	200-400	45	3-10	50-65% CaCl <sub>2</sub> 3% MgSO <sub>4</sub> 5% Altrazine	Polyamide TFC
NF90	Dow Filmtec	200-400	45	3-10	85-95% NaCl >97% CaCl <sub>2</sub>	Polyamide TFC
TS80	TriSep	150	45	2-11	99%	Polyamide
TS40	TriSep	200	50	3-10	99%	Polypiperazineamide
XN45	TriSep	500	45	2-11	95%	Polyamide
UTC20	Toray	180	35	3-10	60%	Polypiperazineamide
TR60	Toray	400	35	3-8	55%	Cross-linked polyamide composite
CK	GE Osmonics	2000	30	5-6.5	94% MgSO <sub>4</sub>	Cellulose acetate
DK	GE Osmonics	200	50	3-9	98% MgSO <sub>4</sub>	Polyamide
DL	GE Osmonics	150-300	90	1-11	96% MgSO <sub>4</sub>	Cross-linked polyamide composite
HL	GE Osmonics	150-300	50	3-9	98% MgSO <sub>4</sub>	Cross-linked polyamide composite

NFX	Synder	150-300	50	3-10.5	99% MgSO <sub>4</sub> 40% NaCl	Proprietary polyamide TFC
NFW	Synder	300-500	50	3-10.5	97% MgSO <sub>4</sub> 20% NaCl	Proprietary polyamide TFC
NFG	Synder	600-800	50	4-10	50% MgSO <sub>4</sub> 10% NaCl	Proprietary polyamide TFC
TFC SR100	Koch	200	50	4-10	>99%	Proprietary polyamide TFC
SR3D	Koch	200	50	4-10	>99%	Proprietary polyamide TFC
SPIRAPR O	Koch	200	50	3-10	99%	Proprietary polyamide TFC
ESNA1	Nitto-Denko	100-300	45	2-10	89%	Composite polyamide
NTR7450	Nitto-Denko	600-800	40	2-14	50%	Sulfonated polyethersulfone
Nano 1nm	Inopor	750	200	1-13	-	TiO <sub>2</sub>
Nano 0.9 nm	Inopor	450	200	1-13	-	TiO <sub>2</sub>
LC	Inopor	200	200	1-13	-	TiO <sub>2</sub>
Nanohelix	Cerahelix	700	70	2-10	-	TiO <sub>2</sub> /ZrO <sub>2</sub> mixed- oxide
Picohelix	Cerahelix	400	70	2-10	-	TiO <sub>2</sub> /ZrO <sub>2</sub> mixed- oxide

**Table 1.** Commercial nanofiltration membranes and specifications by manufacturers [5, 60, 61]

Rejection from NF membranes may be attributed to a combination of steric, Donnan, dielectric and transport effects. The transport of uncharged solutes is primarily through steric mechanism (size based exclusion) and has been studied and well established through numerous studies with UF membranes [8]. For charged membrane interfaces, charge is usually originated from the dissociation of ionizable groups at the membrane surface and from within the membrane pore structure [9, 10, 11]. The dissociation of these surface groups is strongly influenced by the pH of the contacting solution and where the membrane surface chemistry is amphoteric in nature, the membrane may exhibit an isoelectric point at a specific pH [12]. Electrostatic repulsion or attraction of ions present in a solution is based on the valence of ions and the fixed charge on the membrane surface that may vary depending on the local environment. Transport of solute is hindered and can be expressed in terms of both a convective and diffusive element which contributes to the overall transport effect. Lastly, the phenomena of dielectric exclusion is much less understood till date and

couple of theories have been put forward, however the role of dielectric exclusion in separation is still debated [13].

The most widely accepted model that captures all phenomena discussed above is based on the extended Nernst-Planck equation [14]. The equation contains classic expressions for steric and Donnan effects and a third term representing partitioning because of dielectric exclusion. A detailed description of the theory can be found here [15]. The models based on extended Nernst-Planck equation is an extension of the original Donnan-Steric-Pore-Model (DSPM) first proposed by Bowen et al. [16]. The DSPM model was followed by DSPM & DE model proposed by Yaroshchuk [17], and steric electric and dielectric model (SEDE) by Szymczyk and Fievet [18].

### *1.2.2 Conventional nanofiltration using polymer membranes*

#### *1.2.2.1 Synthesis and applications*

Polymeric/organic NF membranes have dominated the global market since 1980 due to their excellent performance and low cost [19]. Important polymers that are being used for making RO and NF membranes are polyamides, cellulose acetate, cellulose diacetate, cellulose triacetate, piperazine, etc. Thin film composite (TFC) membranes were invented in 1970s and were in wide use by the second half of 1980s. A TFC membrane consist of multiple layers of polymeric material supporting a thin top barrier layer having nano-sized pores. The support-layer is generally micro-porous to allow easy flow of permeate. Polyamide TFC membranes are particularly widely accepted due to outstanding performance and better free chlorine resistance than only-polyamide membranes. Figure 4 shows structure of a Polyamide TFC membrane with a support-layer and a carrier-layer.

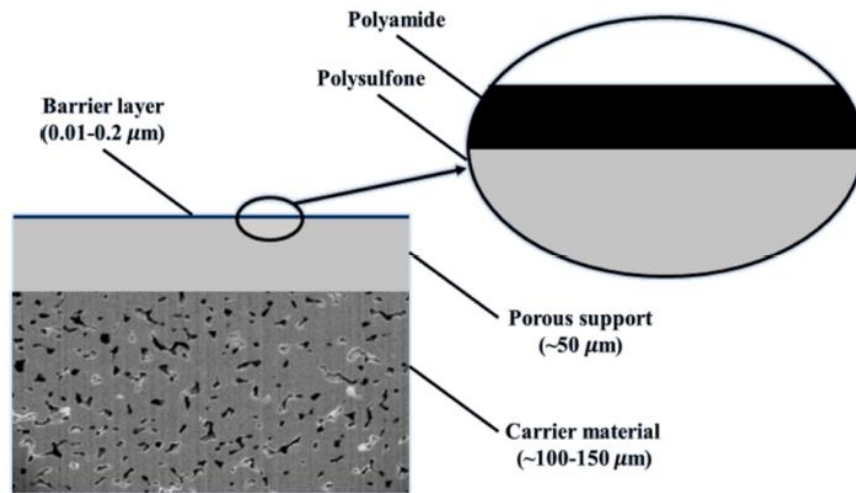


**Figure 4.** Thin film composite membrane structure taken from [19]

NF membranes are synthesized through methods such as Interfacial Polymerization (IP), nanoparticles incorporation (NPs) and grafting polymerization. Grafting polymerization focus more on methods like UV/photo-grafting, electron beam (EB) irradiation, plasma treatment and layer-by-layer (LbL) methods. An IP method typically involves phase inversion followed by interfacial polymerization to produce TFC membranes. Several types of monomers have been used in IP process such as bisphenol A (BPA), tannic acid, m-phenylenediamine (MPD), polyvinylamine reacting with trimesoyl chloride (TMC) or isophthaloyl chloride to form the thin active film layer. The choice and concentration of monomers affect membrane performance and its antifouling properties [20, 21, 22].

In the past, polymer NF membranes have been successfully used to remove >98% As from ground water containing around 190 mg/L of total suspended solids (TSS), 205 mg/L of total dissolved solids (TDS), 0.18 mg/L of As and 4.8 mg/L of iron at pH 7.2 [23]. Other environmental applications of NF include treatment of ground water polluted with pesticides and pesticide transformations products (PTPs) [24], softening of ground water [25], removal of fluoride from fluoride affected areas in ground water [26], removal of radioactive elements such as  $Ra^{2+}_{226,228}$ ,

uranium as uranyl cation  $\text{UO}_2^{2+}$ , or carbonate complexes  $\text{UO}_2(\text{CO}_3)_2^{2-}$ ,  $\text{Rn}_{222}$  from contaminated groundwater [27]. NF membranes have also applications in removal of natural organic matter (NOM) and disinfection by-products' (DBPs) from surface water [28]. Experimental studies with polymer NF membranes to remove pharmaceutically active compounds (PhACs) for drinking water treatment have also shown promise [29].

Application as a pre-treatment step for seawater and brackish water desalination was one of the first applications of polymer NF membranes. The integration of NF as a part of the pre-treatment process in the early 90s led to higher water production (around 60%) and resulted in about 30% cost reduction for RO and multistage flash distiller (MSF) plants [30]. Recently studies have even shown potential for dual-stage NF plants to replace the conventional RO based desalination [31]. Other emerging applications of NF membranes include organic solvent nanofiltration (OSN) employed in pharmaceutical and biotechnology industry for purifying APIs [32, 33]

Lastly, polymer NF has widespread application in wastewater treatment which is the topic of concern for our project. Polymer NF has found its use in conventional wastewater treatment plant, often in municipal wastewater treatment plants, for removal of pharmaceutical and personal care products (PPCPs) such as carbamazepine (CBZ), triclosan (TRI), ibuprofen (IBU), sulfadiazine (DIA), sulfamethoxazole (SMX) and sulfamethazine (SMZ) [34]. Treatment of dairy wastewater, produced wastewater, olive oil mill wastewater and textile wastewater are among other applications. Use of NF membranes in a membrane bio-reactor (NF MBR) is also one of the successful applications but will not be covered in this report. A detailed description and analysis of all wastewater applications is present in the following section.

### 1.2.2.2 Previous studies on IWW treatment

Previous IWW treatment studies with polymer NF are tabulated in Table 2. Previous work done in our lab on NF treatment of IWW wastewater used 6 NF membranes to find the best performance in terms of COD rejection [35]. Previous work also attempted to show the benefits of a combined NF and activated carbon (AC) process to treat the IWW sample. Most of the works are based on removal of low COD wastewater and hence only talk about basic chemical cleaning methods like acidic and caustic cleaning. Other works which have successfully attempted to treat high COD wastewaters have shown good performance in terms of ‘%COD rejection’ but have also reported high membrane fouling. We plan to test more robust and fouling resistant ceramic NF membranes to try and overcome this problem.

Wastewater source & type	Membranes used	Performance	Reference
<b>Produced wastewater</b> Type: Real (3 WW samples) TOC = 136.4 mg/L TDS = 2090 mg/L	NF90 (NF), NF270 (NF) and BW30 (RO).	TOC rejection NF90 = 34 % TDS rejection NF90 = 36% NF90 Flux at 5.5 bar TMP $\approx$ 7 LMH	[36]
<b>Whey effluents</b> Type: Synthetic (Model whey-salt solutions) Salts tested: NaCl, MgSO <sub>4</sub> , KCl, CaHPO <sub>4</sub>	2 commercial NF membranes (NF-90 & NF-45) and 4 lab manufactured membranes.	High flux ( $\approx$ 25 LMH at 6 bar) and selectivity were obtained by NF90. NF-45 and one lab-manufactured membrane were deemed appropriate for this application	[37]
<b>Car wash effluent</b> Type: Real (2 WW samples) COD = 738 mg/L TDS = 89.5 mg/L Turbidity = 68.9 NTU	PVDF100 (polyvinylidene difluoride). PES30 (Polyethersulfone). NF270 (Polyamide).	NF270 flux at 3 bar TMP = 53 LMH COD rejection = 91% TDS rejection = 61% Turbidity rejection = 94%	[38]
<b>Olive mill wastewater</b> Type: Real COD = 40,300 $\pm$ 1000 mg/L TS = 24.8 $\pm$ 0.5 g/L TSS = 6.8 $\pm$ 0.7 g/L Turbidity = 5,111 $\pm$ 478 NTU	NF: NP010 (Microdyn-Nadir), NP030 (Microdyn-Nadir), NF270. RO: XLE, BW30.	Pretreatment: Centrifugation & Ultrafiltration (56.1% COD removal) COD rejection NF270 = 79.2 % COD rejection XLE = 96.3% Flux at 10 bar for NF270 = 28.3 LMH	[39]

<b>Textile wastewater</b> Type: Real COD = 227-627 mg/L SS = 30-526 mg/L Turbidity = 31-85 NTU Salinity = 1.3 -3.1 g/L	NF: DK (MWCO = 200Da) MF: 0.1 µm pore size	Pretreatment: Coagulation and flocculation (CF), Microfiltration DK flux at 10 bar = 28 LMH COD rejection = 60% Color rejection = 100% Salinity rejection = 35%	[40]
<b>Distillery wastewater</b> Type: Real COD = 100,000 mg/L TDS = 51,500 mg/L	NF: Perma PPT-9908 (Polyamide TFC)	Pretreatment: Neutralization and cloth filtration COD rejection = 97.1 %	[41]
<b>Metal effluent</b> Type: Real COD = 165 mg/L	Self-made cellulose acetate NF	COD rejection = 78.9% Average flux = 47 LMH	[42]
<b>Food industry wastewater</b> Type: Real (2 WW samples) COD = 9500, 1160 mg/L TS = 0.25, 0.44 %w/w	NF200 polyamide membrane, SWHR30-80 RO membrane (Dow-Filmtec)	COD rejection NF200 = 92-96 % NF90 flux at 10 bar ≈ 30-35 LMH	[43]
<b>Landfill leachate</b> Type: Real COD = 4,137 ± 30 mg/L TDS = 15110 ± 100 mg/L Turbidity = 115 ± 5 NTU	SB90 (TriSep Cellulose Acetate) MWCO = 500-700 Da	Pretreatment: Coagulation-flocculation NF COD rejection = 90% NF flux at 8 bar = 15 LMH	[44]
<b>IWW from specialized treatment facility (Aevitas)</b> Type: Real COD = 4000 mg/L	NF90, NF270, NFX, NFW, TS80, XN45	Highest COD rejection achieved by NF90 = 63%	[35]

**Table 2.** Previous IWW treatment studies using polymer nanofiltration membranes.

### 1.2.3 Nanofiltration using inorganic membranes

#### 1.2.3.1 Synthesis and applications

Ceramic materials like alumina ( $\gamma\text{-Al}_2\text{O}_3$ ,  $\alpha\text{-Al}_2\text{O}_3$ ), zirconia ( $\text{ZrO}_2$ ), titania ( $\text{TiO}_2$ ), glass ( $\text{SiO}_2$ ) and silicon carbide ( $\text{SiC}$ ) are common inorganic materials used in ceramic MF, UF and NF

membranes [45]. Structure of asymmetric ceramic NF membranes is similar to polymer NF membranes seen before, a thin skin layer on top of a porous sub layer. The top and porous layer can be made of the same or different materials and the corresponding membranes are called ‘integral asymmetric membranes’ and ‘composite membranes’, respectively. Membranes can be fabricated in different configurations such as flatsheet, cylindrical or hollow-fibre. The porous support layer is prepared by shaping a slurry, a suspension of ceramic powders and some additives for controlling the viscosity and drying behavior of the slurry. Shaping is usually performed via classical methods like molding or extrusion. The shaped bodies are heat treated after drying. Intermediate and top layers can be either made via slurry-coating on the support with finer ceramic powders, sol-gel method, dip or spin coating or chemical vapor deposition (CVD). The common sol-gel route contain the formation of polymeric or colloidal particulates in the liquid media (i.e. the formation of sol), establishment of a network among these particulates (i.e. gel formation), drying of the gel followed by heat treatment [46].

First ceramic NF membrane was reportedly manufactured in 2000 [47] with earliest application in treating colored wastewater from textile finishing for recycling [48]. Ceramic MF/UF/NF are also used in drinking water production [49]. Although this market has been and is still currently dominated by polymeric membranes, incorporation of ceramic membranes have been increasing because of their hydrophilic nature and less organic fouling [50]. Other applications include municipal wastewater treatment using ceramic MBR, produced water treatment and food and beverage production. In fact, produced wastewater studies have shown that ceramic MF/UF membranes performed better than polymeric membranes [51]. Similarly, multiple food and beverage applications have reported superior long-term performance over polymeric membranes [52].

1.2.3.2 Previous studies on IWW treatment

Previous IWW treatment studies with ceramic NF are tabulated in Table 3. Multiple studies were found for textile wastewater treatment and in pulp and paper mill effluent, however only one from each is reported here. Since ceramic nanofiltration is relatively new with applications emerging only in the last decade, not many industrial wastewater treatment studies could be found in literature. Our work will try to fill this gap in addressing industrial wastewater treatment with TiO<sub>2</sub> based ceramic NF membrane with the lowest MWCO ever reported for a ceramic NF membrane.

Wastewater source & type	Membranes used	Performance	Reference
<b>PhACs polluted WW</b> Type: Synthetic (mixture of 10 PhACs) Conc. of each PhAC = 10 mg/L	M-SiO <sub>2</sub> , M-TiO <sub>2</sub> , LC1, LC2 (Inopor GmbH)	Best overall rejection by LC2 = 45-100 % with 3 PhACs removed >90%	[53]
<b>Municipal sewage</b> Type: Real COD = 348 - 700 mg/L	Tight-UF (3kDa) from TAMI industry, NF (450 Da) from Inopor GmbH	COD rejection = 80 % by all membranes Flux at 8 bar by 450-Da ≈ 20 LMH	[54]
<b>Textile effluent</b> Type: Real COD = 960-2525 mg/L Turbidity = 35.84-83.34 NTU Conductivity = 2450-7780 μS/cm	Multichannel tubular TiO <sub>2</sub> -ZrO <sub>2</sub> UF ceramic Membrane (MWCO: 30, 50, 150 kDa)	COD rejection = 62-79%. Color rejection = 62-79%. Turbidity rejection > 99%. Flux = 90–160 LMH depending on CFV and MWCOs.	[55]
<b>Pulp and paper mill effluent</b> (Untreated Kraft black liquor) TDS (g/L): 183 ± 2.7 Total hemicelluloses (g/L): 3.56 ± 0.12 Total lignin (g/L): 63.8 ± 1.3	TiO <sub>2</sub> Ceramic NF (MWCO 1000 Da)	Retention of lignin and hemicelluloses: 80%. Avg. flux = 159 LMH	[56]

**Table 3.** Previous IWW treatment studies using ceramic nanofiltration membranes.

### 1.3 Objectives

The objective of this study is to investigate low MWCO (200, 450, 750 Da) TiO<sub>2</sub> ceramic NF membranes as an intermediate treatment step in the treatment train at a facility such as Aevitas. Multiple coagulation-flocculation pretreated wastewater samples will be tested on these membranes to develop a process that could treat most of the IWW below 600 mg/L COD or with a significant COD rejection. Membrane performance evaluation metrics will also include permeate flux testing and membrane area calculations, extent of membrane fouling and chemical cleaning. Additionally, 3 polymer NF membranes will also be tested for comparison purposes. Experimental results will be used to select the best membranes for treatment and as a reference for further pilot-scale testing of some of the membranes.

Since the composition and bulk properties of feed wastewater are time-varying (different from batch-to-batch), membrane performance is expected to have large variations from batch to batch and such variations have been observed previously while working with IWW samples from Aevitas. Therefore, predictive models for COD rejection and flux are needed to avoid time consuming bench-scale testing for every new batch. Bulk wastewater properties along with GC-MS composition analysis technique developed during previous work in our group [35] will be used to build data-driven models for all membranes and investigate the usefulness of such models in treatment of time-varying IWW.

## **CHAPTER-2: Materials and Methods**

### **2.1 Industrial wastewater samples**

#### *2.1.1 Sample collection and storage*

Industrial wastewater samples were collected from Aevitas at two points along their treatment train. These are shown in the flowchart in Figure 2. Based on previous results and literature, these points in the treatment train were most suitable for a nanofiltration unit to be placed. The organic concentration post-PTT and post-FTT treatment are frequently higher than the new discharge targets but low enough to be treated by a NF unit. Since wastewater streams with higher organic concentration tend to foul membranes faster, treating pretreated streams (post-PTT and post-FTT) having lower concentration of organics will also reduce membrane fouling.

6 wastewater samples (WW-A to WW-F) were collected at least one month apart from the facility. Samples were stored in 5-gallon pails secured with lids in a fridge (4 °C) at all times. Pictures of all 6 wastewater samples as received from the plant is shown in Figure 5. Sludge/flocs can be seen settled at the bottom of glass jars for few samples. First, these unwanted particles were separated from each of the wastewater samples by mixing the contents of a pail using a mechanical mixer and then allowing the flocs/sludge to rise/settle for 15 minutes before decanting the clear wastewater portion in a clean pail. These wastewater samples were then used for all characterization and experimentation purposes.

#### *2.1.2 Wastewater characterization*

All wastewater samples were first characterized for bulk properties, namely, Chemical oxygen demand (COD), Soluble chemical oxygen demand (sCOD), pH, Conductivity, Turbidity and Total organic carbon (TOC). COD is an indirect way of measuring the amount of organics and any other oxidizable molecules/ions present in an effluent which might possibly deplete dissolved

oxygen (DO) levels in local water bodies if the effluent is discharged there. sCOD represents the amount of total COD that is present in soluble form. Significant differences in COD and sCOD confirms the presence of undissolved microparticles which are contributing to total COD. Table 4 summarizes the values from bulk wastewater characterization of all 6 wastewaters (A to F). Each bulk property was measured for duplicate samples from the same pail to get an average and error value. WW-B, D & F had relatively low COD ( $< 1000$  mg/L) as compared to WW-A, C & E. WW-E had the highest COD of 10,425 mg/L among all 6 IWW samples. WW-E also had the highest conductivity among all wastewaters (7480  $\mu$ S/cm). Even though WW-E had very high COD, the wastewater was clear with yellowish tint and low turbidity (50.6 NTU) indicating completely dissolved organics. WW-A and C had intermediate COD in the range 3000-5000 mg/L with high turbidity (812 and 503 NTU respectively) indicating presence of solid particulates as well. A significant difference in sCOD and COD for WW-A and C confirms the above hypothesis.

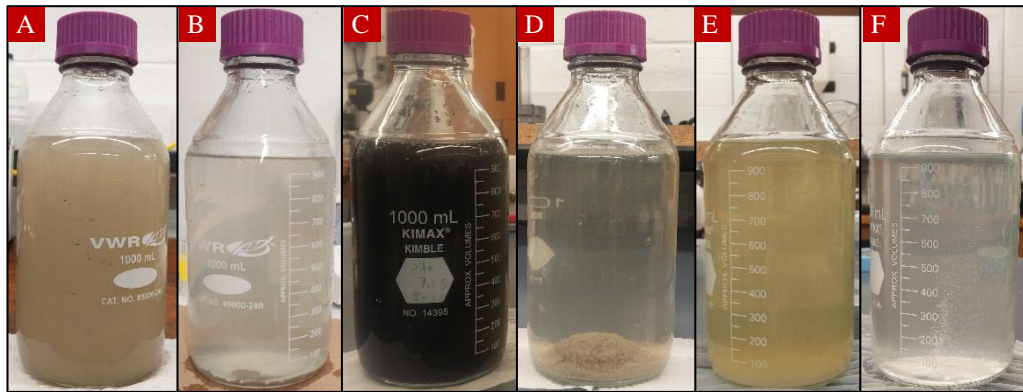


**Figure 5.** Pictures of 6 IWW samples collected from Aevitas. A unique identifier of each WW is mentioned on the top left corner of each panel. Bulk properties of all samples are tabulated in Table 4.

	BULK PROPERTY				
WW	COD (mg/L)	Soluble COD (mg/L)	pH	Conductivity ( $\mu$ S/cm)	Turbidity (NTU)
A	4158 $\pm$ 54	-	7.05 $\pm$ 0.04	4865 $\pm$ 4	812 $\pm$ 33
B	804 $\pm$ 18	-	7.6 $\pm$ 0.2	2532 $\pm$ 5	-
C	3270 $\pm$ 54	3035 $\pm$ 35	6.42 $\pm$ 0.3	6872 $\pm$ 14	503 $\pm$ 12
D	728 $\pm$ 4	654 $\pm$ 28	7.86 $\pm$ 0.004	-	-
E	10425 $\pm$ 125	9940 $\pm$ 20	9.01 $\pm$ 0.07	7480 $\pm$ 120	50.6 $\pm$ 4.1
F	1114 $\pm$ 26	-	9.67 $\pm$ 0.15	3850 $\pm$ 100	16.2 $\pm$ 0.1

**Table 4.** Bulk property characterization of all wastewater samples shown in Figure 5. Two aliquots of each sample were used to calculate the average and error values shown in the table.

In order to analyze the organics composition in each of the wastewaters, a Gas chromatography-Mass spectroscopy (GC-MS) technique was used to separate compound peaks on a GC-MS spectrum and individual peaks were identified using standard NIST (National Institute of Standards and Technology) library of compounds software. A brief summary of GC-MS characterization results for all wastewaters is shown in Table 5. Components identified were majorly long chain ( $C_4$ - $C_{20}$ ) carboxylic acids, alcohols, aromatics, and some nitrogenous compounds. Multiple compounds occurred in more than one sample, for e.g. Benzoic acid was detected in 5 out of 6 IWW samples. Other compounds like ethylene glycol butyl ether, hexadecanoic acid (palmitic acid), decanedioic acid and dodecanedioic acid were detected in 4 IWW samples. Please note that relative concentration of compounds present in each wastewater is not shown in Table 5. For a comprehensive outlook, complete GC-MS dataset for each wastewater is present in Appendix Tables A3-8.

S.No	RT (min)	Compound	Wastewater						Frequency
			A	B	C	D	E	F	
1	8.9	Benzoic acid	✓	✓	✓	✓	✗	✓	5
2	17.3	Decanedioic acid	✗	✓	✓	✓	✗	✓	4
3	18.3	Hexadecanoic acid	✗	✓	✗	✓	✓	✓	4
4	19.4	Dodecanedioic acid	✗	✓	✓	✓	✗	✓	4
5	5	Ethylene glycol butyl ether	✓	✗	✓	✓	✗	✓	4
6	6.9	Nonanoic acid	✗	✓	✓	✓	✗	✗	3
7	18.4	1,11-Undecanedioic acid	✗	✓	✓	✗	✗	✓	3
8	6.2	2-Ethyl hexanoic acid	✗	✓	✗	✓	✗	✓	3
9	3.9	Propan-1,2-diol	✗	✓	✓	✗	✗	✓	3
10	4.8	Octanol	✗	✓	✓	✓	✗	✗	3
11	4	Pentanoic acid	✗	✓	✓	✗	✗	✓	3
12	7	Benzyl alcohol	✗	✗	✓	✓	✗	✓	3
13	9.7	Diethylene glycol butyl ether	✓	✗	✗	✓	✗	✗	2
14	10.6	o-Methyl benzoic acid	✗	✗	✓	✓	✗	✗	2
15	20.5	Octadecanoic acid	✗	✓	✗	✗	✗	✓	2
16	4.1	Cyclohexanol	✗	✓	✗	✗	✗	✓	2
17	7.9	Octanoic acid	✗	✓	✓	✗	✗	✗	2
18	10.8	2-Phenoxy ethanol	✗	✓	✗	✓	✗	✗	2
19	5.4	Phenol	✗	✓	✗	✗	✗	✓	2
20	10	Benzeneacetic acid	✗	✓	✗	✗	✗	✓	2
21	5.1	Hexanoic acid	✗	✗	✓	✗	✗	✓	2
22	16.1	Nonanedioic acid	✗	✗	✓	✗	✗	✓	2
23	6.5	Heptanoic acid	✗	✗	✓	✗	✗	✗	1
24	9.5	Pentanedioic acid	✗	✗	✓	✗	✗	✗	1
25	10.5	6-Hydroxyhexanoic acid	✗	✗	✓	✗	✗	✗	1
26	8.8	1,1,1-Tris(hydroxy methyl) propane	✗	✗	✓	✗	✗	✗	1
27	7.5	1-Methyl pyrrolidinone	✗	✗	✓	✗	✗	✗	1
28	6	Benzonitrile	✗	✗	✓	✗	✗	✗	1
29	3.9	Styrene	✗	✗	✗	✗	✓	✗	1
30	6.1	2-Butanol	✗	✗	✗	✗	✓	✗	1
31	8.1	2-Phenyl ethanol	✗	✗	✗	✗	✓	✗	1
32	8.6	N,N-Dibutylethanolamine	✗	✓	✗	✗	✗	✗	1
33	24.1	Dehydroabietic acid	✗	✓	✗	✗	✗	✗	1
34	22.2	Ricinoleic acid	✗	✓	✗	✗	✗	✗	1
35	7.3	Nonanol	✗	✓	✗	✗	✗	✗	1
36	20.5	Oleic acid	✗	✓	✗	✗	✗	✗	1
37	4.9	Lactic acid	✗	✓	✗	✗	✗	✗	1
38	4.9	Heptan-2-ol	✗	✓	✗	✗	✗	✗	1
39	10.6	2-Methyl benzoic acid	✗	✗	✗	✗	✗	✓	1
40	4.8	2-Ethyl hexanol	✗	✗	✗	✗	✗	✓	1
41	12.7	Salicylic acid	✗	✗	✗	✗	✗	✓	1

**Table 5.** GC-MS characterization of all wastewater samples shown in Figure 5. Compounds present in a wastewater samples are denoted by tick marks and highlighted in green. Compounds are sorted based on frequency of occurrence (out of 6 samples) of a compound shown in the last column. Note that RT stands for ‘retention time’ of a peak/compound

## 2.2 Ceramic NF membranes

Ceramic NF membranes are manufactured by only a handful of companies around the world. Among all the companies that manufacture TiO<sub>2</sub> based ceramic NF membranes, Inopor offered a membrane with the least reported MWCO (200 Da). Due to the challenging separation of dissolved components required for our purpose this membrane was selected for testing along with 3 other membranes from the same manufacturer. These 4 membranes spanned the MWCO from 200 Da to 8500 Da. Membranes were ordered in a single channel tubular format along with a custom-made stainless-steel testing module. Table 6 summarizes the membrane nomenclature and properties along with the reported MWCO for each membrane. Figure 6 shows the tubular membranes and the testing module.

### 2.2.1 Pre-treatment and storage

Ceramic membranes were supplied dry from the manufacturers. A pre-treatment step using a mild-caustic or a caustic chemical cleaner was recommended by the manufacturers before use. Each membrane was pre-treated by circulating a 1% (w/w) solution of Tergazyme, a commercially available caustic enzymatic cleaner for membranes. The solution was circulated for 30 mins at 100 psi with both concentrate and permeate recycle back to the feed tank. Membranes were then flushed with clean water at 100 psi for at least 15 minutes and then stored in DI water as shown in Figure 6. Also, refer to Table 7 in Section 2.5 which summarizes detailed operating conditions for different modes of operation of the system including the ‘ceramic pre-treatment’ mode.



**Figure 6.** Pictures of single channel tubular ceramic membranes stored in DI water. Note that a total of 6 ceramic membranes are shown in the picture but only 4 of them were used for wastewater filtration studies in this report. Panel on the right shows the hollow feed channel inside the tubular membrane which contains the membrane active surface. Each membrane was 25 cm in length with an active membrane area of 55 cm<sup>2</sup>

	Ceramic				Polymeric		
ID	8500-Da	750-Da	450-Da	200-Da	NF90	NFX	NFS
Supplier	Inopor GmbH				Dow Filmtec	Synder Filtration	
Material	Active: TiO <sub>2</sub> , Support: αAl <sub>2</sub> O <sub>3</sub>				Proprietary Polyamide TFC		
MWCO	8500 Da	750 Da	450 Da	200 Da	~200-400Da	~150-300Da	~100-250Da
Average Pore Size	5 nm	1 nm	0.9 nm	-	-	-	-
Average salt rejection (NaCl)	-	-	-	-	98 %	40 %	50 %
Average salt rejection (MgSO <sub>4</sub> )	-	-	-	-	97%	99%	99.5%
Porosity	30-55 %	30-40 %			-	-	-
Zeta-potential	-	-	-16 mV	-	- 46 mV	-	-
Surface nature	Hydrophilic				Hydrophobic		
Cost	400- 600 USD / m <sup>2</sup>				100 - 140 USD / m <sup>2</sup>		

**Table 6.** Membrane nomenclature and properties as reported by the manufacturers and present in literature. MWCO stands for molecular weight cut off which refers to the lowest molecular weight solute in which 90 % of the solute is retained by the membrane. MWCO is usually measured using a mixture of Polyethylene glycols (PEGs). Zeta-potential values reported here were measured at pH 8 using 0.01 M NaCl solution [62, 63]

2.2.2 Pristine membrane performance testing

Clean water permeability (CWP) of a membrane is defined by the slope of line between membrane flux and applied trans-membrane pressure (TMP) when driving clean water through the membrane as per Equation 1. CWP of a membrane is a good indicator of membrane performance and hence it is used as a metric in this study to monitor changes in membrane performance. A baseline CWP of all the pristine membranes was measured twice before any wastewater tests. Results from this are shown below in Figure 7. A complete step-by-step procedure followed to obtain CWP of ceramic membranes is detailed in Section 2.5.1.

$$J = k\Delta P \tag{1}$$

where  $J$  is permeate flux (LMH),  $\Delta P$  is Trans-membrane pressure (bar) and  $k$  is Permeability (LMH/bar).

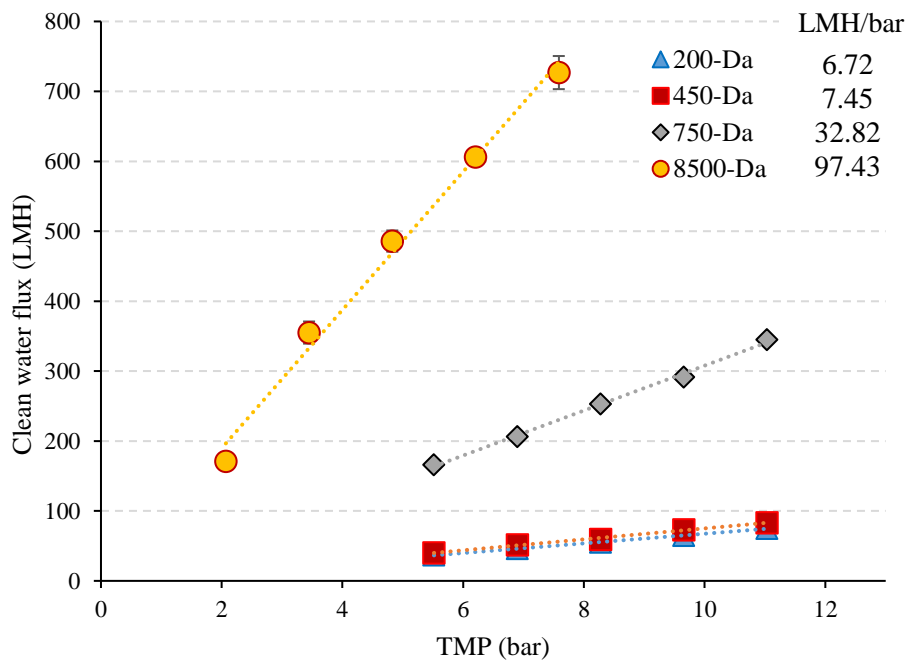
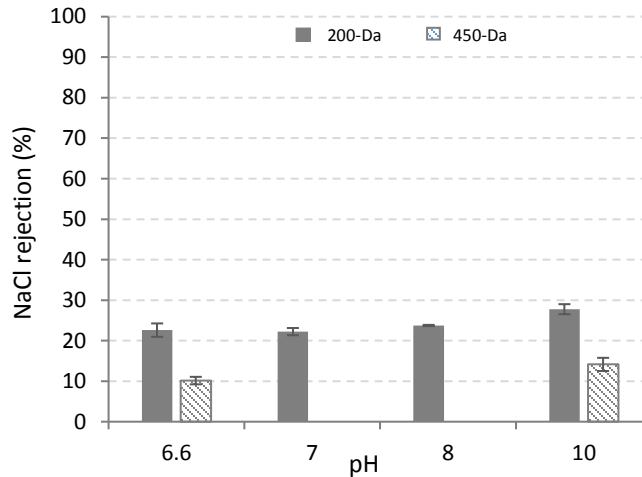


Figure 7. Pristine ceramic membranes CWP plot. Permeability values in LMH/bar are shown in legend

Salt rejection of 200-Da and 450-Da membranes were measured using 2000 ppm NaCl solutions at different pH values. Salt rejections were found to be low (10-30 %) for these membranes due to their low surface charge which is also shown by their low zeta-potential values as compared to polymeric membranes.



**Figure 8.** Salt rejection (NaCl) for pristine ceramic membranes. Error bars are calculated using triplicate conductivity measurements

### 2.3 Polymer NF membranes

3 polymer NF membranes (NF90, NFX, NFS) were chosen for comparison with ceramic NF membranes. These membranes were selected based on previous results from our group [35] where these 3 membranes were observed to achieve a good overall filtration performance. Membranes were ordered dry in flat-sheet roll format and later cut into appropriate shape to fit inside the flat-sheet testing module. Figure 9 shows one such cutout of a flat-sheet membrane and the testing module. Membrane properties as reported by the manufacturers are summarized in Table 6.

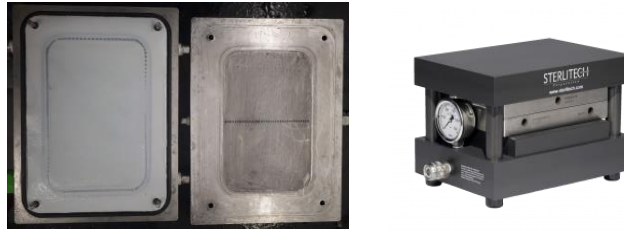


**Figure 9.** Pictures of the flatsheet polymer membrane testing module (right panel) with a membrane cutout placed inside (left panel)

### *2.3.1 Pre-treatment and storage*

Dry membranes are cutout into flat-sheet templates and soaked in 1% solution of Sodium metabisulfite (SMBS) in tap water in plastic bottles. Separate bottles were used to store new cutouts from each of the 3 membranes (NF90, NFX & NFS) to reduce any cross contamination. All cutouts were soaked for a period of at least 24 hour before use so that the membrane is wetted completely. Unused dry membrane rolls were stored in fridge at 4 °C to prevent the membrane from drying as recommended by the manufacturers. Membranes in use were stored in separate containers soaked in 1% SMBS in tap water.

### *2.3.2 Pristine membrane performance testing*

Clean water permeability and salt rejection of monovalent (NaCl) and divalent ( $\text{MgSO}_4$ ) salts were measured for each new cutout of the membrane to serve as a baseline performance metric. Complete step-by-step procedure of measuring the salt rejection of a membrane is present in Section 2.5.3. CWP and salt rejection values of all membrane cutouts used in wastewater filtration experiments are reported in Figure 21 & 22 in Section 4.1.2.

## **2.4 Experimental Setup**

A laboratory scale experimental system as shown in Figure 10 was used for all the high-pressure filtration experiments in this study. The system consists of two HDPE tanks, a Feed tank

and a Clean-in-place (CIP) tank, with a capacity of 20 L and 10 L respectively. Both the tanks are fully equipped to be connected to a chiller/heater using a heat transfer coil present in each tank. A diaphragm pump (Hydra-cell, Wanner Engineering Inc.) is used to send liquid through either of these two tanks towards the membrane module using a three-way valve. This line connecting the pump outlet to module inlet is called the 'feed line'. The feed line consists of a feed rotameter, a feed pressure gauge and a needle valve called feed control valve. The feed line also consists of a relief line and a feed bypass line connecting back to the feed tank. The pressure relief valve on the relief line prevents excessive high pressures in the system and prevents damage to the pump and other system components. The bypass valve is used to open the bypass line which then recirculates the liquid in the feed tank and aids in mixing large amounts of liquids before it can be sent to the membrane module.

The membrane modules used in this study use cross-flow filtration to separate the product, also called 'permeate', from the feed. A high-pressure feed runs tangentially over the active area of a membrane inside the membrane module. The high pressure drives the product/permeate liquid through the membrane pores to the other side of the membrane. The remaining feed liquid recirculated back to the feed tank is called the 'concentrate'.

Similar to the feed line, concentrate line also consist of a concentrate flow-meter, concentrate pressure gauge and a manual concentrate control valve (needle valve). High pressure in the system is achieved by throttling the concentrate needle valve and achieving the required operating pressure. The permeate outlet from the module is connected to a pressure gauge followed by a sampling outlet. Permeate flow-rate is measured manually using the sampling outlet on the permeate line and a stopwatch. Concentrate is recycled back into the feed or CIP tank using a three-way valve as shown. A flexible plastic line is used to recycle permeate back into the feed or the CIP tank by simply attaching it to the required tank.

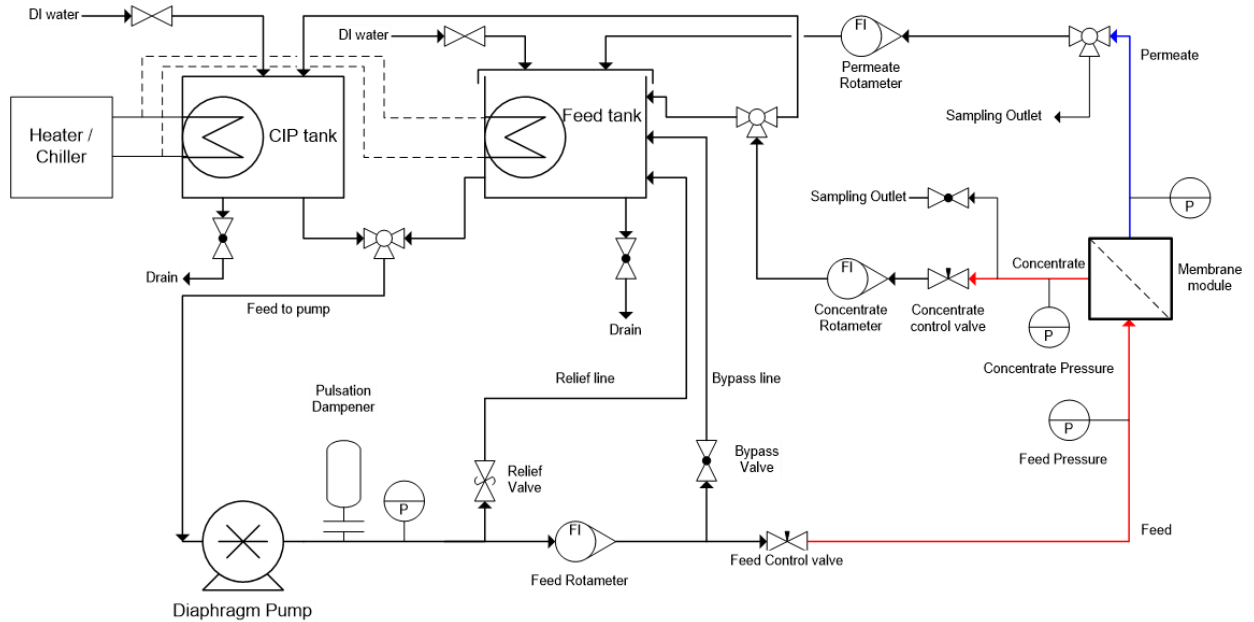


**Figure 10.** Schematic of the experimental setup is shown with membrane module in place. Both ceramic and polymer testing modules can be easily detached from the system using push-to-connect adapters for easy replacement



**Figure 11.** Pictures of the ceramic membrane testing module. Top panel shows the module with ends detached and o-rings placed on the side. Bottom panel shows the module attached to the setup and in operation. Note that the membrane had two permeate outlets (top panel) one of which was blocked (bottom panel) to redirect all permeate from only one outlet.

#### *2.4.1 Ceramic membrane testing module*

A picture of the tubular ceramic membrane testing module is shown in Figure 11. The module consists of a stainless steel framework with detachable ends. The module was fitted with 3 push-to-connect adaptors, one each for the feed, permeate and the concentrate lines. The membrane is kept in the central portion of the module after detaching the ends. One o-ring is placed almost halfway on the glass ends of the membrane on each side carefully. The o-ring separates the feed and the permeate sides of the liquid and prevents any unwanted mixing. The feed is run down the axis of the module where it passes through the inside of the tubular region which is the active side of the membrane. Permeate is collected in the outer annular region of the module. The cross-flow velocity (CFV) through the module with a ceramic membrane in place which had an internal diameter of 7 mm and a constant feed flowrate of 2 L/min (Pump frequency = 16 Hz) was 0.86 m/s.

#### *2.4.2 Polymer membrane testing module*

The polymer membrane testing module (SEPA cell) was previously shown in Figure 9. The SEPA cell consist of two stainless steel portions, one feed spacer (65 mil, where 1 mil = 25.4  $\mu\text{m}$ ), one permeate spacer (17 mil), two o-rings one each for preventing leaks outside the module and preventing mixing of the feed and permeate streams. The module is pressurized using a hydraulic press to seal the two portions together after placing the cutout membrane on the feed portion facing down exposing the active surface of the membrane to the feed side of the SEPA cell. Sepa cell has a slot depth of 0.19 cm, but the actual cross sectional area for feed flow is les due to the thickness of feed spacer. CFV through the module with a feed flow of 1.8 L/min (Pump frequency = 14 Hz) was found by dividing the feed flowrate to the available cross section area  $9.7 \times (0.19 - 65 \times 0.00254) \text{ cm}^2$ , resulting in a CFV of 1.23 m/s.

## 2.5 Filtration tests and Procedures

A summary of the operating conditions during various filtration tests is provided in Table 7. Following subsections elaborate step-by-step procedures taken to complete various filtration tests.

### 2.5.1 Clean water permeability test

Following steps were performed each time to measure CWP of a ceramic membrane. Note that changes in the procedure for a polymeric membrane are highlighted within parenthesis. Firstly, the system is flushed using DI water to prevent any unwanted membrane fouling. Feed tank is then filled with 10 litres of fresh DI water (tap water for polymeric). Chiller is then turned on and set to a temperature of 20 °C and pump is set to a frequency of 16 Hz (14 Hz for polymeric). Feed valve remains closed and bypass valve remains open at this time. Permeate and concentrate valves are checked at this time to ensure they are open and recycling back to the feed tank. Flow is then turned on followed by slowly opening the feed valve to prevent any shock to the membrane after which the bypass valve is closed directing all the feed towards the membrane. Concentrate valve is slowly closed to achieve 120 psi feed pressure. For all practical purposes TMP is assumed to be equal to the feed pressure due to negligible pressure on the permeate side. The system is then allowed to reach a steady state for at least 2 minutes before the permeate sampling valve is opened to record flow-rate. Triplicate flow measurements are taken manually by collecting permeate in a measuring cylinder. Previous steps are repeated for 6 different feed pressures in the range 80-160 psi in the following order: 120,160,100,120,80 psi (for polymeric membranes feed pressures in the range 50-150 psi are used in the order: 90,130,70,110,50,150 psi). All flow-rate readings are used to calculate flux by dividing by membrane area of 55 cm<sup>2</sup> (140 cm<sup>2</sup> for polymeric). A linear regression between

permeate flux (LMH) and TMP (bar) then gives CWP in LMH/bar along with a corresponding confidence interval.

### *2.5.2 Industrial wastewater filtration*

Following steps were performed each time to test the filtration performance of a membrane on industrial wastewater. WW sample is thoroughly mixed and transferred into the feed tank. Chiller is turned on and set to a temperature of 20 °C, pump is set to a frequency of 16 Hz (14 Hz for polymeric). WW is circulated through the pump using the bypass line for a few minutes before sending it towards the membrane. Once the feed valve is open and bypass valve is closed, concentrate needle valve is closed slowly to reach the operating pressure (100/120 psi). A timer is started when the feed pressure first reaches the operating pressure. Feed pressure is continuously monitored throughout the experiment and controlled manually. Permeate flow-rate is measured every 5 minutes for the first 10 minutes, every 10 minutes till 40 minutes and every 20 minutes after that until the end of the experiment (120/180 minutes). Two aliquots of feed and permeate samples are collected at  $t=10, 60, 120$  min during the experiment for COD measurement. One feed sample (100 ml,  $t = 0$  min) and one permeate composite sample (100ml,  $t = 60$  min) are also collected for WW composition analysis using GC-MS. System is flushed twice (15 min each) after each WW filtration test, first using a solution of Sodium dodecyl sulfate (SDS) in tap water and then using tap water to flush the residual SDS from the system.

### *2.5.3 Salt rejection testing*

Following steps were taken to measure the salt rejection of a polymer membrane. A 4 litre stock each for NaCl and MgSO<sub>4</sub> was prepared before each salt rejection experiment. Each solution had 1000 ppm salt concentration. One stock was fed to into the feed tank at a time. The system was operated in full recycle similar to the WW filtration and CWP tests at a constant pressure of

100 psi for 30 minutes. Conductivity of feed and permeate samples was measured in triplicates every 10 minute and % salt rejection was calculated using Equation 2. Steady state values are then reported as % salt rejection.

$$\% \text{ salt rejection} = \frac{(\text{Feed conductivity} - \text{Permeate conductivity})}{(\text{Feed conductivity})} \times 100 \quad (2)$$

#### *2.5.4 Chemical cleaning*

Following procedure was implemented each time to clean ceramic membranes using a chemical cleaning solution. A 4 litre cleaning solution containing 10 g/L (1 % w/w) Tergazyme in DI water was freshly prepared for each membrane. The solution was then transferred to the CIP tank and heated to a temperature of 40 °C (set temperature = 55 °C). Temperature of the cleaning solution was monitored using a temperature probe and always maintained within 40 ± 5 °C. The solution was then circulated through the membrane at 100 psi feed pressure for at least 30 minutes. The cleaning solution was then drained into a pail and the membrane was flushed with DI water for at least 15 minutes to remove any residual cleaning solution.

Filtration test	Experiment Conditions				
	Feed	Feed Pressure (psi)	Feed Temperature (°C)	Pump frequency (Hz)	Duration (min)
<b>Clean water permeability (CWP)</b>	Ceramic: DI Water Polymer: Tap Water	Ceramic: 80-160 Polymer: 50-150	20	Ceramic: 16 Polymeric: 14	-
<b>Salt rejection</b>	1000 ppm salt solution (NaCl/MgSO <sub>4</sub> )	100	20	14	30
<b>WW filtration</b>	Industrial Wastewater	100/120	20	Ceramic: 16 Polymeric: 14	180
<b>Chemical cleaning (Aggressive)</b>	1% w/w Tergazyme solution in DI water	100	40	16	60
<b>Chemical cleaning (mild) Condition A</b>	1% w/w Tergazyme solution in DI water	100	40	16	30
<b>Chemical cleaning (mild) Condition B</b>	1% w/w Tergazyme solution in DI water	100	20	16	30
<b>Chemical cleaning (mild) Condition C</b>	DI water	100	40	16	30
<b>Ceramic pre-treatment</b>	1% w/w Tergazyme solution in DI water	100	20	16	30

**Table 7.** Summary of experimental conditions during various filtration tests. Note that a pump frequency of 16 Hz corresponds to a feed flow of 2 L/min through the system and a cross-flow velocity of 1 m/s through the ceramic tubular membrane.

## **2.6 Chronology of filtration tests**

### *2.6.1 Ceramic nanofiltration*

A full cycle of tests performed while testing one wastewater sample using one ceramic membrane is shown below

- Pristine membrane CWP test (\*\*only required for first WW tested)
- WW filtration test
- Post-WW CWP test
- Chemical cleaning (mild) (\*\*only performed for some experiments)
- Post mild cleaning CWP test (\*\*only required after a mild cleaning step)
- Chemical cleaning (aggressive)
- Post aggressive cleaning CWP test

### *2.6.2 Polymer nanofiltration*

A full cycle of tests performed while testing one wastewater sample using one ceramic membrane is shown below

- Membrane CWP test
- Membrane salt rejection test
- Wastewater test
- Post-WW CWP test
- Post-WW salt rejection test

## **2.7 Analytical procedures**

### *2.7.1 Total & soluble chemical oxygen demand test*

COD tests were carried out using Hach high-range (20-1500 mg/L) COD digester vials. A 2 ml sample was required for each COD test. Appropriate dilutions (2x/4x/10x) in milli-Q were

made in order to measure samples with COD > 1500 mg/L. 2 ml of diluted wastewater sample was then added to a digester vial and shaken vigorously before placing the vial in a Hach DRB200 digital reactor block and digested at 150 °C for 2 hours. The digested vial is then allowed to cool down to room temperature away from light. A control sample using 2 ml of milli-Q water was also prepared using the same procedure. Vials are then placed sequentially in a Hach spectrophotometer after cleaning the glass sides with a Kim wipe (VWR) to provide an unobstructed path for the light. First, the control vial is placed to set a zero value, followed by placing the sample vials and reading the COD measurement. The measured COD value is then appropriately multiplied by the dilution factor to get the actual COD value of the wastewater sample. Two aliquots were used for each wastewater sample to obtain duplicate COD measurements.

To measure soluble COD, a 10 ml sample of undiluted wastewater was first filtered using a syringe filter (0.45 µm) before measuring the COD of the sample using the same procedure described above. Duplicate soluble COD measurements were obtained using two raw wastewater aliquots and two syringe filters.

### *2.7.2 pH & Conductivity test*

pH and conductivity of samples were measured using Hanna HI5522 bench-top meter. pH calibration was verified before every set of measurements using one of the calibration buffers from Hanna. The pH probe was kept submerged in a storage solution (Hanna) at all times by putting a few drops inside the probe cap and then closing the cap on the end of the probe. The cap is removed and the probe is rinsed with DI water before any set of measurements. The probe is dried using a Kim wipe before submerging it into a sample. The probe is allowed to reach a steady state which is indicated by the meter before recording the value. The probe is then rinsed and dried again to measure the next sample. At the end of all samples, probe is rinsed & dried and put back into the

storage solution inside the probe cap. Additionally, the pH meter was also recalibrated using three calibration buffers (Hanna) every month.

Conductivity of samples was measured using a conductivity probe attached to the Hanna bench-top meter. The conductivity probe was rinsed with DI water and dried using a Kim wipe before every use. Conductivity measurements were factory calibrated and hence did not require external calibration. Samples were directly measured by submerging the conductivity probe in the sample and recording the stabilized reading shown on the digital meter.

### *2.7.3 Turbidity test*

Turbidity of wastewater samples was measured using a Turbidity test kit by Hach. The kit consists of four calibration standards, 6 clean glass vials for sample measurement and one digital meter with a sample holder for taking measurements. The calibration of the digital meter was verified using a turbidity standard (NTU = 10) before & after every set of measurements. Wastewater samples are mixed well before transferring them into the glass vials provided with the kit. Vials are closed and shaken vigorously before putting it in the sample holder to take a reading. Duplicate measurements are taken for each wastewater sample by preparing two aliquots. Glass vials are emptied, rinsed and dried to make them ready for next use.

### *2.7.4 Gas chromatography – Mass spectroscopy test*

100 ml of wastewater sample is acidified using 1 M HCl (2-4 ml) to reach a pH between 2 – 2.5. Acidification of samples helps in better extraction and derivatization later on in the process. Once the sample is acidified, it is mixed with 100 ml of Dichloromethane (DCM) in a 500 ml borosilicate separatory funnel inside a fume hood. DCM is an organic solvent insoluble in water but dissolves a variety of organics readily and hence it was used to extract organics present in our wastewater samples. Also, this procedure was observed to work well based on results from [35].

The separatory funnel is then closed and shaken vigorously for at least 3 minutes, while opening the funnel few times during this process to prevent building up excessive pressures which could result in unwanted DCM spills. This completes the extraction of analytes into DCM. The separatory funnel is then placed upright on a stand where two separate phases were clearly visible. DCM being denser than water was separated out at the bottom. The solution was allowed to rest for a minute to obtain a clear phase boundary. The bottom layer is then filtered through 10 grams of Sodium Sulfate on a Grade-1 Whatman filter paper into a glass beaker. Sodium sulfate being hygroscopic in nature absorbs any unwanted traces of water.

A series of operations were now performed to reduce the volume of our sample to 2 ml. This would concentrate analytes and therefore is a necessary step to generate readable signals. Filtered DCM layer is first transferred to a rotary evaporator assembly to undertake the first step in concentrating our sample. The rotary evaporator assembly consists of a chiller, a temperature-controlled water bath, a rotary arm, vacuum system and a condenser. The chiller was set to a temp of -15 °C. Water bath was set to a temperature of 40 °C. Contents from the beaker are transferred into a 250 ml glass round bottom flask. The flask is then attached to the end of the rotary arm and submerged in the water bath by moving and turning the rotary arm. Rotation is then turned on which aids in better heat transfer to the flask. Vacuum system is turned on at this point which results in boiling of DCM. Pure DCM is evaporated and condensed in a separate glass flask with the help of the condenser. The system is operated for 3-4 minutes and the resulting concentrated DCM sample is collected back in a 14 ml glass vial and labelled. This sample is now transferred to a nitrogen purge system where a low-pressure nitrogen stream is used to slowly evaporate DCM and achieve a final sample of 2 ml. 9 samples were simultaneously concentrated using the 9-pins available on the system.

Samples are now derivatized using N-methyl-N-(trimethylsilyl) trifluoroacetamide (MSTFA) mixed with 1% Trichloromethylsilane (TCMS). MSTFA reacts to the analytes and converts them into compounds that can be rendered into a gas phase readily at much lower temperatures. TCMS acts as a catalyst to this reaction. Once the analytes are present in gas phase they can be analyzed using gas chromatography. An internal standard (IS) stock solution was also prepared with 18.8 ng/dL of Anthracene methanol in DCM. 25  $\mu\text{L}$  of sample is pipetted into a 200  $\mu\text{L}$  glass insert placed in a 2 ml glass vial (VWR) followed by 25  $\mu\text{L}$  of IS stock. Next, 25  $\mu\text{L}$  MSTFA (with 1% TCMS) is added to the vial and the vial is closed immediately. Contents are mixed well by placing the vial on a vortex for a few seconds. Vials are then incubated in an oven at 60  $^{\circ}\text{C}$  for 1 hour to complete the derivatization reaction followed by placing them on GC autosamplers for measurement.

The GC-MS analysis was performed using a 6890N gas chromatograph (Agilent), equipped with a DB-17ht column (30 m  $\times$  0.25 mm ID  $\times$  0.15  $\mu\text{m}$  film, J & W Scientific) with a retention gap (deactivated fused silica, 5 m  $\times$  0.53 mm ID), and a 5973 MSD single quadrupole mass spectrometer (Agilent). A 1  $\mu\text{L}$  aliquot of the sample was injected into the chromatograph using a 7683 auto-sampler (Agilent) in splitless mode. The injector temperature was 250  $^{\circ}\text{C}$  and the carrier gas (helium) flow rate was 1.1 mL/min. The transfer line temperature was 280  $^{\circ}\text{C}$  and the MS source temperature was 230  $^{\circ}\text{C}$ . The column temperature was initially at 50  $^{\circ}\text{C}$ , then was increased to 300  $^{\circ}\text{C}$  via an 8  $^{\circ}\text{C}/\text{min}$  ramp and held at 300  $^{\circ}\text{C}$  for 15 min for a total run time of 46.25 min. A full scan mass spectrum between m/z (mass-to-charge ratios) of 50 and 800 were acquired.

## **CHAPTER-3: Performance comparison among ceramic NF membranes**

### **3.1 Introduction**

In order to assess wholesome performance of a membrane filtration process, multiple factors such as membrane selectivity (retention of analytes), flux through the membrane, physical/chemical changes of membrane surface during filtration, fouling propensity & ease of cleaning and maintenance play a major role. Also note that in addition to filtration performance, external economic factors like membrane cost & longevity also affect the industrial adoption of such technology. In this study, four different aspects of filtration performance were tested for 4 ceramic membranes on 3 different industrial wastewater samples from Aevitas. These aspects include COD rejection, permeate flux, CWP before and after filtration & chemical cleaning efficiency using an industrial grade chemical cleaner. WW-A was tested using 200-Da, 450-Da & 8500-Da ceramic membranes. WW-B and C were tested using 200-Da, 450-Da & 750-Da membranes because 8500-Da membrane was damaged during one of the chemical cleaning experiments.

Due to significant differences in COD and Sol-COD for WW-A and WW-C, they were first pre-treated using a lab scale cross-flow microfiltration process using a polymer membrane and the flat-sheet sepa cell. This intermediate MF step was also included to save the costly ceramic membranes from any irreversible damage and ensure reusability to test multiple wastewaters. Synder's V0.2 MF membrane (average pore size = 0.2  $\mu\text{m}$ ) was used to perform the MF step and permeate collected was characterized using the same bulk property measurements and GC-MS analysis as discussed in Section 2. Permeate collected from MF was then used to perform filtration tests on the ceramic membranes. Results from MF of WW-A & C are summarized below in Table 8. Significant amounts of COD and turbidity was rejected during microfiltration for both

wastewater samples. WW-A was reduced to a COD of 2420 mg/L with 42 % rejection, and to a turbidity of 522 NTU with 36 % rejection. WW-C was reduced to a COD of 2718 mg/L with 19 % rejection, and to a turbidity of 132 NTU with 74 % rejection. A high amount of Turbidity rejection did not result in high COD rejection for WW-C which means that solids particles contributing to Turbidity were not contributing to COD as much as the dissolved components. On the other hand, both COD and Turbidity rejections (42 % and 36 % respectively) for WW-A were in the same ballpark indicating presence of a high overlap between components contributing to COD and Turbidity. Low conductivity rejections were observed for both wastewaters (8 % and 16 % for WW-A and WW-C respectively) due to the presence of ionic species in dissolved form and inability of MF membranes in separating ionic salts and species. Slight pH changes were also observed after MF for both wastewaters and both WW-A and WW-C turned out more basic after MF treatment.

	As received				After Microfiltration			
WW	COD (mg/L)	Turbidity (NTU)	Conductivity ( $\mu\text{S}/\text{cm}$ )	pH	COD (mg/L)	Turbidity (NTU)	Conductivity ( $\mu\text{S}/\text{cm}$ )	pH
A	4185 $\pm$ 54	812 $\pm$ 33	4865 $\pm$ 4	7.05 $\pm$ 0.04	2420 $\pm$ 16 (42 % $\downarrow$ )	522 $\pm$ 1 (36 % $\downarrow$ )	4455 $\pm$ 5 (8 % $\downarrow$ )	7.31 $\pm$ 0.01
C	3335 $\pm$ 20	503 $\pm$ 12	6872 $\pm$ 14	6.41 $\pm$ 0.04	2718 $\pm$ 42 (19 % $\downarrow$ )	132 $\pm$ 1 (74 % $\downarrow$ )	5740 $\pm$ 11 (16 % $\downarrow$ )	7.04 $\pm$ 0.03

**Table 8.** Summary of feed and permeate characterization from cross-flow microfiltration pre-treatment step using Synder V0.2 membrane. Highlighted values in the parenthesis show % drop in bulk property. Permeates collected from this step are then used to test the ceramic & polymer NF membranes.

### **3.2 Results – Filtration & Chemical cleaning**

As mentioned earlier, each membrane was tested using a series of experiments and under operating conditions as discussed in Section 2.6.1 and Table 7. Also, since the wastewater samples were collected from Aevitas one month apart, all experiments were completed for one wastewater before moving onto the next. A CWP test for all ceramic membranes was followed by a wastewater filtration test (at 100 psi for WW-A & B and at 120 psi for WW-C) on all membranes. This was followed by a post-wastewater-filtration CWP test for all membranes. Membranes were then chemically cleaned using Tergazyme, an industrial grade membrane cleaner, at 100 psi for 60 minutes at elevated temperature (40 °C). This was followed by post-cleaning CWP test for all membranes. Results for each of these experiments are summarized for all membranes across all 3 wastewater samples and reported in subsequent sections.

#### *3.2.1 COD rejection performance*

Two 10 ml aliquots of both feed and permeate samples were collected at three time points ( $t = 10, 60, 120$  min) during each of the wastewater filtration tests. COD of all these samples were measured and results are tabulated in Table 9. Figure 12 also shows a bar graph comparison between COD rejected from the 4 ceramic membranes for the 3 wastewater samples. Triplicate COD values obtained from feed and permeate samples for each WW filtration experiment was used to calculate the averages and standard deviation errors shown in Figure 12.

200-Da membrane showed the best COD rejection performance followed by 450-Da and 750-Da membrane as expected. Both 200-Da and 450-Da membrane could reduce the COD by 77% for WW-A and the resulting permeate COD (608 and 633 mg/L for 200-Da and 450-Da respectively) were found to be very close to the target COD of 600 mg/L. Similar results were obtained for WW-C where 200-Da membrane achieved the best performance reducing the COD by 60% with the resulting permeate COD of 977 mg/L. This did not meet the 600 mg/L target but still

was a significant improvement in water quality. 450-Da membrane could also reduce a significant amount of COD from WW-C rejecting 49% with a permeate COD of 1264 mg/L. Unlike WW-A & C, COD rejections were relatively low for WW-B for all 3 membranes. 200-Da membrane achieved the highest rejection for WW-B with 30% rejection achieving a permeate COD of 591 mg/L which meets our target. 450-Da membrane could only reduce 19% COD achieving a permeate COD of 652 mg/L while 750-Da membrane could only reduce 9% of the COD and achieved 688 mg/L permeate COD. One of the possible reasons for low COD rejection performance for WW-B could be the low feed COD ( $804 \pm 18$  mg/L) and low turbidity ( $\sim 0$  NTU) of this sample. This observation also suggests that these membranes might not be able to reduce the COD of wastewaters below a certain threshold and therefore low % rejections are observed for low feed COD samples. Secondly, since the composition of WW-B (measured using GC-MS) was found to be very different from other wastewaters, it is possible that WW-B contained dissolved compounds that were being rejected poorly. Unfortunately, none of the major peaks in the GC-MS spectrum for WW-B could be identified as a library compound using NIST-MS library.

WW	Membrane	Time (min)	Feed COD (mg/L)	Permeate COD (mg/L)	Time average Feed COD (mg/L)	Time average Permeate COD (mg/L)	% COD rejection
A	200-Da	10	2638 ± 66	529 ± 11	2594 ± 39	608 ± 70	77
		60	2564 ± 16	661 ± 11			
		120	2580 ± 96	634 ± 2			
	450-Da	10	2758 ± 10	386 ± 10	2721 ± 46	633 ± 216	77
		60	2670 ± 30	728 ± 2			
		120	2736 ± 40	785 ± 7			
	8500-Da	10	2952 ± 60	1280 ± 14	2881 ± 90	1326 ± 50	54
		60	2912 ± 36	1379 ± 9			
		120	2780 ± 28	1318 ± 8			
B	200-Da	10	849 ± 2	574 ± 5	839 ± 9	591 ± 16	30
		60	839 ± 9	604 ± 7			
		120	830 ± 3	597 ± 4			
	450-Da	10	809 ± 8	662 ± 13	807 ± 22	652 ± 9	19
		60	827 ± 3	644 ± 2			
		120	784 ± 11	650 ± 4			
	750-Da	10	786 ± 10	705 ± 12	759 ± 27	688 ± 22	9
		60	758 ± 1	695 ± 5			
		120	732 ± 13	663 ± 2			
C	200-Da	10	2528	940	2473 ± 63	977 ± 33	60
		60	2404	1004			
		120	2488	988			
	450-Da	10	2544	1236	2500 ± 39	1264 ± 28	49
		60	2484	1292			
		120	2472	1264			
	750-Da	10	2488	2040	2500 ± 21	1940 ± 88	22
		60	2488	1908			
		120	2524	1872			

**Table 9.** COD rejection summary from experiments with 4 ceramic membranes and 3 WW samples (A, B, C). Average and standard deviations are calculated using COD values at three time points (t=10, 60, 120 min).

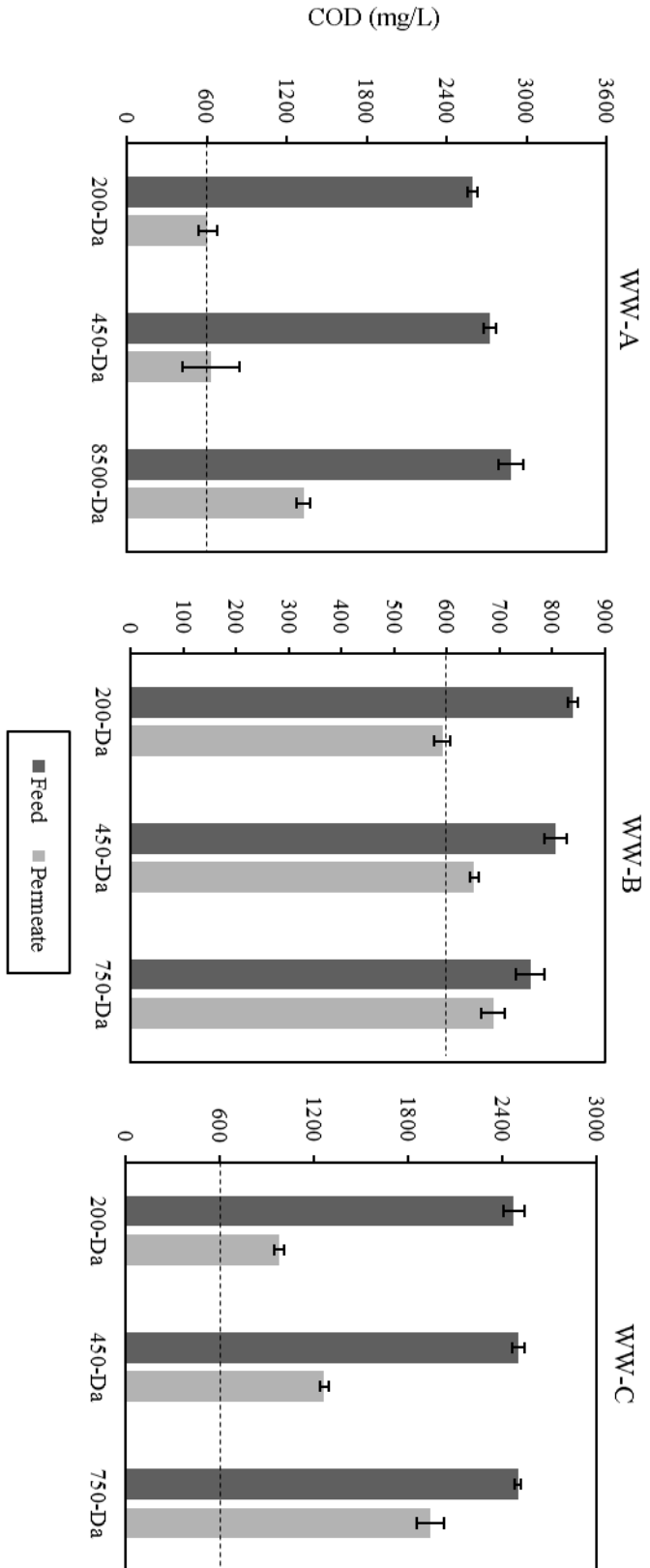


**Figure 12.** Feed and permeate COD bar plots for ceramic membrane testing. Horizontal dashed line represent the COD target for Aevitas to safely discharge the treated effluent (600 mg/L). Corresponding % COD rejection values can be found in Table 9.

### 3.2.2 *Permeate wastewater flux comparison*

Permeate flux is defined by the volume of liquid passing through the membrane per unit area per unit time. A complete profile of permeate flux was recorded for each WW filtration experiment for a duration of 180 minutes at a constant feed pressure. Figure 13 & 14 show the absolute and relative flux profiles obtained for the 3 wastewater samples (WW-A, B, C). Average flux values and standard deviation errors are calculated using triplicate flux measurements.

Absolute flux profiles for WW-A show that highest flux was achieved using 8500-Da membrane (~ 24.5 L/m<sup>2</sup>/h) followed by 450-Da (~ 5.8 L/m<sup>2</sup>/h) and 200-Da membrane (~ 4.8 L/m<sup>2</sup>/h). Note that for WW-A, 450-Da membrane was operated at 150 psi instead of 100 psi due to very low permeate flow at 100 psi incapable of generating enough permeate sample for COD and GC-MS testing. A better comparison is possible in terms of wastewater permeability (LMH/bar) through the membrane, which is calculated by dividing the stabilized permeate flux (LMH) with transmembrane pressure (bar). Assuming that the permeate flux stabilized at the end of each experiment, wastewater permeability values of 0.67, 0.56 and 3.56 LMH/bar were observed for 200-Da, 450-Da and 8500-Da membranes respectively for WW-A. 200-Da membrane was found to be slightly better than 450-Da membrane based on the permeability values. For WW-B, highest absolute flux was achieved by 750-Da membrane (~44.1 L/m<sup>2</sup>/h) followed by 450-Da (~16.4 L/m<sup>2</sup>/h) and 200-Da (~15.3 L/m<sup>2</sup>/h). Corresponding wastewater permeability values were 6.40, 2.38 and 2.22 LMH/bar for 750-Da, 450-Da and 200-Da membranes, respectively. Notice that the flux achieved by 200-Da membrane was only slightly less (< 10 % difference) than 450-Da. For WW-C, highest absolute flux was achieved by 750-Da membrane (~37.1 L/m<sup>2</sup>/h) followed by 200-Da (~10.3 L/m<sup>2</sup>/h) and 450-Da (~9.5 L/m<sup>2</sup>/h). Corresponding wastewater permeability values (4.49, 1.15 and 1.24 LMH/bar for 750-Da, 450-Da and 200-Da) again show that 200-Da could generate slightly more permeate than 450-Da.

Relative flux profiles (Figure 14) from each experiment was calculated by dividing flux at each time point by flux at  $t = 5$  min. Since the TMP is kept constant throughout an experiment, a decrease in relative flux indicates membrane fouling. Fairly constant relative flux profiles were observed for 200-Da and 450-Da membranes for WW-A. Relative flux for 8500-Da membrane increased during the start of the experiment for WW-A, before reaching a steady value. The reason for the initial increase in flux is not clear but could be a consequence of membrane drying and formation of air pockets in the membrane which gradually opened up during the experiment increasing the permeate flow rate. Most importantly, none of the 3 membranes indicated any significant fouling over the duration of 3 hours for WW-A. For WW-B, 200-Da had a steady flux throughout the 3 hour duration indicating no fouling. Relative flux dropped to 0.71 at the end of 3 hours for 450-Da membrane indicating some fouling. Relative flux also dropped to 0.29 for 750-Da membrane indicating severe fouling. In both the cases, it is important to note that rate of flux decline decreased with time and eventually a constant flux value was achieved, implying no further fouling of membranes. Similar results were observed for WW-C, where final relative flux values for 200-Da, 450-Da and 750-Da were found to be 0.80, 0.72 and 0.45, respectively. This implied that 750-Da membrane was fouled more severely followed by 450-Da and 200-Da.

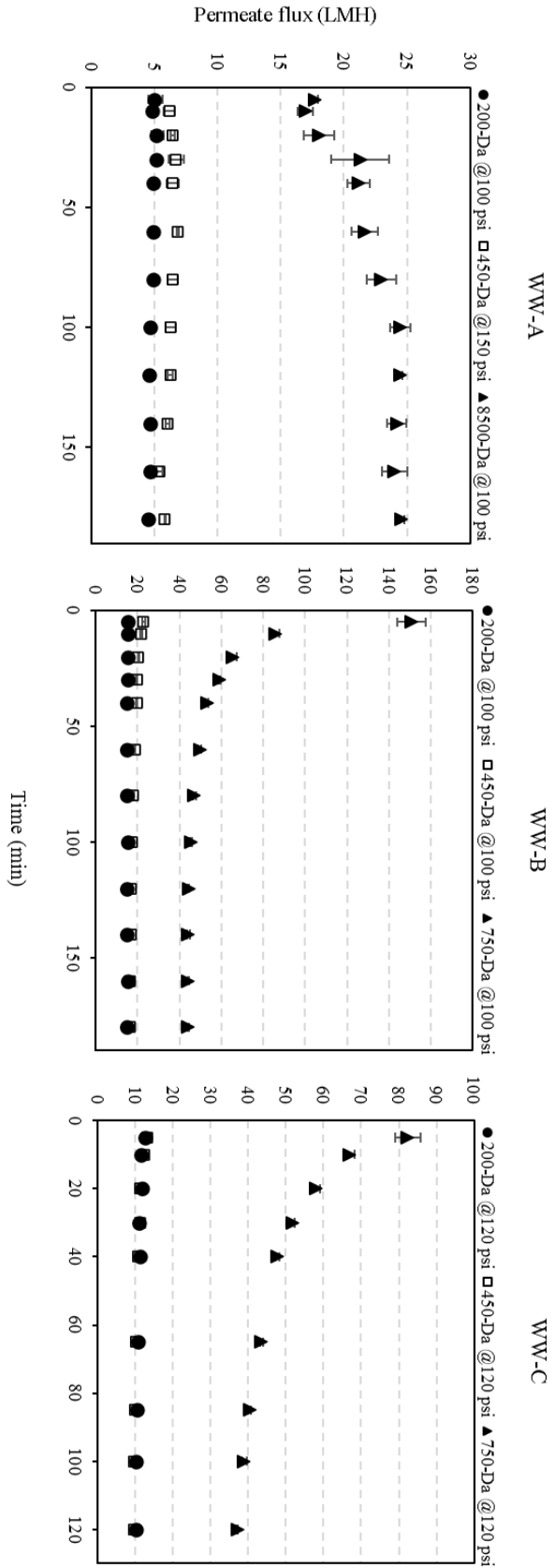


**Figure 13.** Permeate flux profiles during wastewater filtration tests for ceramic membranes. Legends also show the operating pressure during each experiment. Error bars denote the standard deviation in flux measured using triplicate measurements.

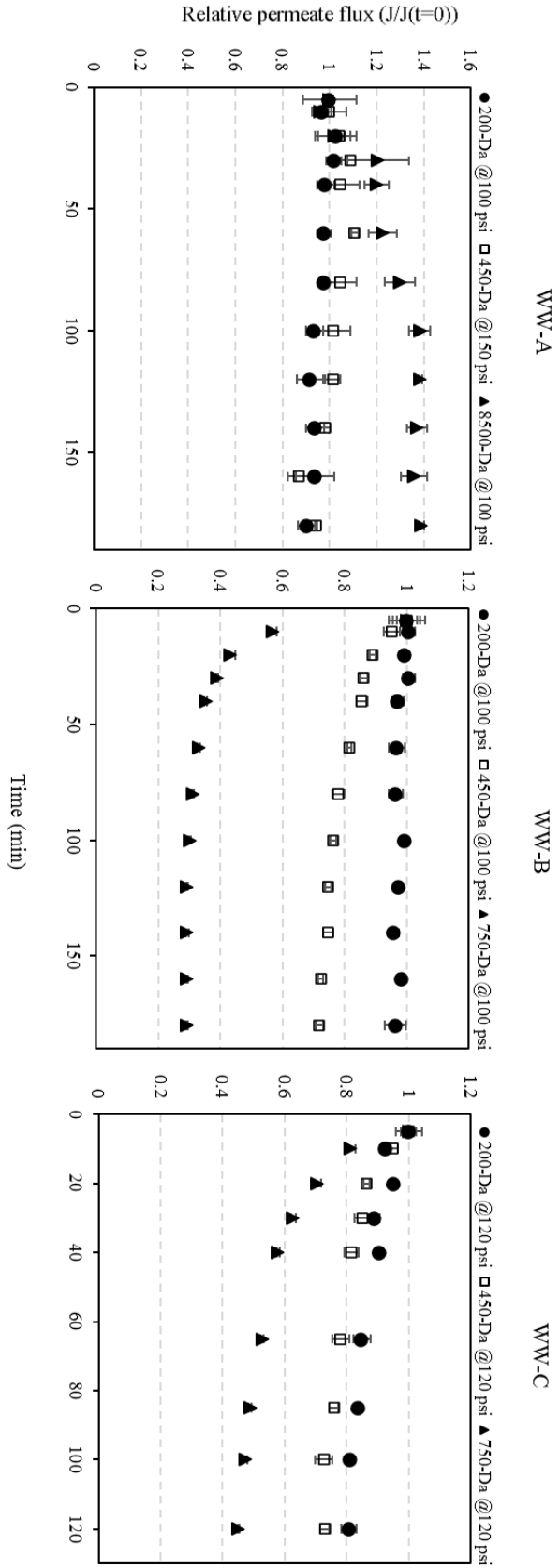


**Figure 14.** Relative permeate flux profiles during wastewater filtration tests for ceramic membranes. Legends also show the operating pressure during each experiment. Error bars denote the standard deviation in relative flux measured using triplicate measurements.

### 3.2.3 Effect of wastewater filtration & chemical cleaning on CWP

Clean water permeability (CWP) was measured for each ceramic membrane before and after WW filtration. An increase/decrease in CWP indicates deviation from baseline performance, which means that the membrane is not completely resistant to foulants/chemicals present in the wastewater. ‘% drop’ in CWP was calculated using Equation 4. Membranes were cleaned in place after WW filtration using a chemical cleaning solution of Tergazyme (concentration: 10 g/L in DI water; cleaning temperature: 40 °C; Duration: 60 minutes, pH = 9.0) procedure for which was previously mentioned in Section 2.5.4. CWP was measured again after chemical cleaning to evaluate cleaning efficacy by calculating ‘% recovery’ using Equation 3.

$$\% \text{ recovery} = \frac{\text{CWP}_{\text{After cleaning}}}{\text{CWP}_{\text{Before filtration}}} \times 100 \quad (3)$$

$$\% \text{ drop} = \frac{\text{CWP}_{\text{Before filtration}} - \text{CWP}_{\text{After filtration}}}{\text{CWP}_{\text{Before filtration}}} \times 100 \quad (4)$$

Figure 15 below summarizes the results from all CWP experiments performed in bar plots. Table 10 contains the calculated values of ‘% drop’ and ‘% recovery’ corresponding to the values shown in Figure 15. CWP experiments were done in duplicates to report the average and error values in the bar plots (except for a few data points where the error bars are not plotted). Also note that results for 8500-Da which was tested using WW-A are not shown in Figure 15. 8500-Da had a CWP of 97.43 LMH/bar before filtration which dropped to 20.53 LMH/bar (79 % drop) post WW filtration. Caustic cleaning at pH 11 using a solution of NaOH, 0.06 % w/w Sodium Dodecyl Sulfate (SDS) and 0.05% w/w Tetrasodium Ethylenediaminetetraacetate (EDTA) was performed but could not recover CWP. Next, an acid cleaning step using Citric acid at pH 2.4 was attempted but no significant recovery was observed. Attempts to recover CWP of 8500-Da membrane using a chemical clean (Tergazyme) followed by heat treatment upto 120 °C at heating and cooling ramps

of 3 °C/min (as recommended by the manufacturers) resulted in further decrease of CWP to 5.81 LMH/bar, possibly damaging the membrane. Results for 8500-Da membrane are summarized in Figure 16. CWP was found to recover only when membranes were cleaned using Tergazyme without any heat treatment as seen in the cases of 200-Da, 450-Da and 750-Da.

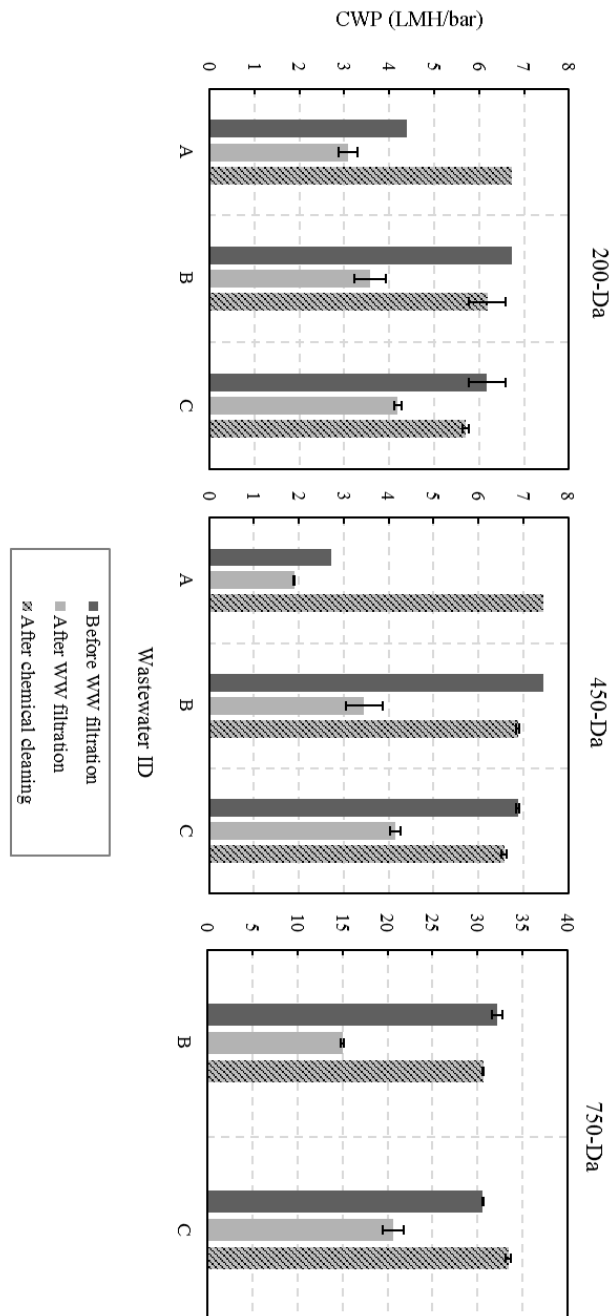


**Figure 15.** Summary plot showing effect of wastewater filtration & chemical cleaning on CWP for ceramic membranes. Error bars are calculated by conducting the complete CWP experiment twice. CWP experiment was only performed once for bars which do not have an error bar.

WW	Membrane	CWP	
		% drop	% recovery
A	200-Da	30	153
	450-Da	31	273
	8500-Da**	79	6
B	200-Da	47	92
	450-Da	54	92
	750-Da	54	95
C	200-Da	32	92
	450-Da	40	95
	750-Da	33	109

**Table 10.** Summary of % drop and % recovery in CWP during testing of ceramic membranes. \*\*Note that the cleaning protocol followed for 8500-Da was different from others which led to very low % recovery in CWP.

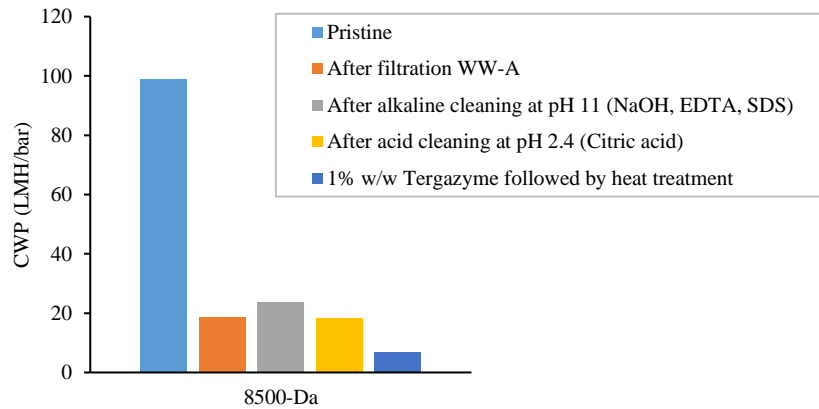


**Figure 16.** Summary of chemical cleaning experiments with various chemicals for 8500-Da membrane

Pristine membrane CWP for 200-Da, 450-Da and 750-Da were found to be 6.7, 7.5 and 32.2 LMH/bar, respectively. Note that dry membranes as received from the manufacturer were directly used for CWP experiments before testing with WW-A which resulted in erroneous results. This can be seen in Figure 15 (Before filtration WW-A) where pristine CWP values for 200-Da and 450-Da were found to be 4.4 and 2.7 LMH/bar, respectively, which were not in the expected range (5-15 LMH/bar) and 450-Da had a lower CWP than 200-Da which should not be the case. A membrane pre-treatment step (refer Section 2.2.1) was carried out on all membranes from then on to get accurate and reproducible results.

All membranes observed a notable decrease in CWP after wastewater filtration with all 3 IWW samples. % drop in CWP for 200-Da membrane were found to be in range 30-47% with a maximum drop of 47% for WW-B. 450-Da membrane follows the same trend where % drop in CWP were found in range 31-54% with maximum drop of 54% for WW-B. Among the two wastewater samples tested with 750-Da membrane, WW-B showed a 54% drop in CWP followed by 33% drop by WW-C. Lastly, 8500-Da membrane which was only tested with WW-A experienced a 79% drop in CWP post filtration. Significant drop in CWP for all membrane show that all membranes were being fouled to some extent during wastewater filtration. From Table 10, it can also be seen that 200-Da membrane showed least drop among membranes tested for all three wastewater samples. It can also be seen that 8500-Da membrane showed highest drop (79%) for WW-A. These results suggest the following order of CWP % drop: 200-Da < 450-Da  $\approx$  750-Da < 8500-Da. It was also noted that some wastewater samples such as WW-B result in higher % drop than other wastewater samples. Post-filtration CWP tests were followed by chemical cleaning step using Tergazyme (1% w/w) to recover membrane CWP. As shown in Table 10, more than 90% recovery in CWP was observed for all membranes and wastewater samples, except for 8500-Da membrane which was possibly damaged while attempting a different cleaning protocol as discussed earlier.

### **3.3 Chemical cleaning & filtration repeatability study – 750 Da membrane**

In the previous section, chemical cleaning was proved to be effective in recovering membrane CWP post wastewater filtration. However, from a process point of view it is equally important to investigate COD rejection performance and wastewater flux recovery after a fouled membrane is chemically cleaned. To this end, we have performed 3 ‘filtration + cleaning’ cycles on 750-Da membrane using WW-C. Detailed experimental procedure and results are discussed in following subsections.

### *3.3.1 Procedure for multiple filtration & cleaning cycles*

Following set of tests were performed to complete one filtration-cleaning cycle. 3 such cycles were performed to get performance data over multiple filtration-cleaning cycles. Mild cleaning tests were introduced in each cycle with differing conditions to investigate significant factors in cleaning of membranes.

1. CWP (Before filtration) – x2 times
2. IWW filtration
3. CWP (After filtration) – x2 times
4. Mild chemical cleaning (Condition A/B/C)
5. CWP (After mild cleaning) – x2 times
6. Aggressive chemical cleaning

Each cycle consist of a mild chemical cleaning step at one of the 3 operating conditions A, B or C followed by an aggressive chemical cleaning step. Cycle-1, Cycle-2 and Cycle-3 are operated with mild cleaning conditions A, B and C respectively. Refer to Table 7 in Section 2.5 for details on conditions (feed conc., feed temp., duration, etc.) for each of the mild chemical cleaning and aggressive chemical cleaning tests. In short, Table 11 below summarizes the chemical cleaning conditions. Note that levels of feed concentration and feed temperature change in conditions A, B and C while duration remains constant. The results will thus help in identifying significance of feed concentration and feed temperature on cleaning efficiency. Also note that an aggressive cleaning step is carried out at high concentration and temperature for a longer duration in order to recover CWP completely before starting the next cycle.

Condition	Feed concentration (% w/w Tergazyme in DI water)	Feed temperature (°C)	Duration (min)
A	High (1%)	High (40)	Moderate (30)
B	High (1%)	Low (20)	Moderate (30)
C	Low (0%)	High (40)	Moderate (30)
Aggressive	High (1%)	High (40)	High (60)

**Table 11.** Summary of chemical cleaning conditions for mild and aggressive cleaning steps

### 3.3.2 Permeate flux and COD rejection performance

Membrane permeability and permeate flux test results are stacked in a chronological manner in Figure 17 (left to right). COD testing results for all 3 cycles are shown in Figure 18. For ‘Cycle-1’, permeate flux at the end of 120 min of filtration was  $37.1 \text{ L.m}^{-2}.\text{h}^{-1}$  (see Figure 17). Initial permeate flux ( $t=5 \text{ min}$ ) during ‘Cycle-2’ increased to 52.8 LMH before dropping down to 24.7 LMH at  $t=120 \text{ min}$ . The initial increase in permeate flux during cycle-2 indicates recovery of wastewater flux to some extent due to chemical cleaning. The increase in permeate flux after chemical cleaning was much more evident during ‘Cycle-3’ where the initial permeate flux ( $t=5 \text{ min}$ ) increased to 72.2 LMH before dropping down to 29.8 LMH at  $t=120 \text{ min}$ . Stabilized permeate flux was achieved within 120 min of filtration during 2<sup>nd</sup> and 3<sup>rd</sup> filtration cycle. 22-35 % COD was rejected during all 3 cycles showing consistent COD rejection performance over all filtration cycles. Performance results discussed above show robustness in membrane performance after repeated high-pressure filtration and chemical cleaning tests.

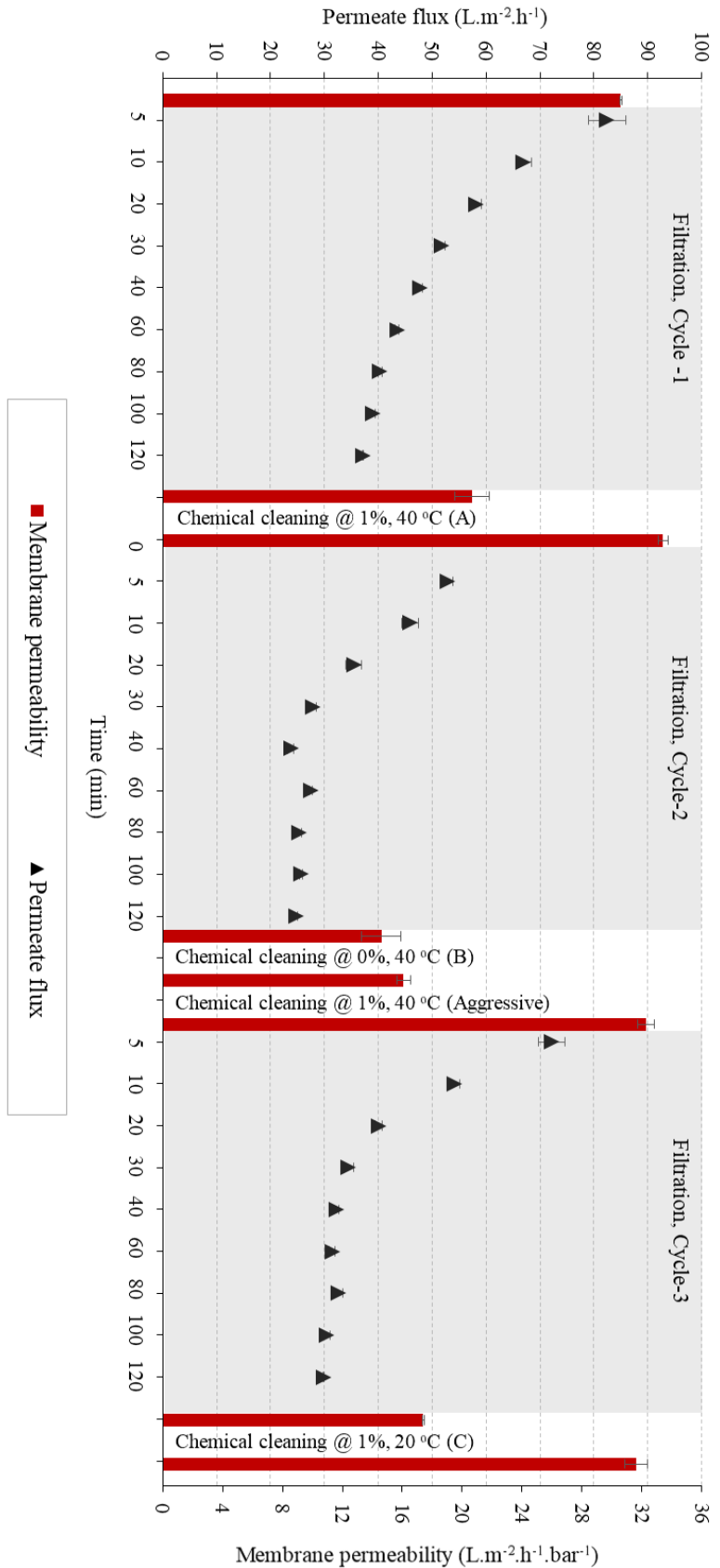


**Figure 17.** Summary of wastewater flux and membrane permeability (CWP) results from 3 filtration-cleaning cycles on 750-Da membrane with WW-C. Note that all experiments are stacked in chronological order from left to right. Intermediate chemical cleaning steps are annotated on the chart showing cleaning conditions (% w/w Tergazyme, Temperature). Permeate flux is denoted by black markers with corresponding g values present on the primary y-axis. Membrane permeability is denoted by red bars with corresponding values present on secondary y-axis. Error bars in CWP denote absolute error from duplicate CWP tests and error bars in permeate flux denote the standard deviation from 5 flux measurements.

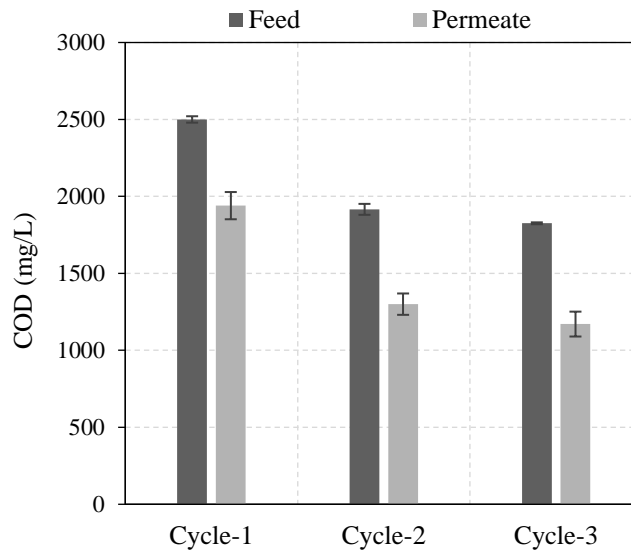


**Figure 18.** Feed and permeate COD during repeated filtration-cleaning cycles of 750-Da membrane with WW-C. Error bars denote standard deviation in COD measured at three time points during filtration ( $t = 10, 60, 120$  min)

### 3.3.3 Chemical cleaning efficiency over multiple filtration cycles

As shown in Figure 17, membrane CWP dropped in the range 14-20 LMH after each wastewater filtration test with an average drop of 44% in CWP for 3 cycles. CWP was found to be completely recovered after chemical cleaning tests, either using one of the chemical cleaning conditions (A, B or C) or using an ‘Aggressive’ cleaning method. For e.g., complete recovery in CWP was observed under condition ‘A’ during cycle-1. No significant recovery was observed for condition ‘B’ during cycle-2. Cleaning test under condition ‘B’ was followed by an aggressive cleaning step to try and recover 100% permeability before beginning the next cycle. Similar to cycle-1, complete recovery in CWP was observed for condition ‘C’ during cycle-3. It is important to note that during the course of repeated filtration and cleaning, membrane permeability (clean membrane) did not change significantly strengthening our claim of membrane robustness due to consistent membrane performance even after 3 filtration-cleaning cycles.

Additionally, CWP recovery under cleaning conditions A, B and C also show that temperature is not a significant factor while concentration of Tergazyme is a significant factor in cleaning.

### **3.4 Conclusion**

Ceramic membranes were found to reject as high as 77% COD for real IWW. Lowest COD rejection observed for the tightest ceramic membrane (average pore size = 200 Da) was found to be 30%. As expected, order of COD rejection among the 4 ceramic membranes was found to be 8500-Da  $\approx$  750-Da < 450-Da < 200-Da. Although the COD target of 600 mg/L was not met for 2 out of 3 IWW samples, significant improvement in COD can reduce downstream treatment/shipping costs for Aevitas.

Permeate flux in the range 5-15 LMH was provided by the 200-Da membrane. All other membranes had higher flux but at the cost of reduced COD rejection performance. Assuming an average permeate flux of 10 LMH, and membrane area of 250 m<sup>2</sup> (10 standard modules from Inopor™), a total of 60,000 L of wastewater can be processed in 24 hours and hence it is a viable option for a medium-scale specialized treatment facility such as Aevitas. Based on ceramic membrane scale up study [57], larger modules are also being developed which will increase capacity and lower membrane cost per unit area in the future.

Stabilized absolute flux profiles for 200-Da and 450-Da membranes show that they were relatively fouling resistant than 750-Da and 8500-Da membrane. CWP for all membranes dropped significantly after wastewater filtration regardless of which IWW sample was filtered which suggests that membranes surface is being fouled/changed quite drastically. However, fouling from all membranes was found to be easily removed by chemical cleaning with 1% w/w Tergazyme

solution. It was also found that temperature of the cleaning solution was not a significant factor in cleaning these membranes.

Since all the membranes had a  $\text{TiO}_2$  active layer and an  $\alpha\text{-Al}_2\text{O}_3$  support layer, 750-Da membrane was chosen as a model membrane to study filtration and cleaning repeatability. Permeate flux was found to recover to a high initial value (at  $t=5$  min) after chemical cleaning, proving effectiveness of the chemical cleaning method used. Consistent COD rejection and no significant deviation in membrane CWP (cleaned membrane) from its baseline permeability shows membrane robustness.

## **CHAPTER-4: Comparison with Polymer Nanofiltration membranes and Predictive modeling of membrane rejections**

### **4.1 Polymer NF filtration performance**

3 polymer NF membranes were also tested in parallel with ceramic NF membranes on 5 out of 6 IWW samples (A, C, D, E, F) tabulated in Table 6. The 3 membranes, namely NF90, NFX and NFS, with reported MWCO in the range ~150-400 Da are commercially available and widely used for industrial purposes. All performance metrics except for chemical cleaning were studied and reported in subsequent sections. New polymer membrane cutouts were used for each IWW sample to reduce any carry-over effects from previous filtration experiments and obtain unbiased results on pristine membranes.

#### *4.1.1 COD rejection & permeate flux*

Figure 19 shows a bar graph comparison for COD rejected from the 3 polymer membranes tested on 5 IWW samples. Feed and permeate samples were collected for COD measurement at three time points ( $t = 10, 60, 120$  min) during wastewater filtration in a similar manner as for ceramic membranes. Permeates for 4 out of 5 IWW sampled were brought down below the target COD of 600 mg/L. WW-E which has the highest feed COD (10,425 mg/L) among all IWW samples could only be brought down to 1023 mg/L COD by NF90 membrane, but still rejecting a significant 90% of the COD. Relatively consistent and high % COD rejection was observed for all polymeric membranes. On an average over all 5 IWW samples, NF90 could reject 89% COD. Similarly, NFX and NFS achieved 77% and 70% average COD rejections, respectively.

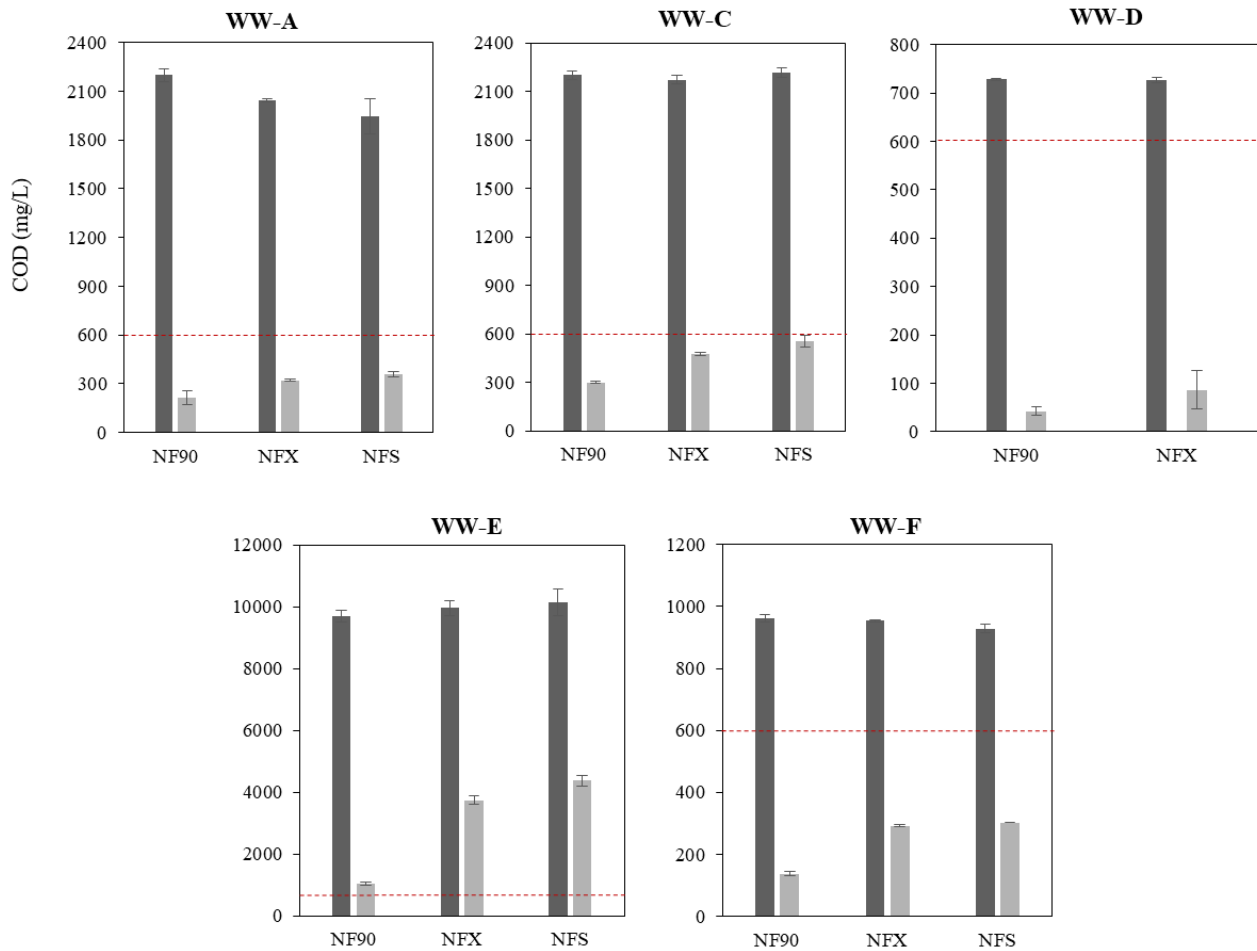


**Figure 19.** Feed and permeate COD's for 3 polymer membranes tested on 5 IWW samples.

Relatively stable permeate flux was observed during all filtration tests, except for WW-A where relative flux for NF90 and NFS membranes dropped below 0.5 (see Figure 20) within 180 minutes of filtration. Flux through NF90 membrane ranged between 5.2-20.6 LMH, with lowest flux observed for WW-C and highest for WW-D, with an average flux of 12.7 LMH. Since WW-C and WW-D have the highest and the lowest feed CODs respectively, permeate flux was found to be weakly negatively correlated with feed COD (correlation coefficient for NF90 = -0.55). A higher permeate flux was achieved by NFX when compared to NF90 for all IWW samples (see Figure 20)

in the range 15.4-23.7 LMH with an average flux of 19.7 LMH. Since NF90 was better at rejecting COD than NFX for all IWW samples, a clear trade-off between rejection and flux could be seen. Highest permeate flux was achieved by NFS at the cost of lowest COD rejection. NFS achieved flux in the range 17.5-36.4 LMH with an average flux of 27.2 LMH.

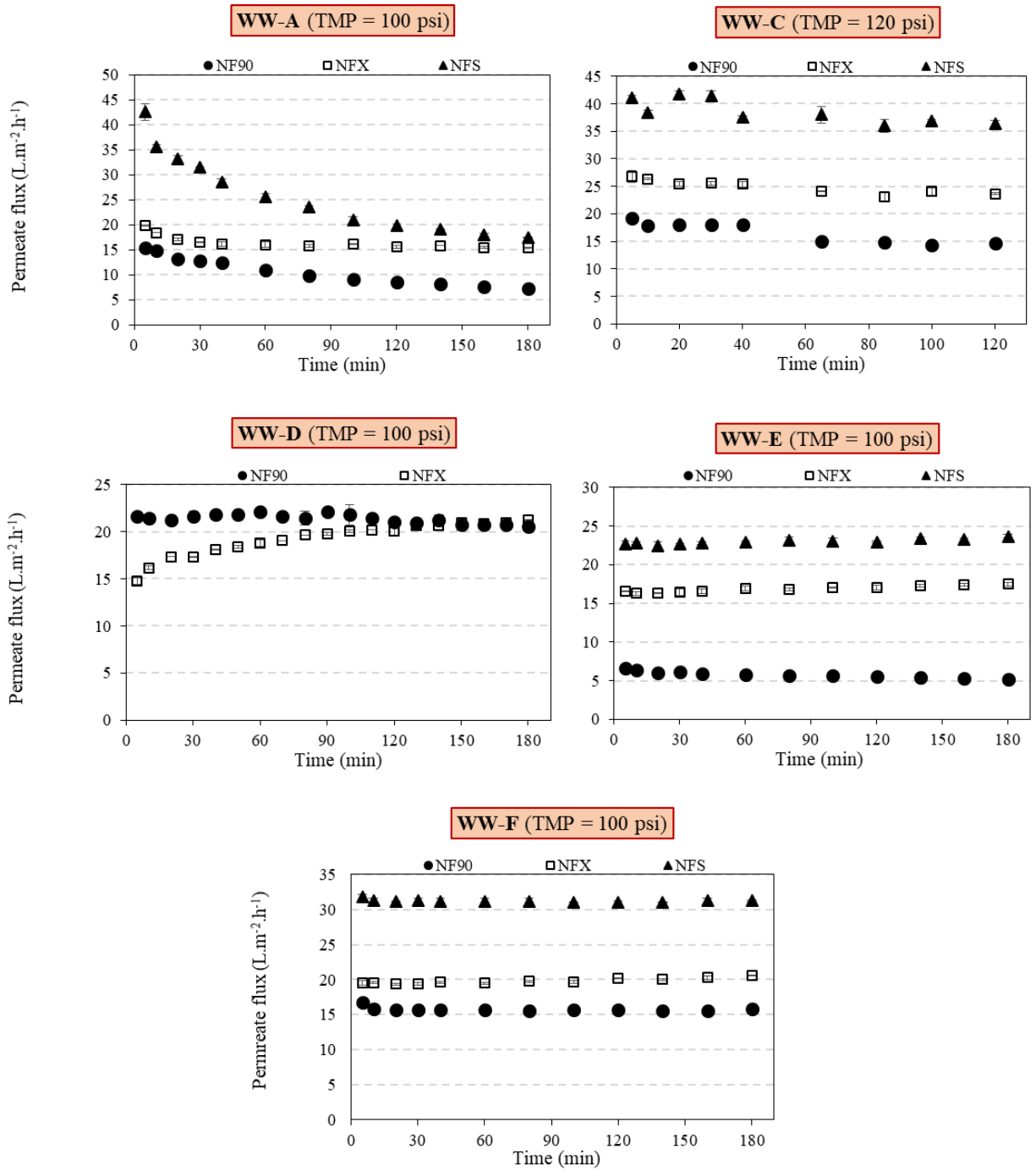


**Figure 20.** Absolute permeate flux profiles for 3 polymer membranes tested on 5 IWW samples.

4.1.2 Effect of wastewater filtration on membrane performance

Membrane permeability and salt rejection was measured for each flat-sheet membrane cutout before and after filtration. Figure 21 shows a bar graph comparison between membrane permeability (LMH/bar) of all membrane cutouts before and after filtration. Each membrane cutout was labelled with the name of IWW sample that was filtered through it (see legend in Figure 21 & 22). Averaging over all membrane cutouts available, CWP for clean membranes was found to be in the following order  $NF90 > NFS > NFX$ . Significant drop in permeability was observed for NF90 after filtration of all IWW samples. A small but clear increase in permeability was observed for NFX and NFS membranes after filtration of all WW samples. A visual inspection of NF90

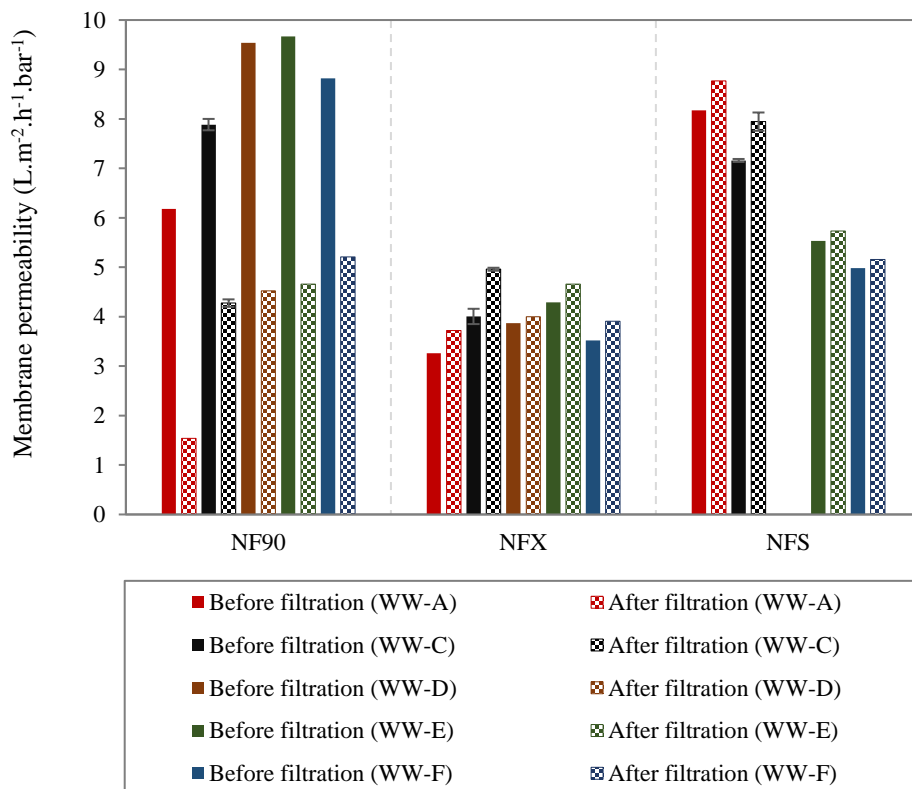


**Figure 21.** Membrane permeability (CWP) before and after filtration for polymer membranes tested on 5 IWW samples. Solid bars represents the CWP for the clean membrane cutouts before filtration and pattern bars represent the CWP of the membranes after wastewater filtration. IWW samples are denoted by different colored bars.

membrane clearly showed cake layer formation on the surface. This also explains one of the reasons behind the highest rejection achieved by NF90 despite having the highest CWP among all the 3 membranes. Accumulation of foulants on membrane surface decrease the effective pore size and therefore increases the rejection. Although the primary reason behind high rejection of NF90 membrane being its high negative surface charge due to which it is able to reject more than 98% of monovalent ions and consequently showing highest rejection of ions present in IWW samples. The slight increase in permeability for NFX and NFS membranes might be due to membrane swelling (which results in increased effective pore size of the membrane) and/or membrane degradation due to chemicals present in the IWW samples.

Figure 22 shows a comparison of salt rejection performance before and after filtration for 4 IWW samples and 3 polymer membranes. Both monovalent and divalent salt rejection seem to decrease for NF90 after filtration of WW-A (monovalent: 87.5% to 82.2%, divalent: 90.9% to 80.7%), but due to a fair 10% error observed with the filtration system while measuring salt rejection of a membrane any significant change in salt rejection could not be confirmed. Salt rejections for all other cases also did not change significantly after filtration as can be seen from Figure 22.

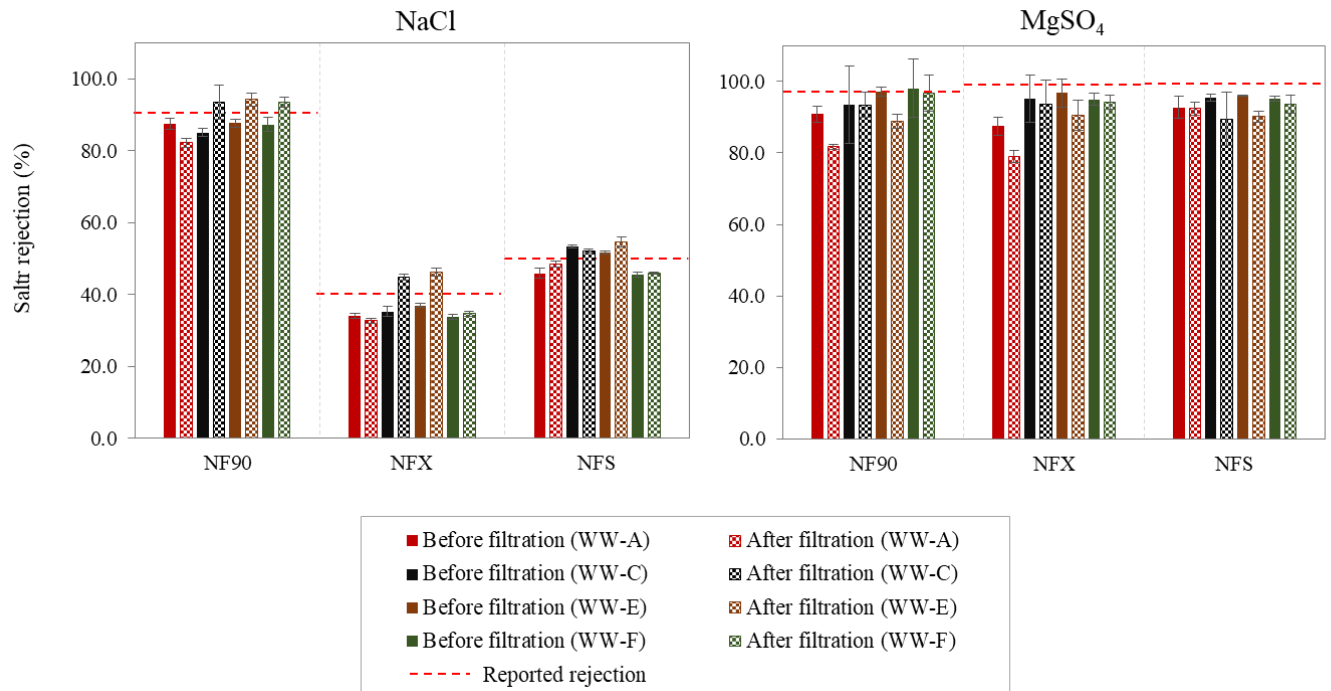


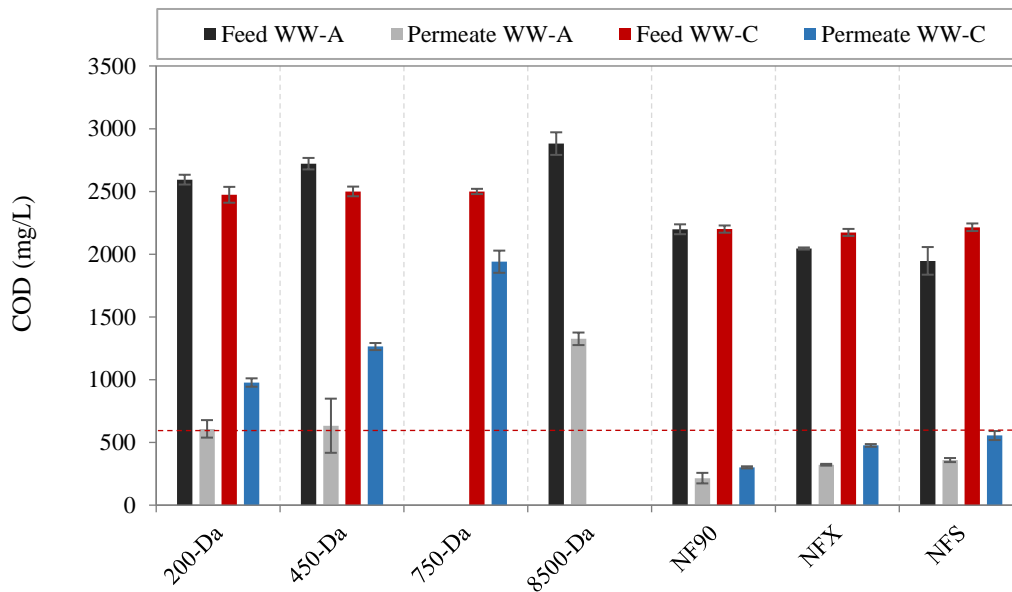
**Figure 22.** Monovalent (NaCl) and divalent (MgSO<sub>4</sub>) salt rejection performance for polymeric membranes before and after wastewater filtration. Error bars are generated using triplicate feed and permeate conductivity measurements at steady state. 4 IWW samples are denoted by different colored bars. % rejection of pristine membranes as reported by the manufacturers is shown by the red dashed line.

## 4.2 Performance comparison – Polymer vs Ceramic membranes

Two IWW samples namely WW-A and WW-C were tested on both ceramic and polymeric membranes. Performance comparison between ceramic and polymeric membranes for both of these IWW samples is shown and discussed in the following subsections

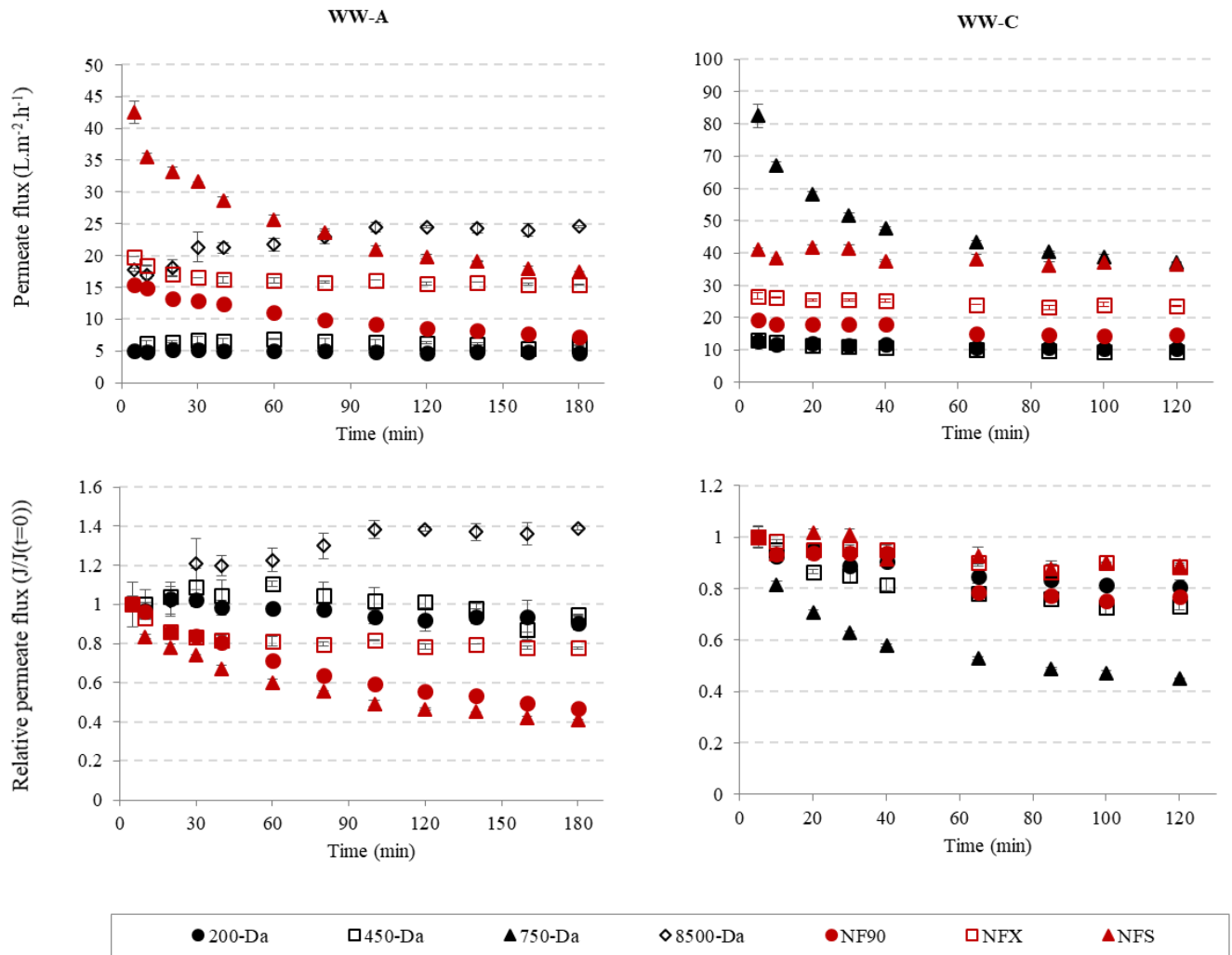
### 4.2.1 Permeate COD and wastewater flux

Figure 23 shows a bar graph comparison between COD rejected by all membranes for WW-A and WW-C. Clearly, polymer membranes were able to reject more COD than the ceramic membranes. In fact all the polymer membranes could bring the permeate COD lower than the best performing ceramic membrane 200-Da for both IWW samples. Figure 24 shows absolute and



**Figure 23.** A comparison of COD rejection between 4 ceramic NF (200-Da, 450-Da, 750-Da and 8500-Da) and 3 polymer NF (NF90, NFX, NFS) membranes on two IWW samples namely, WW-A and WW-C. Red dashed line denote the target COD of 600 mg/L for discharge at Aevitas. Feed and permeate COD values are time averaged using three time points during the filtration experiment ( $t = 10, 60, 120$  min). Error bars denote standard deviation of COD values at those three time points.

relative permeate flux comparison between ceramic and polymeric membranes which are shown using black and red markers respectively. For WW-A and WW-C, ceramic membrane 8500-Da and 750-Da achieved the highest permeate flux respectively among all membranes, but the COD rejection was very low, especially for 750-Da. Keeping the above two ceramic membranes aside, the top two panels in Figure 24 show that polymer membranes achieved higher permeate flux than 200-Da and 450-Da ceramic membranes. A higher decline in relative flux was seen for polymeric membranes as opposed to ceramic membranes for WW-A (see bottom left panel Figure 24). Relative flux for NF90, NFX and NFS dropped down to 0.46, 0.77 and 0.41, respectively, as opposed to 200-Da and 450-Da membranes which only dropped down to 0.90 and 0.94 respectively. This suggests that ceramic membranes were more fouling resistant than polymeric membranes during the 180 minute filtration period for WW-A. All membranes except 750-Da membrane observed similar decline in relative flux ( $\sim 0.8$ ) during WW-C filtration as shown in bottom right panel of Figure 24. This suggests that all membranes except 750-Da were fouled to the same extent and 750-Da was fouled the most by WW-C, with relative flux for 750-Da dropping down to 0.45 at the end of 120 minutes of filtration.



**Figure 24.** Comparison of permeate flux between ceramic NF and polymeric NF membranes. Top two panels compare the absolute flux values for WW-A and WW-C. Bottom two panels compare the relative flux values for WW-A and WW-C. 4 ceramic membranes (200-Da, 450-Da, 750-Da and 8500-Da) are shown using black markers while polymeric membranes (NF90, NFX, NFS) are shown using red markers.

4.2.2 Removal of organic compounds – GCMS analysis

GC-MS spectrum for all feed and permeate samples shown in previous sections were acquired to calculate % peak area reduction. Each spectrum was compared against a spectrum obtained for milliQ water to remove peaks that does not correspond to compounds present in wastewater. A sample of overlaid feed and permeate spectrum for 200-Da membrane and WW-A is shown in Figure 25. Notice how some peaks have reduced area and some are completely removed from the feed spectrum. Automatic peak detection was performed in ‘Bruker Data Analysis’ software with an absolute area under peak threshold equal to 100000 for all feed samples. Corresponding peaks in the permeate samples were then selected and area under peaks calculated using the software. Peak areas were corrected based on area under peak ( $m/z = 280 \pm 0.5$  u) for internal standard (Anthracene methanol). Table 12 summarizes the % peak area reduction obtained

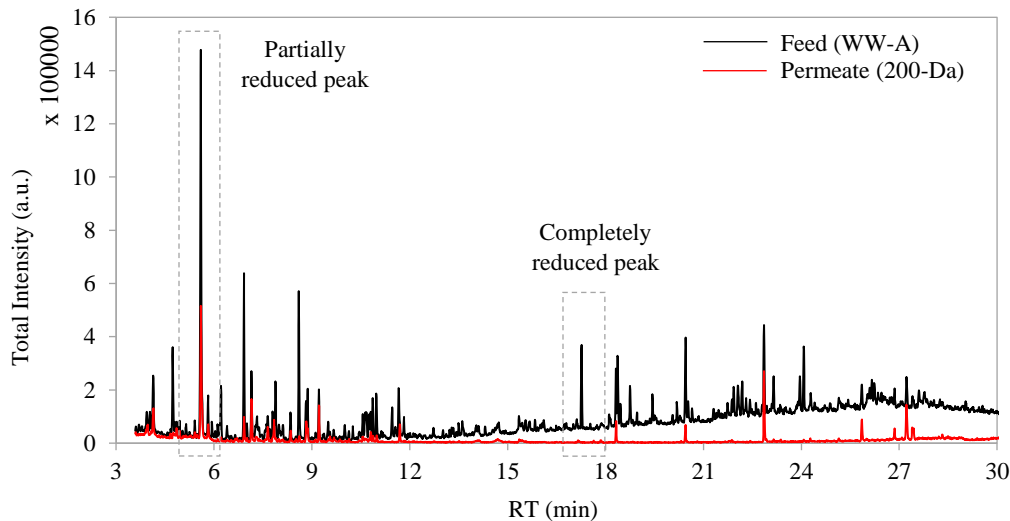


**Figure 25.** Overlaid feed and permeate GC-MS total ion chromatogram (TIC) for WW-A treated using 200-Da ceramic membrane. Example of a partially reduced peak (RT = 5.6 min) and a completely reduced peak (RT = 17.3 min) is annotated on the plot

for all 6 membranes tested with WW-A. Peaks are sorted in decreasing order (from top to bottom) of area under peak in the feed sample so that major contributors are present on top of the table. Similarly, Table 13 summarizes % peak area reduction obtained for 6 membranes tested with WW-C. Note that Table 12 & 13 does not show the relative abundance of peaks identified and other intermediate calculation steps which can be found in Appendix Tables A3-8 (one for each IWW sample). Since WW-A and WW-C were tested on both polymeric and ceramic membranes, a summary of analysis is shown in panels 'b' of Tables 12 & 13.

a.

S.No.	Peak No.	RT (min)	Compound	% Peak area rejection (WW-A)					
				200-Da	450-Da	8500-Da	NF90	NFX	NFS
1	8	5.6	?	51	44	-5	95	90	78
2	13	6.9	Nonanoic acid	79	71	13	98	95	97
3	25	8.6	N,N-Dibutylethanolamine	95	90	61	99	99	99
4	56	20.5	Octadecanoic acid	79	76	75	85	84	85
5	51	18.4	1,11-Undecanedioic acid	99	99	70	99	99	97
6	48	17.3	Decanedioic acid	100	99	68	98	99	98
7	3	4.1	Cyclohexanol	42	49	33	66	51	49
8	21	7.9	Octanoic acid	92	89	71	99	98	95
9	70	24.1	Dehydroabietic acid	95	91	63	99	98	100
10	11	6.2	2-Ethyl hexanoic acid	88	84	18	99	100	97
11	50	18.3	Hexadecanoic acid	56	52	52	67	57	59
12	27	8.9	Benzoic acid	70	79	28	97	87	83
13	53	18.8	?	95	98	91	99	99	96
14	63	22.2	Ricinoleic acid	98	97	95	99	97	99
15	62	22.1	?	99	91	80	97	99	97
16	37	11	?	80	70	2	98	95	92
17	69	24	?	98	98	83	96	97	97
18	68	23.1	?	94	78	43	99	97	97
19	9	5.8	?	44	41	5	82	79	71
20	38	11.5	?	96	89	18	97	95	95
21	16	7.3	Nonanol	72	68	16	97	91	95
22	61	21.9	?	96	93	68	98	99	96
23	36	10.9	?	80	71	-5	96	94	96
24	44	15.3	?	78	84	21	97	86	82
25	1	3.9	Propan-1,2-diol	15	6	31	22	15	32
26	18	7.6 <sup>(1)</sup>	?	35	41	-9	93	65	56
27	19	7.8	?	72	71	6	99	95	99
28	80	27.6	?	94	88	95	92	94	90
29	32	10.6 <sup>(1)</sup>	?	80	68	4	96	94	97
30	81	27.8	?	88	88	90	90	93	97
31	57	20.5	Oleic acid	98	98	95	97	96	97
32	33	10.7	?	81	76	-4	96	98	98
33	76	26.2	?	97	96	-13	96	94	94
34	59	21.7	?	85	81	82	87	88	84
35	54	19.4	Dodecanedioic acid	98	98	85	98	97	95
36	71	24.3	?	83	88	74	92	80	80
37	31	10.6 <sup>(2)</sup>	?	58	44	-22	95	68	69
38	74	26	?	83	85	74	91	74	89
39	52	18.5	?	97	96	93	98	97	96
40	75	26.1	?	94	94	25	98	97	95
41	34	10.8 <sup>(1)</sup>	?	82	75	-9	97	96	100
42	55	20.2	?	91	92	26	99	98	97
43	41	11.8	?	93	89	9	97	97	98
44	77	26.2	?	85	99	27	92	96	94
45	35	10.8 <sup>(2)</sup>	2-Phenoxy ethanol	44	26	-24	94	38	27
46	22	8	?	85	81	29	100	97	96
47	47	15.7	?	96	97	68	93	87	96
48	29	9.5	?	76	80	12	95	90	99
49	42	13.6	?	97	96	33	99	99	96
50	46	15.5	?	89	85	62	92	91	85
51	72	25.2	?	72	76	61	92	68	86
52	7	5.4	Phenol	63	87	0	100	84	78
53	23	8.1	?	84	80	22	97	96	98
54	45	15.4	?	79	53	39	91	82	77
55	39	11.6	?	90	95	15	97	91	96
56	43	14	?	84	79	22	90	91	85

57	30	10	Benzeneacetic acid	91	84	65	87	74	86
58	60	21.9	?	82	65	14	94	95	100
59	65	22.4	?	85	92	49	97	94	97
60	12	6.4	?	88	73	33	95	92	87
61	4	4.8	Octanol	62	92	86	90	88	88
62	17	7.6 <sup>(2)</sup>	?	76	71	19	98	93	90
63	5	4.9	Lactic acid	9	29	37	12	-8	7
64	2	4	Pentanoic acid	78	51	27	84	88	77
65	58	20.7	?	89	96	89	95	99	90
66	49	18.1	?	90	85	63	96	91	96
67	64	22.3	?	92	96	64	99	95	97
68	15	7.3	?	69	47	-15	96	96	71
69	10	5.9	?	88	100	79	96	99	89
70	6	4.9	Heptan-2-ol	36	37	30	84	79	50
Rejection > 90%				26	24	5	59	48	42

**b.**

Criteria	Compound / RT(min)
Diff > 15% & Polymeric > 90%	5.6, Nonanoic acid, Benzoic acid, 11.0, Nonanol, 10.9, 7.6 <sup>(1)</sup> , 7.8, 10.6, 10.7, 10.8, 2-phenoxy ethanol, 8, 9.5, 25.2, 7.6 <sup>(2)</sup> , 7.3
Diff > 15% & Ceramic > 90%	None
Ceramic > 90% & Polymeric > 90%	N,N-Dibutylethanolamine, 1,11-Undecanedioic acid, Decanedioic acid, Octanoic acid, Dehydroabietic acid, 18.8, Ricinoleic acid, 22.1, 24, 23.1, 11.5, 21.9, 27.6, Oleic acid, 26.2, Dodecanedioic acid, 18.5, 26.1, 20.2, 11.8, 26.2, 15.7, 13.6, 11.6, 22.4, Octanol, 20.7, 18.1, 22.3, 5.9
Diff > 15% & Ceramic < Polymer < 90%	Cyclohexanol, 5.8, Heptan-2-ol
Diff > 15% & Polymeric < Ceramic < 90%	None
Diff < 15% & Ceramic < 90% & Polymeric < 90%	Octadecanoic acid, Hexadecanoic acid, Propan-1,2-diol, 21.7, Lactic acid, Pentanoic acid

**Table 12. a.** Organic compounds rejection for 6 membranes tested on WW-A. Peaks are sorted in decreasing order of area under peak found in the feed sample, so major contributors to organic concentration are found towards the top of the table. Unidentified peaks are marked using ‘?’. Compounds/peaks which observed more than or equal to 90% rejection are highlighted in green. A count of total peaks reduced ( $\geq 90\%$ ) is present in the last row for each membrane out of 70 peaks. **b.** Segregation of peaks based on 6 different criterias to analyze the differences in rejection for ceramic and polymeric membranes, where ‘Diff’ stands for  $|\text{Polymeric} - \text{Ceramic}|$ . For unidentified peaks, corresponding retention time (RT) is mentioned.

**a.**

S.No	Peak No.	RT (min)	Compound	% Peak area rejection (WW-C)					
				200-Da	450-Da	750-Da	NF90	NFX	NFS
1	15	6.2	2-Ethyl hexanoic acid	91	71	39	100	98	96
2	78	18.4	1,11-Undecanedioic acid	98	90	63	100	99	100
3	39	8.8	Benzoic acid	66	47	25	84	93	90
4	20	6.9	?	89	67	41	100	98	97
5	48	10.5 <sup>(1)</sup>	?	73	36	20	97	36	37
6	12	5.6	?	68	31	17	96	77	70
7	80	19.4	Dodecanedioic acid	99	93	67	100	100	100
8	75	17.3	Decanedioic acid	100	95	64	100	100	100
9	16	6.4	?	88	59	30	100	93	88
10	66	13.5	?	92	67	36	99	97	98
11	24	7.3	?	86	70	40	99	99	97
12	58	11.4	?	96	79	53	100	99	100
13	32	7.8	?	82	70	41	98	97	98
14	30	7.6	?	85	68	34	99	98	92
15	29	7.5	?	87	43	30	99	93	92
16	55	11	?	94	79	49	100	99	98
17	22	7.1	?	64	51	32	82	73	78
18	54	10.9	?	95	80	50	99	99	99
19	25	7.4	?	81	73	33	98	91	89
20	14	6.1	?	89	59	34	99	94	91
21	2	4	Pentanoic acid	100	75	62	100	99	96
22	49	10.6	2-Methyl benzoic acid	76	45	28	99	87	86
23	67	13.6	?	99	85	66	100	94	100
24	5	4.7	?	97	68	38	96	89	80
25	70	15.7	?	100	98	70	99	100	100
26	47	10.5 <sup>(2)</sup>	?	76	43	26	99	51	50
27	79	18.4	?	100	99	76	99	99	100
28	50	10.6	?	95	72	40	99	99	100
29	33	7.9	?	85	67	41	100	98	100
30	46	10.3	?	99	98	72	100	98	99
31	52	10.7 <sup>(1)</sup>	?	97	81	46	100	100	100
32	9	5.1	Hexanoic acid	97	79	61	94	94	98
33	34	8	?	90	68	38	100	100	99
34	51	10.7 <sup>(2)</sup>	?	98	69	38	100	99	100
35	27	7.5	?	93	73	35	97	97	80
36	83	20.5	Octadecanoic acid	72	49	45	81	81	84
37	3	4.1	Cyclohexanol	58	39	38	57	61	52
38	36	8.1	?	96	83	44	100	97	99
39	59	11.5	?	99	81	64	98	98	98
40	11	5.4	Phenol	45	10	12	97	50	10
41	77	18.3	Hexadecanoic acid	62	38	41	76	60	76
42	26	7.4	?	90	74	11	100	93	79
43	62	12.2	?	70	14	9	99	57	41
44	61	12.1	?	72	40	23	87	52	53
45	17	6.4	?	97	78	40	89	88	73
46	31	7.7	?	89	81	39	100	99	100
47	28	7.5	?	97	90	24	100	92	100
48	53	10.8	?	71	33	32	98	53	40
49	86	21.9	?	100	99	77	94	98	97
50	6	4.8	2-Ethyl hexanol	89	27	43	91	75	57
51	72	16.1	Nonanedioic acid	100	96	67	99	97	92
52	56	11.1	?	98	92	81	100	99	100
53	21	7	Benzyl alcohol	50	-38	5	87	59	31
54	71	16	?	97	94	71	95	97	87
55	8	5	Ethylene glycol butyl ether	86	-9	31	100	88	61
56	44	10	Benzeneacetic acid	98	94	25	98	96	88

57	23	7.2	?	87	92	33	93	80	88
58	65	13.4	?	99	100	95	100	93	99
59	74	17.1	?	64	70	69	100	78	72
60	64	12.7	Salicylic acid	84	69	29	98	92	77
61	57	11.2	?	93	92	79	97	98	100
62	18	6.5	?	76	75	50	87	88	85
63	73	16.8	?	100	90	61	96	100	96
64	42	9.5	?	100	57	10	92	96	96
65	68	14	?	94	94	62	100	95	100
66	45	10.1	?	75	33	28	100	94	98
67	7	4.9	Propan-1,2-diol	84	-19	39	78	58	37
68	63	12.6	?	93	100	67	100	100	98
69	35	8	?	82	56	20	100	84	70
70	81	19.6	?	97	92	81	95	81	96
71	82	20.1	?	95	100	60	98	99	98
72	41	9.4	?	95	72	29	96	98	94
73	69	15.6	?	98	94	68	97	98	100
74	85	21.8	?	91	89	76	97	97	99
75	10	5.2	?	69	48	52	90	79	80
76	84	21.4	?	100	84	81	94	99	98
Rejection > 90%				41	21	1	66	52	45

**b.**

Criteria	Compound / RT(min)
Diff > 15% & Polymeric > 90%	Benzoic acid, 10.5 <sup>(1)</sup> , 5.6, 7.8, 7.6, 7.4, 2-methyl benzoic acid, 10.5 <sup>(2)</sup> , 7.9, Phenol, 12.2, 17.1, Salicylic acid, 10.1, 8, 5.2
Diff > 15% & Ceramic > 90%	None
Ceramic > 90% & Polymeric > 90%	2-ethyl hexanoic acid, 1,11-undecanedioic acid, Dodecanedioic acid, Decanedioic acid, 13.5, 11.4, 11, 10.9, Pentanoic acid, 13.6, 4.7, 15.7, 18.4, 10.6, 10.3, 10.7 <sup>(1)</sup> , Hexanoic acid, 8, 10.7 <sup>(2)</sup> , 7.5, 8.1, 11.5, 7.5, 21.9, Nonanedioic acid, 11.1, 16, Benzeneacetic acid, 13.4, 11.2, 16.8, 9.5, 14, 12.6, 19.6, 20.1, 9.4, 15.6, 21.8, 21.4
Diff > 15% & Ceramic < Polymer < 90%	7.1, 12.1, Benzyl alcohol
Diff > 15% & Polymeric < Ceramic < 90%	None
Diff < 15% & Ceramic < 90% & Polymeric < 90%	Octadecanoic acid, Cyclohexanol, Hexadecanoic acid, 6.5, Propan-1,2-diol

**Table 13. a.** Organic compounds rejection for 6 membranes tested on WW-C. Peaks are sorted in decreasing order of area under peak found in the feed sample, so major contributors to organic concentration are found towards the top of the table. Unidentified peaks are marked using ‘?’. Compounds/peaks which observed more than or equal to 90% rejection are highlighted in green. A count of total peaks reduced ( $\geq 90\%$ ) is present in the last row for each membrane out of 76 peaks. **b.** Segregation of peaks based on 6 different criterias to analyze the differences in rejection for ceramic and polymeric membranes, where ‘Diff’ stands for  $|\text{Polymeric} - \text{Ceramic}|$ . For unidentified peaks, corresponding retention time (RT) is mentioned.

The best performing ceramic membrane in terms of COD rejection (200-Da) was found to remove 26 out of 70 peaks for WW-A and 41 out of 76 peaks for WW-C. On the other hand, the best performing polymeric membrane for COD rejection (NF90) could remove 59 out of 70 peaks for WW-A and 66 out of 76 peaks for WW-C. Based on analysis tables shown in panel b of Table 12 & 13, all peaks that were removed by a ceramic membrane were also removed by a polymeric membrane but not vice-versa. 17 peaks including compounds like benzoic acid, nonanoic acid, nonanol and 2-phenoxy ethanol were removed by polymeric membranes but not by a ceramic membrane for WW-A (see Table 12.b.). 16 peaks including compounds like benzoic acid, 2-methyl benzoic acid, phenol and salicylic acid were removed by polymeric membranes but not by a ceramic membrane for WW-C (see Table 13.b.). Surprisingly, a majority of aromatic compounds identified in WW-C were removed using a polymeric membrane but not by a ceramic membrane. RT=5.6 min, RT=7.8 min, RT=7.6 min and RT=8.0 min also belonged to this class of compounds and were found both in WW-A and WW-C. Other compounds like N,N-dibutylethanolamine, 1,11-undecanedioic acid, decanedioic acid, octanoic acid, dehydroabiatic acid, ricinoleic acid, oleic acid, dodecanedioic acid, octanol, 2-ethyl hexanoic acid, nonanedioic acid, benzene acetic acid, RT=13.6 min, RT=15.7 min, RT=11.5 min were removed more than 90% both by ceramic and polymeric membranes. A small class of compounds like cyclohexanol, propan-1,2-diol, octadecanoic acid and hexadecanoic acid were not removed effectively by either polymeric or ceramic membranes. Cyclohexanol and propan-1,2-diol had low molecular weights (100 and 76 g/mol respectively) and therefore low rejections. Incomplete rejection phenomena for octadecanoic acid and hexadecanoic acid was observed for multiple wastewater samples and average rejections (50-70%) were observed in all cases but the real reason behind this observation is still unknown.

### **4.3 Predictive modeling using GC-MS compound removal dataset**

#### *4.3.1 Introduction*

IWW may contain up to 100 different organic compounds in a single batch of wastewater. Every batch of wastewater received by Aevitas has a different composition of compounds present in it, mostly due to working with numerous clients and changes in client's day-to-day activities in generating wastewater. Nanofiltration treatment of such a WW is able to reject every organic to a certain degree which ranges from anywhere between 0 to 100 % depending on physical and chemical properties of that compound, interaction with the membrane and interaction with other compounds in the wastewater matrix. This % rejection value for each component in the wastewater can be measured using Gas chromatography-Mass spectroscopy (GC-MS) of the feed and permeate (treated wastewater) samples from lab scale testing. A dataset of % rejection of all the compounds identified and all the membranes tested can then be used to build regression models for prediction on unseen compounds. A good model can eliminate the need for lab scale testing and help in decision making for eg. choosing membranes, deciding future treatment steps etc. This section shows such a predictive model building approach and testing results for compounds identified in 6 real IWW samples when tested with 5 nanofiltration membranes.

A large peak rejection dataset was collected as shown in Tables 12, 13 and Tables A3-8 in Appendix. In this section, we attempt to build model(s) for predicting % peak area rejections for each membrane. Rejection results were combined into a single table (Table A2) by only keeping the peaks that were matched with library compounds. Rejections for compounds that occurred in multiple wastewaters were averaged and the error values show the standard deviation in rejection observed for that compound. Note that the magnitude of error values shows the variation in rejection of a compound across different wastewaters. Interestingly, most of the compounds that

occurred in multiple wastewaters had low error values and therefore similar rejection values were observed except for a few compounds which are highlighted in Table A2 (see Appendix). Based on this observation, the following modeling exercise assumes that compound rejection is only affected by the physical/chemical properties of the compound and membrane and does not depend on interaction with other compounds in the wastewater matrix.

Separation of organic compounds during nanofiltration depends on numerous factors and their contributions to the degree of rejection cannot be captured in a first principles model easily. However, it is known that for any class of compounds for e.g. polyethylene glycols (PEGs), % rejection by a membrane is related to the molecular weight (MW) of the compound through characteristic rejection curve which is typically used to determine a membrane's molecular weight cut off (MWCO). Other chemical properties like acid dissociation constant (pKa) in conjunction with solution pH describes the extent to which a compound is dissociated and present in its ionic form. This affects rejection depending on the attractive/repulsive electrostatic force experienced due to surface charges present on the membrane. 4 such chemical properties are selected to describe the properties of the compounds in our dataset :

- a. Molecular weight (MW)
- b. Acid dissociation constant (pKa)
- c. Octanol-water partition ( $K_{ow}$ )
- d. Solubility in pure water at 20 °C (Sol)

A compound-property dataset was collected using online NCBI (National Center for Biotechnology Information) database and concatenated with the membrane rejections from lab scale testing to get a final dataset shown in Table 14. Input matrix (MW, pKa,  $K_{ow}$ , Sol) will be referred as 'X' and output matrix containing rejections (200-Da, 450-Da, 750-Da, 8500-Da, NF90, NFX, NFS) will be referred as 'Y' from here on in the report. The dataset is segregated into training and testing sets for the purpose of demonstrating prediction of the final trained model on unseen observations. 7 out of 41 observations were randomly selected and removed from the original dataset to make a testing set with 7 observations and a training set with 34 observations. The testing set observations are highlighted in Table 14.

S.No	RT (min)	Compound	MW (g/mol)	pKa	K <sub>ow</sub>	Sol (g/L)	% rejection (Observed)						
							200 Da	450 Da	750 Da	8500 Da	NF90	NFX	NFS
1	9.7	Diethylene glycol butyl ether	162	15.12	0.56	997	-	-	-	-	100	80	78
2	6.5	Heptanoic acid	130	4.4	2.42	2.82	-	-	-	-	98	96	93
3	9.5	Pentanedioic acid	132	4.34	-0.29	638	-	-	-	-	96	95	91
4	10.6	o-Methyl benzoic acid	136	3.96	2.46	1.18	-	-	-	-	98	95	87
5	10.5	6-Hydroxyhexanoic acid	132	4.71	0.62	69.7	-	-	-	-	98	98	93
6	8.8	1,1,1-Tris(hydroxy methyl) propane	134	14.01	-1.48	1000	-	-	-	-	72	70	53
7	7.5	1-Methyl pyrrolidinone	99	17	-0.38	999	-	-	-	-	98	72	51
8	6	Benzonitrile	103	19.33	1.56	2.06	-	-	-	-	97	69	39
9	3.9	Styrene	104	20	2.95	0.3	25	0	12	-	-	-	-
10	6.1	2-Butanol	74	17.6	0.61	181	87	67	47	-	-	-	-
11	8.1	2-Phenyl ethanol	122	15.88	1.36	20	79	40	27	-	-	-	-
12	6.9	Nonanoic acid	158	5.23	3.42	0.284	79	71	-	13	98	97	97
13	8.6	N,N-Dibutylethanolamine	173	14.77	2.65	3.46	95	90	-	61	99	99	99
14	20.5	Octadecanoic acid	284	4.95	7.4	0.0005	75	62	45	75	83	83	85
15	18.4	1,11-Undecanedioic acid	216	4.65	2.7	5.1	99	95	63	70	99	99	98
16	17.3	Decanedioic acid	202	4.72	2.1	1	100	97	64	68	99	100	99
17	4.1	Cyclohexanol	100	18.18	1.2	42	50	44	38	33	61	56	50
18	7.9	Octanoic acid	144	4.89	3.05	0.789	92	89	-	71	98	97	94
19	24.1	Dehydroabiatic acid	300	4.55	4.8	0.006	95	91	-	63	99	98	100
20	6.2	2-Ethyl hexanoic acid	144	5.14	2.64	2	89	77	39	18	99	99	97
21	18.3	Hexadecanoic acid	256	4.95	6.4	0.00004	58	49	35	52	70	62	63
22	8.9	Benzoic acid	122	4.2	1.9	3.4	68	63	25	28	94	90	86
23	22.2	Ricinoleic acid	298	4.99	6.19	3.46	98	97	-	95	99	97	99
24	7.3	Nonanol	144	16.84	3.77	0.14	72	68	-	16	97	91	95
25	3.9	Propan-1,2-diol	76	14.47	-0.9	998	50	0	39	31	64	42	32
26	20.5	Oleic acid	282	4.99	7.64	0.00001	98	98	-	95	97	96	97
27	19.4	Dodecanedioic acid	230	4.65	3.2	0.04	98	95	67	85	99	99	99
28	10.8	2-Phenoxy ethanol	138	15.1	1.16	26	44	26	-	0	95	41	36
29	5.4	Phenol	94	9.98	1.5	82	54	49	12	0	99	67	44
30	10	Benzeneacetic acid	136	4.55	1.4	16.6	95	89	25	65	93	85	87
31	4.8	Octanol	130	17.7	3.1	1.1	62	92	-	86	91	91	87
32	4.9	Lactic acid	90	3.86	-0.72	999	9	29	-	37	12	0	7
33	4	Pentanoic acid	102	4.81	1.4	24	89	63	62	27	94	86	84
34	4.9	Heptan-2-ol	116	17.68	2.31	3.5	36	37	-	30	84	79	50
35	10.6	2-Methyl benzoic acid	136	3.96	2.5	1.1	76	45	28	-	99	87	86
36	5.1	Hexanoic acid	116	5.09	1.9	10.3	97	79	61	-	96	95	95
37	4.8	2-Ethyl hexanol	130	17.7	3.1	1.1	89	27	43	-	91	75	57
38	16.1	Nonanedioic acid	188	4.15	1.6	2.4	100	96	67	-	99	98	95
39	7	Benzyl alcohol	108	15.02	1.1	42.9	50	2	5	-	85	37	29
40	5	Ethylene glycol butyl ether	118	15.12	0.8	998	86	15	31	-	97	63	54
41	12.7	Salicylic acid	138	2.79	2.3	2.2	84	69	29	-	98	92	77

**Table 14.** Complete dataset showing 41 observations, 4 input variables (MW: Molecular weight, pKa: Dissociation constant, K<sub>ow</sub>: Octanol-water partition coefficient, Sol: Solubility) and 7 output variables (one for each membrane tested 200-Da, 450-Da, 750-Da, 8500-Da, NF90, NFX and NFS). 7 highlighted observations were selected randomly and separated into a testing dataset; remaining observations were used for training models.

#### 4.3.2 Preliminary PLS model

A partial least squares (PLS) model is a functional mapping between an input matrix (X) and output matrix (Y) described using equations 5 & 6 shown below. Error matrices E and F\* (in  $X = TP' + E = \sum t_h p'_h + E$  and  $Y = UQ' + F^* = \sum u_h q'_h + F^*$ ) are minimized while maximizing correlation between X and Y ( $\hat{u}_h = b_h t_h$ ) using the NIPALS PLS algorithm [58] to learn model parameters p, q and b. Once the simplified model parameters w\* and c are calculated using p, q and b, predictions can be made for new observations using equations 5 & 6. PLS regression has been accepted as a robust modeling method when dealing with multivariate dataset such as ours.

$$\mathbf{T}_{(N \times A)} = \mathbf{X}_{(N \times K)} \mathbf{w}^*_{(K \times A)} \quad (5)$$

$$\hat{\mathbf{Y}}_{(N \times M)} = \mathbf{T}_{(N \times A)} \mathbf{c}'_{(A \times M)} = \mathbf{X}_{(N \times K)} \mathbf{w}^*_{(K \times A)} \mathbf{c}'_{(A \times M)} \quad (6)$$

where, N = number of observations,

A = number of components in PLS model,

K = number of input variables (K=4 for our case),

M = number of output variables (M=5 for our case)

A PLS model was built using Aspen ProMV on training set with 26 observations, 4 input variables (MW, pKa, K<sub>ow</sub>, Sol) and 5 output variables (200-Da, 450-Da, NF90, NFX and NFS). 750-Da and 8500-Da membrane were excluded from the model due to less number of observations. Score and loadings plot for this model are shown in Figure 26, panels 'c' and 'b', respectively. Model summary (output-space) is shown in Figure 26, panel 'a'. The loadings plot shows that rejections from all 5 membranes are positively correlated with each other due to tightly clustered red markers in the third quadrant. Also, the rejections are negatively correlated with both 'pKa' and

‘Solubility’ because both variables are present in the exact opposite quadrant with a high magnitude of  $w^*$  values. The first component of the model suggests that MW is correlated with rejections and therefore compounds with high MW are easily rejected, but the second component shows otherwise, hence they are only weakly positively correlated. The score plot shows clustering of compounds. A closer look at ‘regions-A’ and ‘region-C’ marked in Figure 26 shows that region-A has all carboxylic acids while compounds in region-C are all some form of alcohol. Region-B formed in the 2<sup>nd</sup> quadrant of the score plot has 5 long chain monocarboxylic acids (C<sub>16</sub>-C<sub>20</sub>). The combination of score and the loadings plot also reveals that on an average dicarboxylic acids have high rejections (>90 %) followed by intermediate rejections (80-90 %) for monocarboxylic acids followed by the least rejections for alcohols since the direction of increasing rejection is defined by the ‘c’ loadings vector, moving along the opposite direction in the score plot will decrease rejection predictions. Score plot also reveals that Lactic acid does not follow this general trend and have very low rejections (<30 %).

Although weak correlations can be learnt using this PLS model it is not the best model for prediction since the  $R^2$  &  $Q^2$  for Y-space using 2 components is 0.40 and 0.09, respectively. A PLS model built on all 34 training observations had even lower  $R^2$  and  $Q^2$  values. These low values indicate that the original dataset might contains subsets which are behaving very differently, or in other words, variables inside each subset might have very different effects on final rejections.

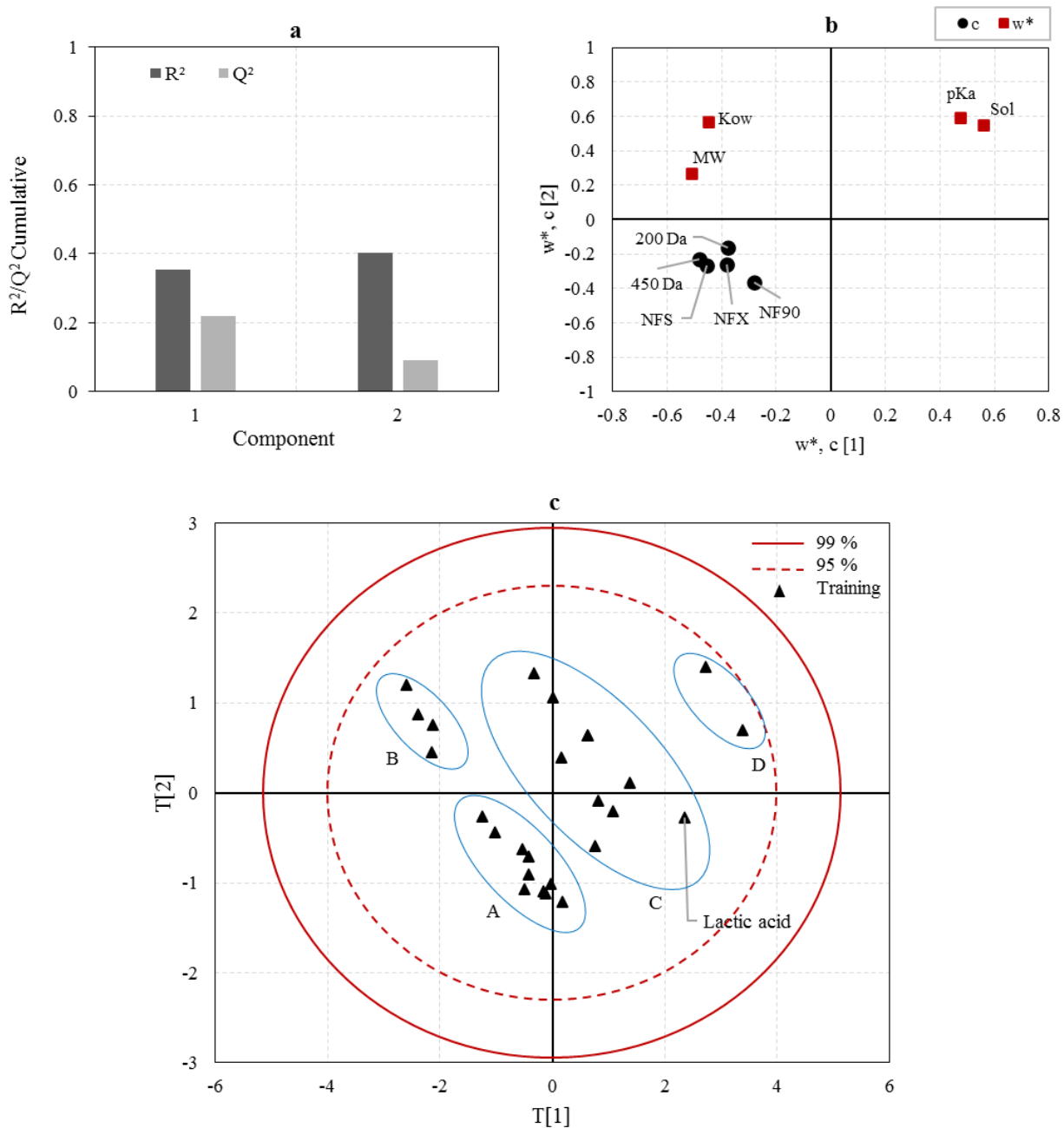


**Figure 26.** Plots for 2 component preliminary PLS model; **a.** Model summary showing  $R^2$  and  $Q^2$  values for Y-space ; **b.**  $w^*,c$  loadings plot between 1<sup>st</sup> and 2<sup>nd</sup> component; **c.** Score plot between 1<sup>st</sup> and 2<sup>nd</sup> components for the PLS model, where region A consisted of short chain monocarboxylic and dicarboxylic acids, region B had long chain monocarboxylic acids, region C consisted mainly of alcohols and regions D had short chain acids or alcohols.

#### 4.3.3 Grouped PCA-PLS predictive modeling approach

To overcome the shortcoming mentioned in the previous section, separate PLS regression models can be built for each subset. These subsets/groups can be learnt using a PCA model score plot which will automatically group together compounds with similar properties. A similar approach was followed by Dahua et al [59], where they modeled a biological indicator crucial in drug delivery by partitioning chemical compounds into clusters using a combination of 4D molecular similarity and PCA.

This combined PCA-PLS modeling approach flowchart is shown in Figure 27. First a PCA model will be trained on the inputs (MW, pKa, K<sub>ow</sub>, Sol) of the training data and subsets of compounds will be recognized using the score plot, this can be done manually or using a clustering algorithm. Observations within each group/subset will then be used to train multiple PLS models. So, if 4 groups were identified by PCA, a total of 4 PLS models will be trained. Note that for a new testing observation, the PCA model will classify the observation into one of the groups, and hence the PCA model decides which PLS model will be used to predict the output for that observation.

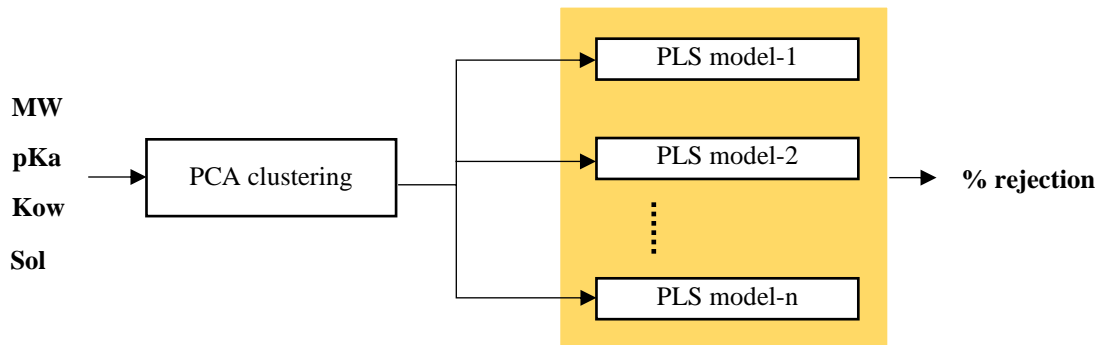


**Figure 27.** Grouped PCA-PLS modeling flowchart. The prediction layer is highlighted in yellow. Complete prediction layer is trained twice in this report, once for ceramic membranes (200-Da & 450-Da) and second time for polymeric membranes (NF90, NFX, NFS).

#### 4.3.4 Grouped PCA-PLS models training

First, a PCA model was built on X and corresponding score plot is shown in Figure 28. Note the different regions on the plot where observations are clustered. The 4 groups of compounds were manually identified using score plot which are listed in Table 15. Note that the clustering is very similar to the clustering observed in the PLS score plot earlier. Group-1 compounds consist of monocarboxylic and dicarboxylic acids, most of Group-2 compounds are alcohols, Group-3 consist of short chain ( $C_2$ - $C_5$ ) alcohols/acids, and Group-4 consist of long chain ( $C_{16}$ - $C_{20}$ ) monocarboxylic acids.

Group-1	Group-2	Group-3	Group-4
Heptanoic acid	Benzonitrile	Diethylene glycol butyl ether	Dehydroabietic acid
o-Methyl benzoic acid	Styrene	Pentanedioic acid	Ricinoleic acid
6-Hydroxyhexanoic acid	2-Butanol	1,1,1-Tris(hydroxy methyl) propane	Hexadecanoic acid
1,11-Undecanedioic acid	2-Phenyl ethanol	Propan-1,2-diol	Oleic acid
Octanoic acid	N,N-Dibutylethanolamine	Lactic acid	
2-Ethyl hexanoic acid	Cyclohexanol	Ethylene glycol butyl ether	
Benzoic acid	2-Phenoxy ethanol		
Dodecanedioic acid	Phenol		
Benzeneacetic acid	Octanol		
Pentanoic acid	2-Ethyl hexanol		
2-Methyl benzoic acid	Benzyl alcohol		
Hexanoic acid			
Salicylic acid			

**Table 15.** Grouping of chemical compounds present in the training set using PCA score plot

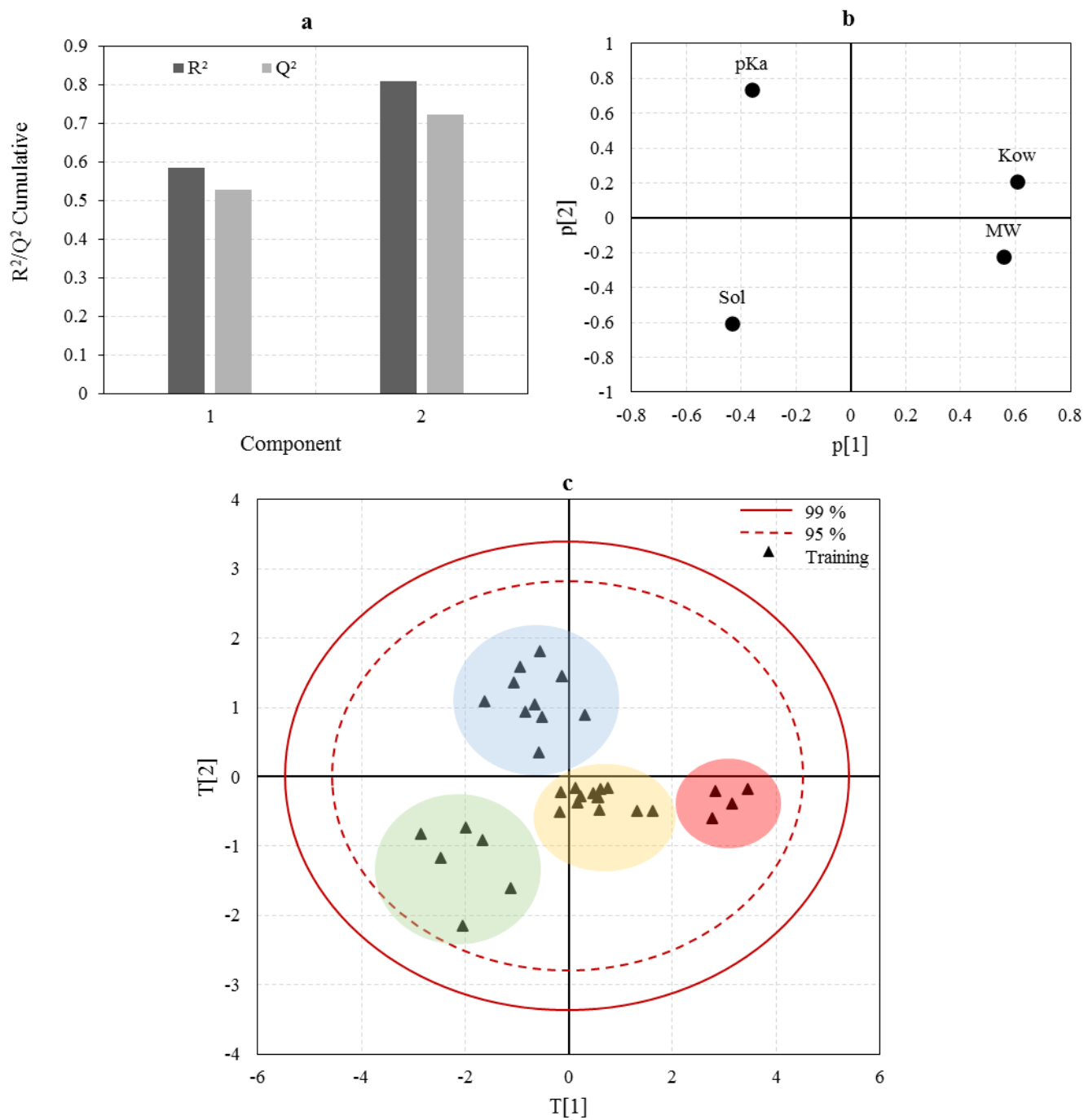


**Figure 28.** Plots for 2 component PCA model on X ; **a.** Model summary showing R<sup>2</sup> and Q<sup>2</sup> values ; **b.** Loadings plot between 1<sup>st</sup> and 2<sup>nd</sup> component, each point on the loadings plot refers to an input variable which is shown as a data label ; **c.** Score plot between 1<sup>st</sup> and 2<sup>nd</sup> components for the PCA model, compounds were found to be weakly clustered into four groups highlighted with different backgrounds on the plot (gold: Group-1, blue: Group-2, green: Group-3, red: Group-4)

PLS models are now built separately for each group as shown in the model flowchart in Figure 27. Also note that the PLS model layer (PLS model-1 to PLS model-n) shown in Figure 27 is trained separately for ceramic and polymeric membranes, and therefore ceramic and polymeric PLS models have 2 (200-Da & 450-Da) and 3 (NF90, NFX, NFS) output variables respectively. In this report, the PLS models have been trained for 5 membranes. PLS models were not built for other two membranes (750-Da and 8500-Da) due to less number of observations. Following Table 16 summarizes the nomenclature for PLS models trained.

PLS models		
Group	Ceramic	Polymeric
1	C-Model-1	P-Model-1
2	C-Model-2	P-Model-2
3	-	P-Model-3
4	C-Model-4	P-Model-4

**Table 16.** PLS model nomenclature. One PLS model is trained for each group and each membrane type. No PLS model was trained for Group-3 compounds for ceramic membranes due to less number of observations

#### 4.3.5 Model training and testing results

PLS models were trained using NIPALS algorithm with leave-one-out cross validation strategy coded in Matlab. All the following results were generated using the same customized functions and verified using Aspen ProMV. Results were not generated directly using Aspen ProMV due to its inability to perform leave-one-out cross validation which is required when working with small datasets such as ours. For both ceramic and polymeric membranes, a General PLS model was also trained which is trained on all observations. This model is only shown for comparison purposes with the Grouped PCA-PLS modeling approach.

4.3.5.1 Performance metrics –  $R^2$ ,  $Q^2$ , RMSEE, RMSEP

All performance metrics are calculated on the output space (% rejection) of the models. Equations 7 to 10 are used to calculate the performance metrics for each model.

$$R^2 = 1 - \frac{\sum_{i=1}^n (y_i - \hat{y}_i)^2}{\sum_{i=1}^n (y_i - \bar{y}_i)^2} \quad \text{where } i \in \text{training set} \quad (7)$$

$$Q^2 = 1 - \frac{\sum_{i=1}^n (y_i - \hat{y}_{i,cv})^2}{\sum_{i=1}^n (y_i - \bar{y}_i)^2} \quad \text{where } i \in \text{training set, } \hat{y}_{i,cv} \text{ is cross validated prediction} \quad (8)$$

$$\text{RMSEE} = \sqrt{\frac{\sum_{i=1}^n (y_i - \hat{y}_i)^2}{n}} \quad \text{where } i \in \text{training set} \quad (9)$$

$$\text{RMSEP} = \sqrt{\frac{\sum_{i=1}^n (y_i - \hat{y}_i)^2}{n}} \quad \text{where } i \in \text{testing set} \quad (10)$$

Note that each of the outputs  $y_i$  shown in equations 7 to 10 is a vector (2 dimensional for ceramic models and 3 dimensional for polymeric) so all subtraction and squaring operations are done element wise.  $R^2$  describes how well the model performs on the training set,  $Q^2$  describes the predictive power of the model, RMSEE stands for root mean square error in estimation which is calculated on the training set, similarly RMSEP stands for root mean square error in prediction which is calculated on the corresponding testing set.

Before calculating RMSEP, testing set observations need to be classified into one of the predefined groups using the PCA model. All 7 testing observations were plotted on the PCA score plot shown in Figure 29. Based on regions defined for the 4 groups earlier, three of the compounds were estimated to be from Group-1, two from Group-2 and one each from Group-3 & 4. Table 17 lists down the testing observations and their estimated groups. Notice how the three testing

observations estimated to be from Group-1 were all acids which was our generalized idea of compounds belonging to Group-1. Similarly, the two testing observations estimated to be from Group-2 were alcohols. This shows that PCA is a great tool to automate grouping of similar compounds.

Results from model training and testing are summarized in Table 18. Low  $R^2$  and  $Q^2$  values are observed for General PLS models (Ceramic:  $R^2 = 0.40$ ,  $Q^2 = 0.12$  ; Polymeric:  $R^2 = 0.34$ ,  $Q^2 = 0.09$ ) which is why these models are not used for final predictions. On the other hand, a Grouped PCA-PLS model for ceramic membranes had an  $R^2 = 0.71$  and  $Q^2 = 0.46$ . Note that this Grouped PCA-PLS model consist of three PLS models ('C-Model-1', 'C-Model-2' and 'C-Model-4'). Metrics for each individual PLS model are also shown in the same table. Compounds from Group-2 which are modeled using 'C-Model-2' are not well predicted due to low  $Q^2$  (0.05) value, but the average predictive performance over all groups of compounds is fair with a  $Q^2 = 0.46$ . Similarly, the Grouped PCA-PLS model for polymeric membranes had an  $R^2 = 0.89$  and  $Q^2 = 0.67$  showing good predictive performance. Looking into the individual models that are within this grouped model, we find that compounds from Group-2 (model 'P-Model-2') were the most difficult to predict due to least  $Q^2$  (0.33) among the four PLS models.

Improved RMSEE was observed for Grouped PCA-PLS model (RMSEE = 19.1) when compared with General PLS model (RMSEE = 27.5) for ceramic membranes. However, only a marginal improvement in testing performance was observed (RMSEP = 22.5, 23.3 for Grouped PCA-PLS and General PLS model respectively). The Grouped PCA-PLS model for ceramic membranes is chosen over the General PLS model due to higher  $Q^2$ . For polymeric membranes, Grouped PCA-PLS model achieved good results with significantly improved metrics when

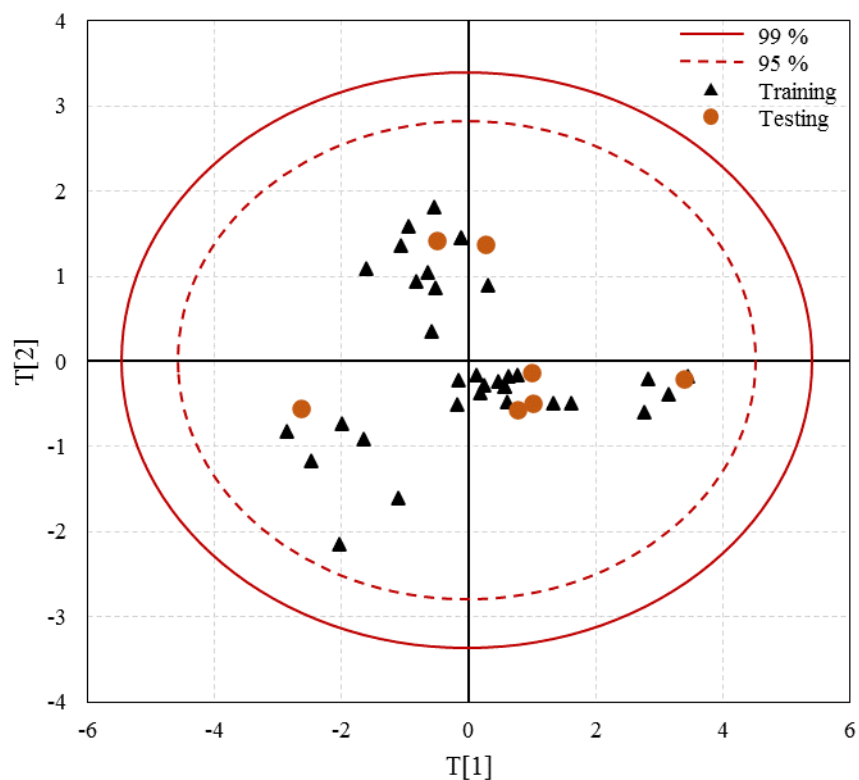


**Figure 29.** PCA score plot with both training and testing sets. Score values (T[1] & T[2]) for 7 testing set observations are shown in orange circles alongside training data to visualize how testing set observations are classified based on their position on the score plot.

Compound	Estimated Group
Nonanoic acid	1
Decanedioic acid	1
Nonanedioic acid	1
Nonanol	2
Heptan-2-ol	2
1-Methyl pyrrolidinone	3
Octadecanoic acid	4

**Table 17.** Testing set compounds and their estimated groups based on PCA score plot analysis in Figure 29.

Ceramic membrane models (2 output variables: 200-Da, 450-Da)						
Model	No. of training observations	No. of testing observations	R <sup>2</sup>	Q <sup>2</sup>	RMSEE	RMSEP
General PLS model	24	6	0.40	0.12	27.5	23.3
Grouped PCA-PLS model	24	6	0.71	0.46	19.1	22.5
C-Model-1	10	3	0.44	0.31	13.2	21.2
C-Model-2	10	2	0.52	0.05	25.9	15.2
C-Model-4	4	1	0.90	0.61	8.18	35.16
Polymer membrane models (3 output variables: NF90, NFX, NFS)						
Model	No. of training observations	No. of testing observations	R <sup>2</sup>	Q <sup>2</sup>	RMSEE	RMSEP
General PLS model	31	7	0.34	0.09	31.0	25.5
Grouped PCA-PLS model	31	7	0.89	0.67	12.6	12.3
P-Model-1	13	3	0.53	0.40	4.6	4.5
P-Model-2	8	2	0.44	0.33	22.1	12.4
P-Model-3	6	1	0.96	0.49	9.6	20.63
P-Model-4	4	1	0.90	0.57	7.5	16.4

**Table 18.** Group-wise model summary for ceramic and polymeric membranes.

Membrane	R <sup>2</sup>	Q <sup>2</sup>	RMSEE	RMSEP
200-Da	0.73	0.36	10.91	13.6
450-Da	0.71	0.51	15.6	18.01
NF90	0.85	0.50	6.9	8.1
NFX	0.90	0.68	7.4	6.0
NFS	0.91	0.74	7.5	6.9

**Table 19.** Membrane-wise performance metrics for all 5 membranes. Corresponding Grouped PCA-PLS models were used to calculate predictions for each membrane

compared to its corresponding General PLS model. More than 50% improvement in both RMSEE and RMSEP was observed for Grouped PCA-PLS model. It should be noted that the absolute values of RMSEE and RMSEP for each of the Grouped PCA-PLS models shown in Table 18 are a combination of errors in % rejection for multiple membranes, 2 membranes for ceramic membrane models and 3 membranes for polymeric membrane models. Equation 11 is the general equation relating the RMSE for individual membranes to the overall model RMSE. Individual membrane RMSE values are important in understanding how far off our model predictions lie from the actual ‘% rejection’ values. For e.g.  $RMSEP_{200-Da} = 10$  would mean that the model has a RMSE of 10% for 200-Da membrane while testing. This would imply that 68% of our testing observations have predictions within 10% of the actual membrane rejection, assuming data points are coming from a gaussian distribution. Individual membrane RMSE values are reported in Table 19 along with individual membrane  $R^2$  and  $Q^2$  values to quantify prediction performance for each membrane. Based on predictions from the Grouped PCA-PLS models, RMSEE & RMSEP for all polymer membranes was observed to be low ( $< 10$ ) as shown in Table 19. Slightly higher RMSE values were observed for 200-Da membrane with an RMSEP of 13.6. Worst training and testing performance were observed for 450-Da membrane with an RMSEP equal to 18.0, which means that on an average the error in prediction for 450-Da membrane could be as high as 18%. For all practical purposes of decision making at any industry like Aevitas, an acceptable error in performance prediction could be around 15%. Based on this assumption, it is reasonable to say that all membranes except 450-Da showed good predictability while error in prediction for 450-Da membrane were slightly above the 15% margin.

$$RMSEE_{model} = \sqrt{\sum_{i=1}^n RMSEE_i^2} \quad , \quad \text{where } n = 2, 3 \text{ for our case} \quad (11)$$

#### 4.3.5.2 Observed vs Predicted plots

Based on predictions from Grouped PCA-PLS models, observed % rejections were plotted against predicted % rejections to obtain Observed vs Predicted plots for each membrane shown in Figure 30 & 31. Both training and testing set observations are shown on the same plot. Note that both the training and testing sets shown in the plots contain observations from all the groups of compounds identified earlier using PCA modeling. For the sake of simplicity, observation from different groups are not differentiated in the plots and marked as a single large training and testing sets. Low predictability for 450-Da membrane could be seen from 450-Da plot in Figure 30. 3 testing observations out of 6 had significantly large error in prediction (>20 %). For all other membranes, a fair agreement between observed and predicted values was visible.

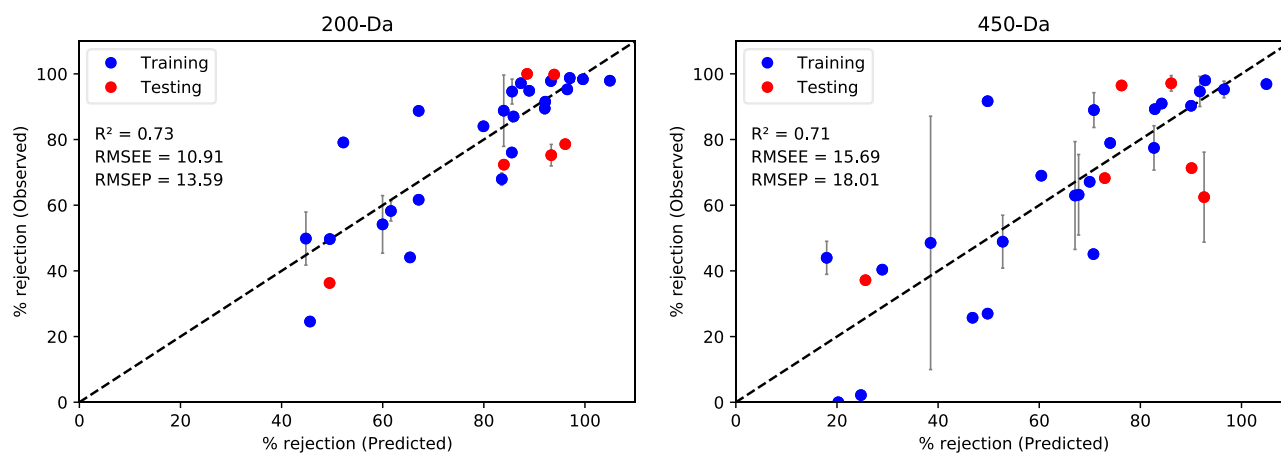


**Figure 30.** Observed vs Predicted plots for 200-Da (left) and 450-Da (right) ceramic membranes. Each point on the plot correspond to an observation either from the training set (blue) or the testing set (red).  $R^2$  and RMSEE reported on each plot are calculated using points from the training set while RMSEP is calculated using points from the testing set. Error bars denote the standard deviation in % rejection for compounds that occurred in multiple wastewater samples

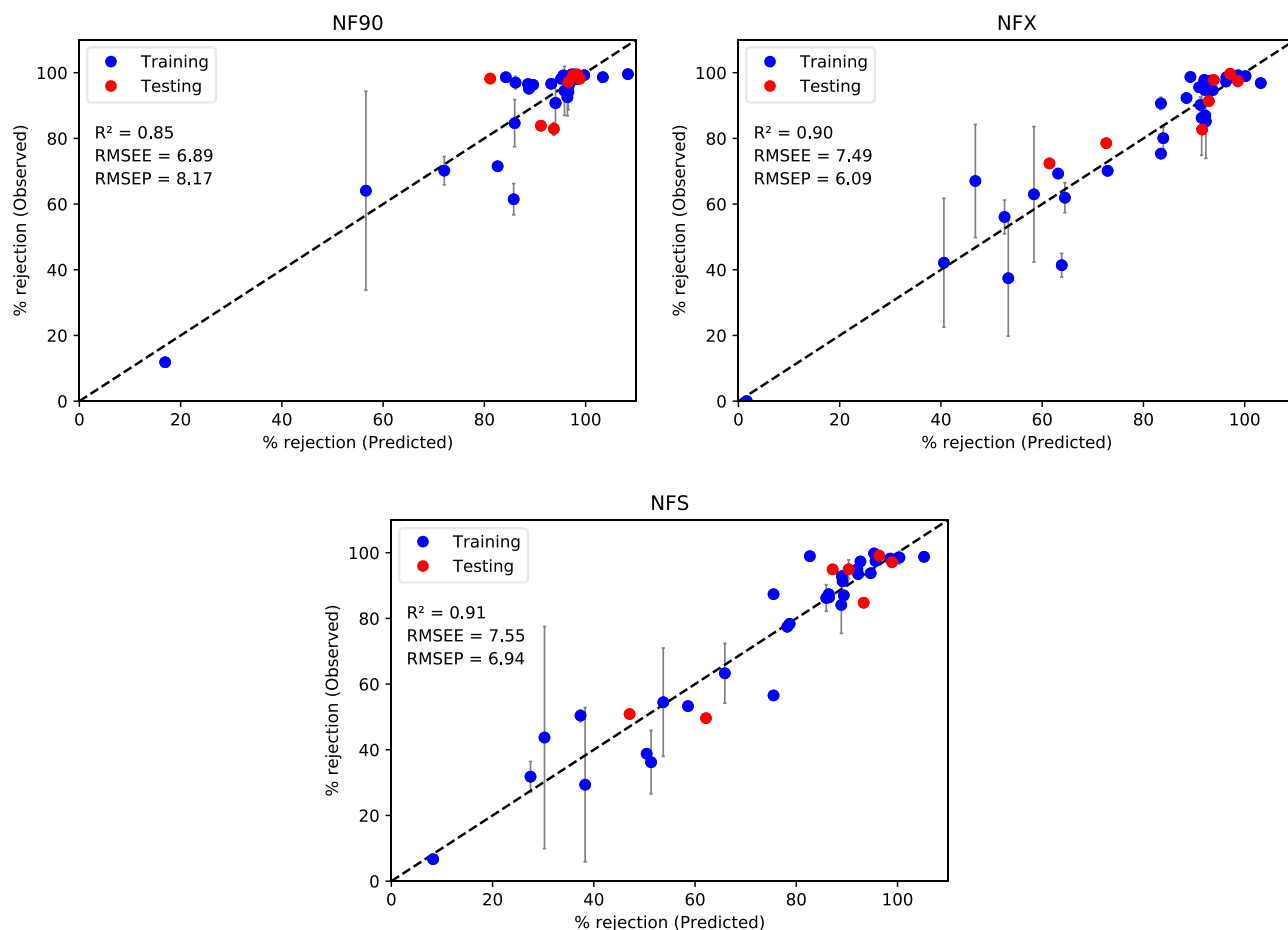


**Figure 31.** Observed vs Predicted plots for NF90 (top left), NFX (top right) and NFS (bottom) polymer membranes. Each point on the plot correspond to an observation either from the training set (blue) or the testing set (red).  $R^2$  and RMSEE reported on each plot are calculated using points from the training set while RMSEP is calculated using points from the testing set. Error bars denote the standard deviation in % rejection for compounds that occurred in multiple wastewater samples

#### 4.3.5.3 Cross testing results

A cross testing exercise was performed to emphasize the importance and benefits of Grouped PCA-PLS modeling approach for dataset such as ours. A subset from the training set corresponding to compounds from Group-1 was named ‘Train set-1’. Similarly, a subset from the testing set corresponding to compounds from Group-1 was named ‘Test set-1’. This was done for compounds belonging to all the four groups. Prediction performance metric RMSEP was then calculated for each testing subset using all models trained previously, nomenclature for which is shown in Table 16. The General PLS models were also included in this exercise where RMSEP for each test subset was calculated separately for comparison purposes to identify the best model for each test subset. Results are tabulated in Table 20.

Cross testing of models for ceramics show that some testing sets have better predictions when predicted using model trained on observations from a different group. Such instances are highlighted in red background in the table. For instance, observations from Test set-1 are better predicted using C-Model-2 when compared to predictions using C-Model-1 with RMSEP values of 12.8 and 21.2, respectively. This suggests that maybe merging training sets 1 & 2 might produce a model that is able to predict both the test sets 1 & 2 reasonably well. The overall error in prediction for this new model (RMSEP = 20.33) is slightly less than the corresponding General PLS model and Grouped PCA-PLS model but it has a significantly lower cross validated  $Q^2$  value ( $Q^2 = 0.24$ ) when compared to the old Grouped PCA-PLS model ( $Q^2 = 0.46$ ). The low RMSEP value might be an artifact of the choice of the random testing set. This leads us to believe that the old Grouped PCA-PLS model is a better model for prediction.

For polymer membranes, grouped modeling approach is clearly better than a General PLS model due to significantly higher  $Q^2$  and lower RMSEP values. This is also supported by the cross-

testing results where the RMSEP metrics show that testing observations from a particular set are only predicted well when using a model which was trained on the same class of compounds. With the General PLS model, higher RMSEE and RMSEP values are observed for each of the 4 groups. This shows that the General PLS model is providing fair predictions for all the groups while compromising on predicting a single group very well.

CERAMIC MEMBRANES								
RMSEE					RMSEP			
Subset	Train set-1	Train set-2	Train set-4	Train set-4	Test set-1	Test set-2	Test set-4	Test set-4
Number of observations	10	10	4	4	3	2	1	1
C-Model-1	13.2	-	-	-	21.2	160.1	82.4	82.4
C-Model-2	-	25.9	-	-	12.8	15.2	254.5	254.5
C-Model-4	-	-	8.1	-	193.9	169.4	35.1	35.1
General PLS model	16.9	35.6	25.5	25.5	17.4	25.2	32.8	32.8
POLYMERIC MEMBRANES								
RMSEE					RMSEP			
Subset	Train set-1	Train set-2	Train set-3	Train set-4	Test set-1	Test set-2	Test set-3	Test set-4
Number of observations	13	8	6	4	3	2	1	1
P-Model-1	4.6	-	-	-	4.5	120.1	197.2	46.8
P-Model-2	-	22.1	-	-	18.6	12.4	303.0	116.8
P-Model-3	-	-	9.6	-	210.0	268.2	20.6	327.9
P-Model-4	-	-	-	7.5	175.6	306.2	2803	16.4
General PLS model	16.6	31.4	47.9	33.7	17.3	23.5	32.3	38.8

**Table 20.** Summary of cross testing results. Cells highlighted in red are instances when a test subset was better predicted (low RMSEP) using a model that was not trained on observations from the same group as the test subset. Cells highlighted in gray show RMSEP values when a test subset was predicted using a model trained on observations from the same group as the test subset.

#### **4.4 Key learnings – Polymer NF vs Ceramic NF membranes**

Based on COD rejection results, polymeric membranes were found to achieve higher % COD rejection than ceramic NF membranes. GC-MS analysis also brought out that polymeric NF membranes were good at rejecting aromatic compounds namely, benzoic acid, 2-methyl benzoic acid, salicylic acid, phenol, 2-phenoxy ethanol.

Even though the stabilized absolute permeate flux was dependent on IWW composition and its bulk properties, higher wastewater flux was achieved by polymer NF membranes than ceramic NF membranes (at constant TMP) for both IWW samples tested, namely, WW-A & C. When compared to 200-Da ceramic NF membrane, polymer NF90 could achieve 56% more flux for WW-A and 42% more flux for WW-C. Polymeric NFX and NFS could achieve more than 2 times the flux achieved by 200-Da and 450-Da ceramic membranes.

200-Da and 450-Da ceramic membranes were found to be more fouling resistant and suitable for filtration of WW-A. Polymeric NF membranes except NFX experienced a large decline in flux during 180 minutes of filtration ( $< 0.5$ ) for WW-A, making them unsuitable for filtration of WW-A. This observation corroborates the enhanced fouling resistance claimed by the manufacturers.

Ceramic NF membranes were found to be easily cleaned and regenerated in 30 minutes and possibly even less (not tested in this study) using 1% w/w solution of an enzyme based industrial cleaner (Tergazyme). Multiple filtration cleaning cycles on one of the model membranes 750-Da showed perfect regeneration of membrane CWP every time showing membrane robustness.

## **Chapter-5: Conclusions and future work**

### **5.1 Conclusions**

In the last couple of years, IWW treatment using conventional technologies has become challenging for Aevitas and other similar facilities due to stricter sewer discharge regulations imposed by the city of Brantford. High COD concentrations, bio-toxicity and varied composition of wastewater pose problems in downstream processing of wastewater at a municipal facility which typically use biological treatment methods. Thus, an imperative need of an intermediate treatment technology to work in tandem with conventional treatment units at such facilities is required to meet the required targets. Development of membrane nanofiltration (NF) has led to widespread applications in industries due to its low energy cost, no chemical usage and room temperature applicability. NF treatment has been successfully adopted in treating single source feed applications such as desalination, ground water treatment, surface water treatment, wastewater treatment to remove trace pharmaceuticals and personal care products, organic solvent nanofiltration (OSN) to purify pharmaceutical drugs and many more. Although promising, NF has several drawbacks including membrane fouling and membrane incompatibility with chemicals present in feed. Recent developments in TiO<sub>2</sub> based ceramic NF membranes has potential to enhance fouling resistance and endure harsher chemical and physical conditions as per the claims by the manufacturers. Our study has investigated performance of state-of-the-art ceramic NF membranes on multiple IWW samples acquired from Aevitas along with conventional polymer NF membranes for comparison purposes. Moreover, a data-driven modeling strategy was developed for prediction of organics compounds removal.

Ceramic membranes resulted in significant improvement in COD for 2 out of 3 IWW samples but were still not at par with the COD rejections obtained by the polymeric membranes. For two IWW samples tested both on ceramic and polymeric membranes, COD was best rejected

at an average of 68.5 % by a ceramic membrane (200-Da) as opposed to an average of 88.3 % by a polymeric membrane (NF90). GC-MS analysis further indicated better overall peaks reduction by polymeric membranes, especially in removing majority of the identified aromatic compounds which could not be removed as effectively by the ceramic membranes. Ceramic membranes were able to achieve permeate flux in the range 5-40 LMH at a TMP of 100-150 psi, where maximum flux was achieved by the membrane with highest MWCO. Interestingly, 200-Da membrane could achieve slightly higher permeate flux than 450-Da membrane but also rejected higher COD at the same time, hence making it the most suitable pick out of all the 4 ceramic membranes tested. When compared to the polymeric membranes, once again polymeric membranes achieved higher permeate fluxes at same TMP conditions. On an average over two IWW samples (WW-A & C), NF90 was able to achieve 49% more flux than 200-Da ceramic membrane. NFX and NFS were found to achieve more than 2 times the flux achieved by 200-Da membrane. A brief summary of membrane areas required to process 100,000 L wastewater per day is shown in Table 21. Although, ceramic membranes did not surpass conventional polymeric membranes in COD rejection and flux performance, severe flux decline was observed for polymeric membranes but not for 200-Da and 450-Da ceramic membranes indicating better fouling resistance in ceramic membranes. Based on above discussion, it can be concluded that 200-Da, NF90 and NFX membranes are promising candidates for such a process and should be studied further.

Membrane	Average flux (LMH)	Membrane area required to process 100,000 L/day (m <sup>2</sup> )	Typical membrane areas in commercially available modules
200-Da	10.1	412.5	Upto 1.3 m <sup>2</sup> per element and 58.5 m <sup>2</sup> per module
NF90	12.7	328.1	37 m <sup>2</sup> per '8 inch diameter, 40 inch length spiral wound module'
NFX	19.7	211.5	27 m <sup>2</sup> per '8 inch diameter, 40 inch length spiral wound module'

**Table 21.** Membrane area calculations based on flux achieved by 200-Da, NF90 and NFX membranes

An artificial intelligence approach was applied for the first time in predicting the complex rejection behavior of NF membranes based on properties of a molecule. Preliminary PLS model results and past work in the field of ‘quantitative structure-activity relationship’ (QSAR) modeling helped in building a combined PCA-PLS modeling architecture. A fair agreement in observed and predicted rejections was found based on average cross validated score  $Q^2 = 0.46$  for ceramic membranes, and  $Q^2 = 0.67$  for polymeric membranes. During model testing, RMSEP was found to be less than 15% for 4 membranes out of 5. 450-Da membrane had the highest RMSEP of 18%. Since removal of peaks from GC-MS is directly related to removal of COD, predictions from such models can be used to predict COD rejection if all peaks in a feed GC-MS spectrum were identified. Moreover, such models may play a key role in treating time-varying feed wastewater which may contain unseen compounds which have never been tested in a laboratory before. An early prediction available for such samples would aid in decision making. In conclusion, composition analysis of IWW using GC-MS when combined with data-driven modeling techniques could help in building useful models for day-to-day activities in wastewater treatment facilities receiving multi-source time-varying wastewater.

## **5.2 Future work**

Further experimental work should include long duration testing (24 – 48 h) of the recommended membranes in a non-recycle mode with high recovery to simulate a real industrial setting. Additionally, chemical/physical cleaning methods for polymer NF membranes NF90 and NFX need to be investigated. In regards to permeate flux, this report shows the permeate flux obtained at a constant TMP, however in order to find the maximum permeate flux that could be achieved by a membrane without accumulating extra fouling, a range of TMP values could be tested in a single experiment to determine the critical pressure.

One of the major problems in handling real IWW samples from Aevitas was its changing COD. Several samples were found to reduce their COD and change color while storage. This phenomena was slowed when the samples were stored in fridge at 4 °C, but never halted. One of the reasons behind the slow decrease in COD was presence of micro amounts of coagulants from the coagulation-flocculation process in the plant. Thus, micro-flocs kept forming and settling even while the sample was sitting. This creates problems in head-to-head comparison of membrane performance. Solution to this problem was not addressed methodically in this work but may prove helpful in future work. Tracking COD change for few weeks while mixing the wastewater sample vigorously before each COD measurement could help in identifying shelf life of the sample. Although, the samples can be left for a period of time to come to a stabilized condition before testing them, such a strategy might not simulate a real industrial setting where the wastewater needs to be treated immediately after coming out of the flocculation tanks. Another way to alleviate this problem could be to test all membranes at once using a high throughput system. Use of a high throughput system will also resolve the problem of COD reduction due to dilution and adsorption within the membrane testing system during every experiment. Collection and testing of samples after aeration treatment (removes micro-flocs) might also be a good idea to get a cleaner feed sample.

One of the most time intensive tasks during this project was GC-MS sample preparation, measurement and analysis. Although a standardized procedure was carefully followed each time, variation in area under peak for ‘internal standard’ (used as a basis for other peaks) was found to be high, and therefore calculating relative peak areas based on this IS could have incorporated extra errors in ‘% area reduction’ rather than correcting for the instrument variability. Acquiring duplicate GC-MS spectrum for each sample could help in getting accurate results and is therefore recommended for future experiments. Trying a new internal standard or using two internal

standards could be helpful in rectifying this problem and also identifying if the current variation is due to interference of IS with sample components. Since GC-MS was found to be a promising IWW characterization tool, future research could also look into fast GC-MS techniques to reduce characterization time and produce rapid predictions for quick decision making.

Usage of updated NIST20 (2020) standard mass spectra library for compound identification is highly recommended to identify newer pollutants and chemicals such as surfactants and pharmaceuticals which might be present in our wastewater. Compound identification in current GC-MS spectrums were performed using NIST v2.0f (2008) mass spectra library.

Size exclusion being one of the major separation mechanisms for membranes, it is also necessary to know and utilize particle size distribution using techniques such as Dynamic Light Scattering (DLS) in addition to GC-MS characterization. State-of-the-art DLS methods can measure particle sizes down to 1-2 nm range and as high as 3.5  $\mu\text{m}$ . Some preliminary DLS measurements on feed and permeate samples from microfiltration of WW-A were acquired using a Malvern Mastersizer 3000. A multimodal distribution was observed for feed which turned into a bimodal distribution after microfiltration completely removing two of the peaks. Given that a DLS measurement takes less than 5 minutes to perform and provides valuable information which could be used for predicting filtration and fouling performance, future work can include DLS as a wastewater characterization tool.

More wastewater testing is needed to increase the number of observations present for model building. A larger dataset would help build a better model. Future work should include usage of the updated peak reduction model in predicting COD rejection and permeate flux through a membrane.

Since real wastewater samples have a lot of unknown compounds and solid particles, rejection for some molecules could be affected due to unknown reasons. A synthetic wastewater recipe with carefully selected group of compounds and predictor variables could help in building great models and find informative correlations between rejection and molecular properties/structure. Compounds should be selected in a way such that a wide range for every property/structure (predictors) is covered. This will ensure that the data cloud does not contain highly dense or empty regions in the n-dimensional space (where n is the number of predictor variables) and the user ends up with a biased model towards some classes of compounds.

## Appendix

Table A1. Discharge targets at Aevitas

<b>Parameter</b>	<b>Limit</b>	<b>Unit</b>
Nitrification inhibition	6.3	%
Chemical Oxygen Demand	600	mg/L
Biological Oxygen demand	300	mg/L
Total Suspended Solids (TSS)	350	mg/L
Total Kjeldhal Nitrogen (TKN)	100	mg/L
Total Phosphorous	10	mg/L
Oil and Grease - animal and vegetable	150	mg/L
Oil and Grease - mineral and synthetic/hydrocarbon	15	mg/L
pH	6.0-10.5	mg/L
Temperature	< 60 °C	mg/L
Phenolic Compounds	1	mg/L
PCB	0.004	mg/L
Aluminium	50.0	mg/L
Arsenic	1.0	mg/L
Cadmium	0.7	mg/L
Chloride	1500.0	mg/L
Chromium	2.8	mg/L
Cobalt	5.0	mg/L
Copper	2.0	mg/L
Cyanide	1.2	mg/L
Fluoride	10.0	mg/L
Iron	50.0	mg/L
Lead	0.7	mg/L
Mercury	0.0	mg/L
Molybdenum	5.0	mg/L
Nickel	2.0	mg/L
Selenium	0.8	mg/L
Silver	0.4	mg/L
Sulphide (as H <sub>2</sub> S)	1.0	mg/L
Tin	5.0	mg/L
Titanium	5.0	mg/L
Zinc	3.0	mg/L

Table A2. Error in rejection for compounds occurring in multiple wastewaters. Error values more than 15% are highlighted in red

S.No	RT [min]	Compound	% peak area reduction									
			200-Da		450-Da		NF90		NFX		NFS	
			Avg	Err	Avg	Err	Avg	Err	Avg	Err	Avg	Err
1	9.7	Diethylene glycol butyl ether					100	0	80	3	78	
2	6.5	Heptanoic acid					98		96		93	
3	9.5	Pentanedioic acid					96		95		91	
4	10.6	o-methyl benzoic acid					98	1	95	1	87	1
5	10.5	6-hydroxyhexanoic acid					98		98		93	
6	8.8	1,1,1-Tris(hydroxy methyl) propane					72		70		53	
7	7.5	1-methyl pyrrolidinone					98		72		51	
8	6	Benzonitrile					97		69		39	
9	3.9	Styrene	25									
10	6.1	2-butanol	87		67							
11	8.1	2-phenyl ethanol	79		40							
12	6.9	Nonanoic acid	79		71		98	1	97	2	97	2
13	8.6	N,N-Dibutylethanolamine	95		90		99		99		99	
14	20.5	Octadecanoic acid	75	3	62	14	83	2	83	2	85	0
15	18.4	1,11-undecanedioic acid	99	1	95	5	99	0	99	0	98	1
16	17.3	Decanedioic acid	100	0	97	2	99	1	100	0	99	1
17	4.1	Cyclohexanol	50	8	44	5	61	5	56	5	50	2
18	7.9	Octanoic acid	92		89		98	0	97	1	94	1
19	24.1	Dehydroabietic acid	95		91		99		98		100	
20	6.2	2-ethyl hexanoic acid	89	2	77	7	99	0	99	1	97	1
21	18.3	Hexadecanoic acid	58	3	49	8	70	4	62	5	63	9
22	8.9	Benzoic acid	68	2	63	16	94	5	90	2	86	4
23	22.2	Ricinoleic acid	98		97		99		97		99	
24	7.3	Nonanol	72		68		97		91		95	
25	3.9	Propan-1,2-diol	50	35	0	6	64	30	42	20	32	5
26	20.5	Oleic acid	98		98		97		96		97	
27	19.4	Dodecanedioic acid	98	1	95	3	99	1	99	1	99	2
28	10.8	2-phenoxy ethanol	44		26		95	2	41	4	36	10
29	5.4	Phenol	54	9	49	39	99	1	67	17	44	34
30	10	Benzeneacetic acid	95	4	89	5	93	6	85	11	87	1
31	4.8	Octanol	62		92		91	7	91	2	87	1
32	4.9	Lactic acid	9		29		12				7	
33	4	Pentanoic acid	89	11	63	12	94	7	86	11	84	9
34	4.9	Heptan-2-ol	36		37		84		79		50	
35	10.6	2-methyl benzoic acid	76		45		99		87		86	
36	5.1	Hexanoic acid	97		79		96	2	95	1	95	3
37	4.8	2-ethyl hexanol	89		27		91		75		57	
38	16.1	Nonanedioic acid	100		96		99	1	98	1	95	3
39	7	Benzyl alcohol	50		2		85	7	37	18	29	23
40	5	Ethylene glycol butyl ether	86		15		97	2	63	21	54	17
41	12.7	Salicylic acid	84		69		98		92		77	

**Supplementary data file**

Description:

The accompanying excel spreadsheet contains Table A3 through A8, containing GC-MS analyzed dataset, one for each wastewater sample A through F. 6 sheets are present in total with sheet names denoting Table number.

Filename: AgnihotriSatyam\_WastewaterAnalysis\_GCMSdata.xlsx

Location: [MacSphere](#) Open Access Dissertations and Theses, McMaster University

## References

- [1] I. Huisman, MEMBRANE SEPARATIONS | Microfiltration, Elsevier BV, 2000.
- [2] R. Davis, "Microfiltration in Pharmaceuticals and Biotechnology," *Current Trends and Future Developments*, p. 29–67, 2019.
- [3] A. Moslehyani and P. Goh, "Recent Progresses of Ultrafiltration (UF) Membranes and Processes in Water," *Membrane Separation Principles and Applications*, p. 85–110, 2019.
- [4] D. Zhao and S. Yu, "A review of recent advance in fouling mitigation of NF/RO membranes in water treatment:," *Desalin. Water Treat*, p. 870–891, 2015.
- [5] A. Mohammad, Y. Teow, W. Ang, Y. Chung, D. Oatley-Radcliffe and N. Hilal, "Nanofiltration membranes review: Recent advances and future prospects," *Desalination* , p. 226–254, 2015.
- [6] "Synder Filtration," [Online]. Available: <https://synderfiltration.com/nanofiltration/membranes/>.
- [7] P. Eriksson, "Nanofiltration Extends the Range of," *Environmental Progress*, pp. 58-62, 1988.
- [8] W. Deen, "Hindered transport of largemolecules in liquid-filled pores," *AIChE J.*, p. 1409–1425, 1987.
- [9] M. Ernst, A. Bismarck, J. Springer and M. Jekel, "Zeta-potential and rejection rates of a polyethersulfone nanofiltration membrane in single salt solutions," *J. Membr. Sci.*, p. 251–259, 2000.
- [10] G. Hagemeyer and R. Gimbel, "Modelling the salt rejection of nanofiltration membranes for ternary ionmixtures and for single salts at different pH values," *Desalination*, p. 247–256, 1998.
- [11] M. Hall, D. Lloyd and V. Starov, "Reverse osmosis of multicomponent electrolyte. Part II. Experimental verification," *J. Membr. Sci.*, p. 39–53, 1997.
- [12] A. Childress and M. Elimelech, "Effect of solution chemistry on the surface charge of polymeric reverse osmosis and nanofiltration membranes," *J. Membr. Sci.*, p. 253–268, 1996.

- [13] D. Oatley, L. Llenas, R. Pérez, P.M.Williams, X. Martínez-Lladó and M. Rovira, "Review of the dielectric properties of nanofiltration membranes and verification of the single oriented layer approximation," *Adv. Colloid Interface*, p. 1–11, 2012.
- [14] T. Tsuru, S. Nakao and S. Kimura, "Calculation of ion rejection by extended Nernst–," *J. Chem. Eng. Jpn*, p. 511–518, 1991.
- [15] W. Bowen and J. Welfoot, "Modelling the performance of membrane nanofiltration—," *Chem. Eng. Sci.*, p. 1121–1137, 2002.
- [16] W. Bowen, A. Mohammad and N. Hilal, "Characterisation of nanofiltration membranes for predictive purposes — use of salts, uncharged solutes and atomic force microscopy," *J. Membr. Sci.*, p. 91–105, 1997.
- [17] A. Yaroshchuk, "Dielectric exclusion of ions from membranes," *Adv. Colloid Interface*, pp. 193-230, 2000.
- [18] A. Szymczyk and P. Fievet, "Investigating transport properties of nanofiltration membranes by means of a steric, electric and dielectric exclusion model," *J. Membr. Sci.*, p. 77–88, 2005.
- [19] Z. Yang, Y. Zhou, Z. Feng, X. Rui, T. Zhang and Z. Zhang, "A Review on Reverse Osmosis and Nanofiltration Membranes for Water Purification," *polymers*, vol. 11, no. 1252, 2019.
- [20] T. Tsuru, S. Sasaki, T. Kamada, T. Shintani, T. Ohara, H. Nagasawa, K. Nishida, M. Kanezashi and T. Yoshioka, "Multilayered polyamide membranes by spray-assisted 2-step interfacial polymerization for increased performance of trimesoyl chloride (TMC)/m-phenylenediamine (MPD)-derived polyamide membranes," *J. Membr.*, p. 504–512, 2013.
- [21] M. A. Seman, M. Khayet and N. Hilal, "Development of antifouling properties and performance of nanofiltration membranes modified by interfacial polymerisation," *Desalination*, pp. 36-47, 2011.
- [22] M. Seman, M. Khayet and N. Hilal, "Nanofiltration thin-film composite polyester polyethersulfone-based membranes prepared by interfacial polymerization," *J. Membr. Sci.*, pp. 109-116, 2010.
- [23] P. Pal, S. Chakraborty and L. Linnanen, "A nanofiltration–coagulation integrated system for separation and stabilization of arsenic from groundwater," *Sci. Total Environ.*, p. 601–610, 2014.
- [24] H. Madsen and E. Søggaard, "Applicability and modelling of nanofiltration and reverse osmosis for remediation of groundwater polluted with pesticides and pesticide transformation products," *Sep. Purif. Technol.*, p. 111–119, 2014.

- [25] C. Galanakis, G. Fountoulis and V. Gekas, "Nanofiltration of brackish groundwater by using a polypiperazine membrane," *Desalination*, p. 277–284, 2012.
- [26] S. Chakraborty, M. Roy and P. Pal, "Removal of fluoride from contaminated groundwater by cross flow nanofiltration: transport modeling and economic evaluation," *Desalination*, p. 115–124, 2013.
- [27] M. G. Khedr, "Radioactive contamination of groundwater, special aspects and advantages of removal by reverse osmosis and nanofiltration," *Desalination*, pp. 47-54, 2013.
- [28] C. Martínez-Huitle and E. Brillas, "Electrochemical alternatives for drinking water disinfection," *Angew. Chem. Int. Ed.*, p. 1998–2005, 2008.
- [29] I. Vergili, "Application of nanofiltration for the removal of carbamazepine, diclofenac and ibuprofen from drinking water sources," *J. Environ. Manag.*, p. 177–187, 2013.
- [30] M. A.-K. Al-Sofi, "Seawater desalination — SWCC experience and vision," *Desalination*, pp. 121-139, 2001.
- [31] R. Cheng, T. Tseng and K.L.Wattier, "Two-Pass Nanofiltration Seawater Desalination Prototype Testing and Evaluation," U.S. Department of the Interior, Bureau of Reclamation,, Long Beach, CA, 2013.
- [32] G. Székely, J. Bandarra, W. Heggie, B. Sellergren and F. Ferreira, "A hybrid approach to reach stringent low genotoxic impurity contents in active pharmaceutical ingredients: combining molecularly imprinted polymers and organic solvent nanofiltration for removal of 1,3-diisopropylurea," *Sep. Purif. Technol.*, p. 79–87, 2012.
- [33] W. Siew, A. Livingston, C. Ates and A.Merschaert, "Molecular separation with an organic solvent nanofiltration cascade — augmenting membrane selectivity with process engineering," *Chem. Eng. Sci.*, p. 299–310, 2013.
- [34] Y.-L. Lin, J.-H. Chiou and C.-H. Lee, "Effect of silica fouling on the removal of pharmaceuticals and personal care products by nanofiltration and reverse osmosis membranes," *J. Hazard. Mater.*, p. 102–109, 2014.
- [35] S. Alizadeh, "Design and optimization of membrane filtration and activated carbon processes for industrial wastewater treatment based on advanced and comprehensive analytical characterization methodologies," Department of Chemical engineering, McMaster University, 2019.
- [36] S. Mondal and S. R. Wickramasinghe, "Produced water treatment by nanofiltration and reverse osmosis membranes," *Journal of Membrane Science*, p. 162–170, 2008.

- [37] H. Alkhatim, M. Alcaina, E. Soriano, M. Iborra, J. Lora and J. Arnal, "Treatment of whey effluents from dairy industries by nanofiltration membranes," *Desalination*, pp. 177-184, 1998.
- [38] W. Lau, A. Ismail and S. Firdaus, "Car wash industry in Malaysia: Treatment of car wash effluent using ultrafiltration and nanofiltration membranes," *Separation and Purification Technology*, pp. 26-31, 2013.
- [39] T. Coskun, E. Debik and N. M. Demir, "Treatment of olive mill wastewaters by nanofiltration and reverse osmosis membranes," *Desalination*, pp. 65-70, 2010.
- [40] E. Ellouze, N. Tahri and R. B. Amar, "Enhancement of textile wastewater treatment process using Nanofiltration," *Desalination*, pp. 16-23, 2012.
- [41] S. K. Nataraj, K. M. Hosamani and T. M. Aminabhavi, "Distillery wastewater treatment by the membrane-based," *WATER RESEARCH*, pp. 2349-2356, 2006.
- [42] L. Feini, Z. Guoliang, M. Qin and Z. Hongzi, "Performance of Nanofiltration and Reverse Osmosis Membranes in Metal Effluent Treatment," *Chinese Journal of Chemical Engineering*, pp. 441-445, 2008.
- [43] I. Galambos, J. M. Molina, P. Jfiray, G. Vatai and E. Bekfissy-Molnar, "High organic content industrial wastewater treatment," *Desalination*, pp. 117-120, 2004.
- [44] R. d. Almeida, A. M. Costa, F. d. A. Oroski and Juacyara, "Evaluation of coagulation–flocculation and nanofiltration processes in landfill leachate treatment," *Journal of Environmental Science and Health, Part A*, pp. 1091-1098, 2019.
- [45] M. Lee, Z. Wu and K. Li, "Advances in ceramic membranes for water treatment," *Chemical Eng & Applied Chemistry*, pp. 43-82, 2015.
- [46] S. Akbarnezhad, S. M. Mousavi and R. Sarhaddi, "Sol-gel synthesis of alumina-titania ceramic membrane: Preparation and characterization," *Indian Journal of Science and Technology*, pp. 1048-1051, 2010.
- [47] P. Puhlfür, I. Voigt, R. Weber and M. Morbé, "Microporous TiO<sub>2</sub>-membranes with a cut off < 500 Da," *J. Membr. Sci.*, pp. 123-133, 2000.
- [48] I. Voigt, M. Stahn, S. Wöhner, A. Junghans, J. Rost and W. Voigt, "Integrated cleaning of coloured waste water by ceramic NF membranes," *Sep. Pur. Tech.*, pp. 509-512, 2001.
- [49] M. Y. Li, G. X. Wu, Y. T. Guan and X. H. Zhang, "Treatment of river water by a hybrid coagulation and ceramic membrane process," *Desalination*, pp. 114-119, 2011.

- [50] B. Hofs, J. Ogier, D. Vries, E. F. Beerendonk and E. R. Cornelissen, "Comparison of ceramic and polymeric membrane permeability and fouling using surface water," *Separation and Purification Technology*, pp. 365-374, 2011.
- [51] K. S. Ashaghi, M. Ebrahimi and P. Czermak, "Ceramic ultra- and nanofiltration membranes for oilfield produced water treatment: A mini review," *he Open Environmental*, pp. 1-8, 2007.
- [52] M. S. Li, Y. J. Zhao, S. Y. Zhou and W. H. Xing, "Clarification of raw rice wine by ceramic microfiltration membranes and membrane fouling analysis," *Desalination*, pp. 166-173, 2010.
- [53] Y.-y. Zhao, X.-m. Wang, H.-w. Yang and Y.-f. F. Xie, "Effects of organic fouling and cleaning on the retention of pharmaceutically active compounds by ceramic nanofiltration membranes," *Journal of Membrane Science*, pp. 734-742, 2018.
- [54] F. C. Kramer, R. Shang, S. G. Heijman, S. M. Scherrenberg, J. B. v. Lier and L. C. Rietveld, "Direct water reclamation from sewage using ceramic tight ultra- and nanofiltration," *Separation and Purification Technology*, pp. 329-336, 2015.
- [55] J. S. Barredo-Damas, M. Alcaina-Miranda, A. Bes-Piá, M. Iborra-Clar, A. IborraClar and J. Mendoza-Roca, "Ceramic membrane behavior in textile wastewater ultrafiltration," *Desalination*, pp. 623-628, 2010.
- [56] A. Arkell, J. Olsson and O. Wallberg, "Process performance in lignin separation from softwood black liquor by membrane filtration," *Chem. Eng. Res. Des.*, pp. 1792-1800, 2014.
- [57] I. Voigt, H. Richter, M. Stahn, M. Weyd, P. Puhlfürß, V. Prehn and C. Günther, "Scale-up of ceramic nanofiltration membranes to meet large scale applications," *Separation and Purification Technology*, pp. 329-334, 2019.
- [58] S. Wold, M. Sjöström and L. Eriksson, "PLS-regression: a basic tool of chemometrics," *Chemometrics and Intelligent Laboratory Systems*, pp. 109-130, 2001.
- [59] D. Pan, M. Iyer, J. Liu, Y. Li and A. J. Hopfinger, "Constructing Optimum Blood Brain Barrier QSAR Models Using a Combination of 4D-Molecular Similarity Measures and Cluster Analysis," *J. Chem. Inf. Comput. Sci.*, pp. 2083-2098, 2004.
- [60] R. Metzler, R. Rauschert and V. Prehn, "Inopor," [Online]. Available: <http://inopor.com/images/documents/downloads/en/productsheet/datasheet-ceramic-nf-membranes.pdf>.
- [61] "Cerahelix," [Online]. Available: <https://www.cerahelix.com/products/>.

- [62] A. Imbrogno, A. Tiraferri, S. Abbenante, S. Weyand, R. Schwaiger, T. Luxbacher and A. I. Schäfer, "Organic Fouling through Magnetic Ion Exchange-Nanofiltration (MIEX-NF) in Water Treatment," *Journal of Membrane Science*, 2017.
- [63] I. Caltran, L. Rietveld, H. Shorney-Darby and S. Heijman, "Separating NOM from salts in ion exchange brine with ceramic nanofiltration," *Water Research*, 2020.